Sharanappa Nembenna

β−Diketiminate Ligand Supported Group 2 Metal Hydroxide, Halide, Oxygen Bridged Heterobimetallic and Heterotrimetallic Complexes: Synthesis and X-ray Structural Studies

---

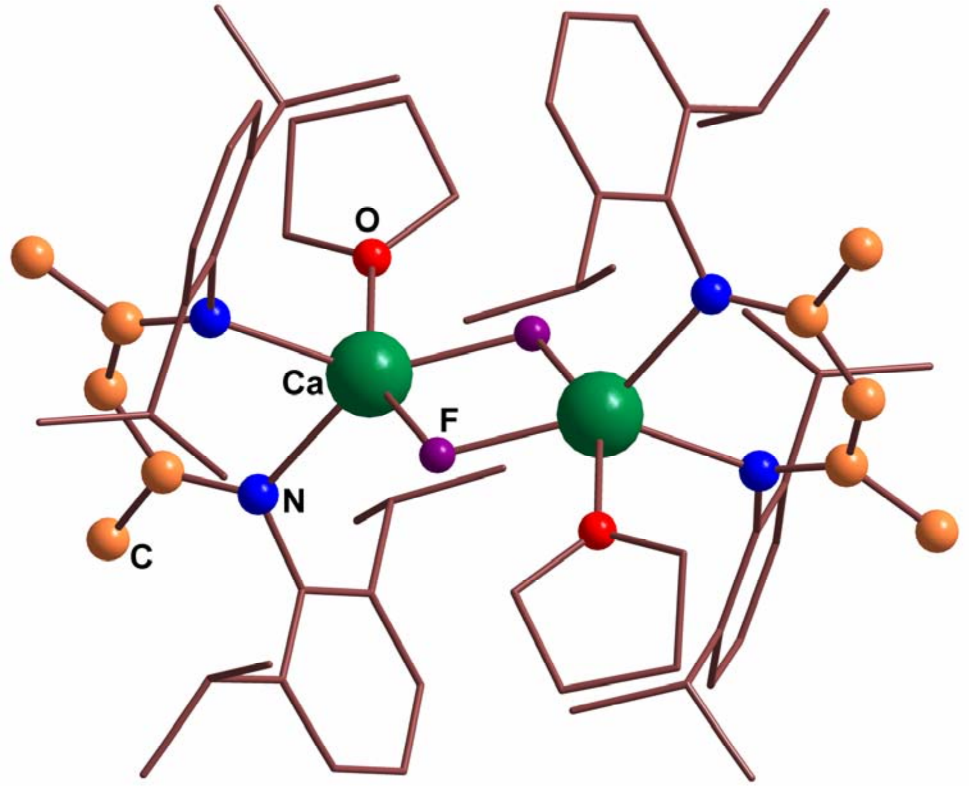

Göttingen 2007

β−Diketiminate Ligand Supported Group 2 Metal Hydroxide, Halide, Oxygen Bridged Heterobimetallic and Heterotrimetallic Complexes: Synthesis and X-ray Structural Studies

Dissertation
zur Erlangung des Doktorgrades
der Mathematisch-Naturwissenschaftlichen Fakultäten
der Georg-August-Universität zu Göttingen

Vorgelegt von

Sharanappa Nembenna
Aus Kallur
(INDIA)

Göttingen 2007

D 7

Referent: Prof. Dr. Dr. h. c. mult. Herbert W. Roesky

Korreferent: Prof. Dr. Dietmar Stalke

Tag der mündlichen Prüfung: 30.10.2007

Dedicated to my mother Channabasamma

and

My eldest brother late Mallikarjungouda

Acknowledgement

The work described in this doctoral thesis has been carried out under the guidance and supervision of Prof. Dr. Dr. h. c. mult. Herbert W. Roesky at the Institut für Anorganische Chemie der Georg-August-Universität in Göttingen between April 2004 and September 2007.

My grateful thanks to

Prof. Dr. Dr. h. c. mult. Herbert W. Roesky

for his constant advice, guidance, motivation, suggestions, and discussions throughout this work. I would like to thank him for his personal attention and the freedom I enjoyed during my stay in Göttingen.

I would like to thank Prof. G. M. Sheldrick, Prof. D. Stalke, Prof. J. Magull, Dr. M. Noltemeyer, Mr. H. Ott, Ms. A. Hofmeister, Mr. A. Pal, and Mr. H.-G. Schmidt for their kind help in X-ray crystallographic studies. I thank Dr. R. B. Oswald for the theoretical studies. And also I thank Dr. P.-J. Wilbrandt, Mr. M. Hahn, Ms. U. Bethe, for the SEM and EDX analyses. I express my sincere thanks to Prof. Dr. N. S. Hosmane, Northern Illinois University, Dekalb USA and Prof. Dr. K. V. Katti, Missouri Columbia USA for their encouragement and sharing their ideas with me during their stay in Göttingen.

I could not have finished my research work without the help from technical and non technical staff from our institute. I thank Mr. W. Zolke, Mr. J. Schöne, Dr. G. Elter, Dr. M. John (NMR studies), Dr. D. Böhler, Mr. T. Schuchhardt (mass spectral measurements), Mr. M. Hesse (IR spectral measurements), Mr. M. Schlote, and the staff of analytical division for their timely help. I am also thankful to all the members of glass blowing section, work shop, chemical store as well the security of our institute for their co-operation and help in all kind of situations.

I wish to offer my sincere thanks to the members of our group starting with ex-members, Dr. S. K. Pandey, Dr. S. Singh, Dr. U. N. Nehete, Dr. L. Pineda, Dr. H. Zhu, Dr. J. Chai, Dr. S.

Shravankumar, Dr. V. Jancik, Dr. S. K. Mandal, Dr. V. M. Jimenez-Perez, Dr. Y. Zhi, Mr. T. Blunk, Mr. C. Ene, and the present members Dr. S. Nagendran, Mr. P. M. Gurubasvaraj, Mr. Y. Ying, Dr. G. Nikiforov, Dr. D. Ghoshal, Mr. Z. Zhang, Mr. S. Sarish, Mr. B. Nekouei, Mr. S. S. Sen, and Mr. A. Jana, for their cooperation and help during the course of this work. Especially I would like to thank Dr. S. Singh, Dr. U. N. Nehete for their help to start my research in our lab and in learning new lab techniques. And also my special thanks to Dr. S. Nagendran and Dr. K. Starke for their support and kind help.

I am also greatly indebted to many teachers in the past and present, starting from school education till the completion of the studies in the university. I am greatly thankful to all my family members especially, my mother and my brothers, Mr. Mayashankaragouda, Mr. Gundappagouda, Mr. Amarappagouda, and relatives, specially my brother-in-law Mr. B. Nagabhushanagouda, and my close friend Dr. V. V. Sanjeevkumar, for their motivation and support in accomplishing this work.

The financial support from the Göttinger Akademie der Wissenschaften and the Deutsche Forschungsgemeinschaft (DFG) is gratefully acknowledged.

I will be always indebt to this Georg-August-Universität, Göttingen, and beautiful city of Göttingen, for obtaining my Ph.D. and making my stay here peaceful and happy.

I bow down in front of THE ALMIGHTY GOD for providing me the health, strength, and this opportunity in my life.

Table of Contents

Abbreviations

δ	chemical shift
λ	wavelength
μ	bridging
$\widetilde{\nu}$	wave number
Ar	aryl
av	average
b	broad
^{o}C	Celsius
calcd.	calculated
Cp	cyclopentadienyl
Cp*	pentamethylcyclopetadienyl
d	doublet
decomp.	decomposition
EI	electron impact ionization
eqv.	equivalents
eV	electron volt
h	hours
Hz	Hertz
*i*Pr	*i*so-propyl
IR	infrared
K	Kelvin
L	$[CH\{(CMe)(2,6\text{-}i\mathrm{Pr}_2C_6H_3N)\}_2]$
L^{I}	$[CH\{Et_2NCH_2CH_2N(CMe)\}_2]$

L^{II}	$[HC\{C(CH_2)\}(CMe)(2,6\text{-}i\text{Pr}_2C_6H_3N)_2]$
m	multiplet
m/z	mass/charge
Mp	melting point
M^+	molecular ion
Me	methyl
MS	mass spectrometry, mass spectra
NMR	nuclear magnetic resonance
ppm	parts per million
q	quartet
s	singlet
sept	septet
t	triplet
THF	tetrahydrofuran
V	volume
w	weak
Z	number of molecules in the unit cell

1. Introduction

This section of the thesis gives the background and an overview of the area in several sections before the work is presented.

1.1. *β*-Diketiminate ligands

In recent years, the *β*−diketiminate ligands (Figure 1) have emerged as potential spectator ligands, in view their strong binding to metals, their tunable, steric, and electronic effects, and their diversity in bonding modes.[1] The first complexes of *β*−diketiminate ligands were prepared in the mid to late 1960's as homoleptic complexes of Co, Ni, Cu, and Zn.[2-14] When R_1 or R_5 is a small moiety such as H, Me and $SiMe_3$, the substance easily forms a dimer and allows higher coordination to the metal center, whereas a bulky aryl group on the nitrogens usually leads to the isolation of monomeric species with low coordination numbers at the metal center. For example, the N-aryl substituted ligand **L** (L = $CH\{(CMe)(2,6\text{-}i\text{Pr}_2C_6H_3N)\}_2$) has stabilized the first example of a monomeric LAl[15] complex where aluminum is in the +1 oxidation state. Also, an unprecedented germylene hydroxide LGeOH,[16] that contains a hydroxyl group attached to a Ge(II) center was stabilized by the same ligand. To date, various *β*−diketiminate complexes containing main group,[17-23] transition,[24,25] and lanthanide elements[26-29] have been synthesized and structurally characterized. Most of them have found application in catalysis (e.g. Al[30], Cr,[31-34] Mg,[35] Ni,[36] Pd,[36] Ti[37], Zn,[35] and Zr[38]) and also in bioinorganic chemistry as model compounds (e.g. Cu[39,40]).

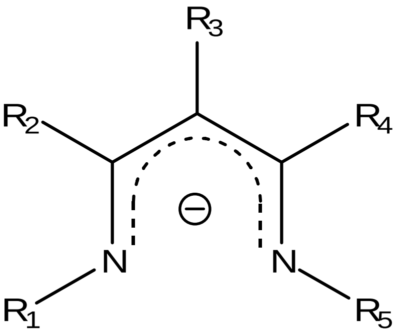

I

Figure 1. Schematic representation of β-diketiminate ligand.

Nevertheless, β–diketiminate complexes of the alkaline earth metals are few in number and their chemistry is not well established. Therefore, this thesis deals with group 2 hydroxide, halide, oxygen bridged heterobi- and trimetallic complexes stabilized by the β–diketiminate ligand.

The ligand, **L** can be prepared in good yield by the method of Feldman and coworkers (Scheme 1). The direct condensation of 2,4-pentanedione, and 2,6-di-*iso*-propylaniline in the presence of HCl in boiling ethanol afforded the ligand hydrochloride, this upon neutralization with Na_2CO_3 gave the free ligand as colorless crystals (Scheme 1).[36]

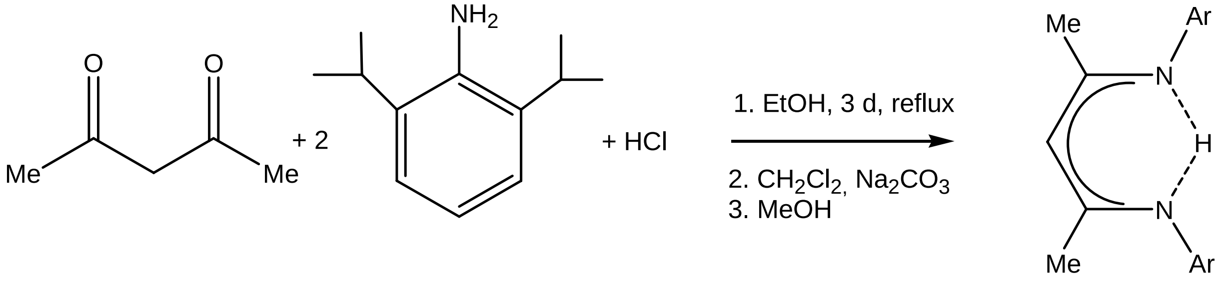

Ar = 2,6-$i$$Pr_2C_6H_3$

LH

Scheme 1. Synthesis of a sterically encumbered β -diketiminate ligand

1.2. *β*−Diketiminate supported group 2 metal hydroxides

There is a great deal of interest in the synthesis and characterization of novel main group hydroxide complexes due to their potential applications as precursor for the synthesis of heterobi- and heteropolymetallic compounds that act as versatile catalysts in organic transformations.[41] In addition, the hydroxide complexes can function as model compounds for the insoluble or unstable metal hydroxides M(OH)x. In view of these applications, Roesky et al. have reported the synthesis of various metal hydroxide complexes such as the N-bonded silanetriol[42,43] $RSi(OH)_3$ ($R = 2,6\text{-}i\mathrm{Pr}_2\mathrm{C}_6\mathrm{H}_3\mathrm{NSiMe}_3$), the aluminium(III) dihydroxide $LAl(OH)_2$,[44] the aluminium(III) monohydroxide LAl(Me)OH,[30] by tailor made synthetic strategies and unveiled their interesting reactivity. Recently, our group also reported an unprecedented germylene hydroxide LGe(OH),[16] which contains a hydroxyl group attached to a Ge(II) center, the gallium(III) dihydroxide $LGa(OH)_2$,[45] and the gallium(III) monohydroxide LGa(Me)OH [46] (see Chart 1). These examples portray the evolution of the group 13 and 14 hydroxide chemistry. Nevertheless, the organometallic hydroxide chemistry with respect to group 2 elements is still at its infancy. This is due to the higher percentage of ionic character in the M−OH (M = an alkaline earth metal) bond and also due to a fast ligand exchange.

The magnesium hydroxide[47] complex $\{[\mathrm{Tp}^{\mathrm{Ar,Me}}]\mathrm{Mg}(i\text{-OH})\}_2$; Ar = $p\text{-}\mathrm{Bu}_t\mathrm{C}_6\mathrm{H}_4$ stabilized by the tris (1-pyrazolyl)hydroborate ($\mathrm{Tp}^{\mathrm{Ar,Me}}$) ligand was prepared by Parkin et al. Another example of a magnesium hydroxide $[\mathrm{LMg(OH)\cdot THF}]_2\cdot 4\mathrm{THF}$[48] was obtained by Bochmann and coworkers. The latter compound was isolated by a serendipitous hydrolysis, when $\mathrm{LMg}(\eta^1\text{-}\mathrm{C}_3\mathrm{H}_5)(\mathrm{THF})$ was kept at −26 °C for crystallization and it lacks a direct synthetic route.

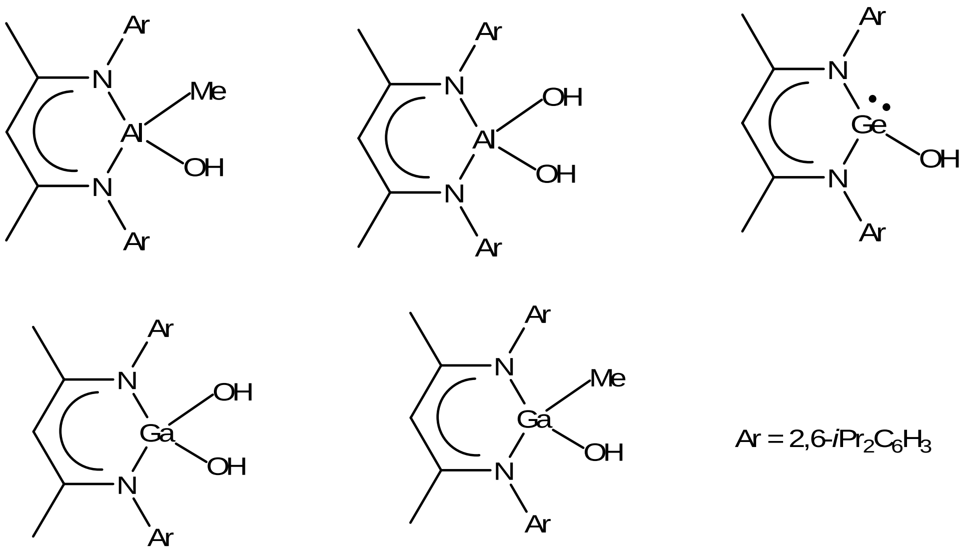

Chart 1. *β*-Diketiminate supported main group metal hydroxides .

The first part of this thesis deals with the direct synthetic route for the preparation of the *β*−diketiminate magnesium hydroxide complex. By understanding the potential lying behind this novel synthetic strategy, we have extended this approach to isolate the hitherto unknown hydroxide complexes of heavier alkaline earth metals.

In contrast to the chemistry of Mg, syntheses and isolation of complexes of the heavier alkaline earth metals Ca, Sr, and Ba have always been plagued by their high reactivity. [49-51] Over the last decade, however, rapid development in the organometallic chemistry of the elements in this group of the periodic table has been observed: its early cyclopentadienyl chemistry[52,53] has evolved to synthetic routes for alkyl, [54,55] allyl, [56] benzyl,[57] and aryl complexes.[58-61] Recently, a heteroleptic calcium hydride $[LCa(H)\cdot THF]_2$ was also reported by Harder and coworkers.[62] Its unusual stability against ligand exchange and formation of insoluble CaH_2 is presumably due to the rather bulky and strongly chelating *β*−diketiminate ligand that forms a cage around the central $(CaH)_2$-core. It suggests that the **L** ligand might also be successful in the synthesis of the kinetically more labile calcium hydroxide complex $[LCa(OH)\cdot THF]_2$. To the best of our knowledge, the Ca−OH functionality has only been observed in larger mixed metal (Li/Ca) clusters.[63] This hydroxides could also be of interest in sol-gel coatings,[64] polymerization catalysis[65] or as a potential precursor in the syntheses of well-defined heterobimetallic catalysts.[30]

1.3. *β*−Diketiminate supported group 2 metal halides

In view of the increasing importance of the heteroleptic complexes in polymerization reactions, we have attempted for the synthesis of magnesium and calcium complexes that contain both the halide and *β*−diketiminate ligand.[66,67] In accordance with the recent theoretical studies on CpM−MCp (M = alkaline earth metals) group 2 elements,[68,69] these *β*−diketiminate ligand stabilized group 2 metal halides might also be considered as promising precursor to prepare low valent group 2 compounds with metal-metal bond. In recent years, such studies are well documented in low valent zinc chemistry.[70-72] And also Roesky et al. prepared manganese(I) compound, which is stabilized by the *β*−diketiminate ligand.[73]

Since the first isolation of organomagnesium compounds by Barbier and Grignard at the beginning of the 20th century, they have become the potential reagents for the synthetic organic and organometallic chemists, due to the ease with which they can be prepared and the wide array of reactions that they undergo.

Roesky et al. have reported the Grignard analogues such as $LMgI{\cdot}OEt_2$[74] and L^I MgBr.[75] The former compound was obtained by the reaction of $LLi{\cdot}OEt_2$ with MgI_2 and the latter compound lacks a direct synthetic route. Therefore, this thesis also deals with the synthesis of the solvent free and monomeric *β*−diketiminate supported magnesium chloride complex.

CaF_2 is the most important fluoride of the alkaline earth metals since its mineral fluorspar is the only large-scale source of hydrogen fluoride. Moreover, CaF_2 is a high melting solid (1418

^{o}C), whose low solubility in water allows quantitative precipitation in analytical chemistry.[76] Although, CaF_2 is the feedstock for most of the fluorine compounds, up to now it is not available to organometallic chemistry because of its poor solubility in common organic solvents.[77] To address this issue our group has reported the first soluble CaF_2 complex $[(Cp^*TiF_2)_6CaF_2(THF)_2]$.[78] This complex was prepared by adding a solution of Cp^*TiF_3 to a suspension of calcium metal in the presence of mercury at 0 ^{o}C. And also the reaction of CaF_2 (prepared *in situ*) with either $[(C_5Me_5)TiF_3]$ or $[(C_5Me_4Et)TiF_3]$ results in the formation of either $[\{(C_5Me_5)TiF_3\}_4CaF_2]$ or $[\{(C_5Me_4Et)TiF_3\}_4CaF_2]$. In all these examples CaF_2 is trapped in a soluble organometallic matrix.[79] Nevertheless, it did not allow to explore the chemistry of the Ca–F bond. Therefore, it is very interesting to synthesize a well-defined hydrocarbon-soluble molecular compound of composition LCaF. This target has never been accomplished, but there are some ill-defined substituted calcium monofluoride species. Thus the arylcalcium fluoride (ArCaF) is formed as a reactive brown solid by vaporization and co-condensation of calcium metal with excess ArF at 77 K.[80] And also the deposition of calcium vapor with argon at 9 K generates calcium atoms and calcium clusters which react with MeF to form species of composition $MeCa_xF$ ($x = 1, 2$). None of these compounds have been structurally characterized.[81,82] Also, the synthesis of the well-defined LCaF complex gains importance in view of its expected use as soluble precursor for the preparation of CaF_2 coatings which would eradicate the high resources and energy consuming methods conventionally used for making such coatings.[83] These CaF_2 coatings are used as window material for both infrared and ultraviolet wavelengths and exhibit extremely weak birefringence. Therefore, when applied on the surface of substrates such as glass or metal they impart a change in its optical properties. Moreover, thin layers of CaF_2 have been used recently as fluoride ion conductors.[84,85]

1.4. Heterobi- and trimetallic oxygen bridged complexes

Heterobi- and heteropolymetallic compounds find various applications ranging from advanced materials to valuable catalysts. The compounds with different metal centers have often modified the fundamental properties of the individual metal atoms.[86] Roesky and co workers have developed various heterobi- and trimetallic oxygen bridged systems (see Chart 2). Some of them are used as catalysts in various polymerization reactions.[30,87-92] Furthermore, group 2 metal oxides find applications in a wide range of man-made materials such as catalysts, ferroelectrics, metallic conductors, and superconductor materials.[63,93]

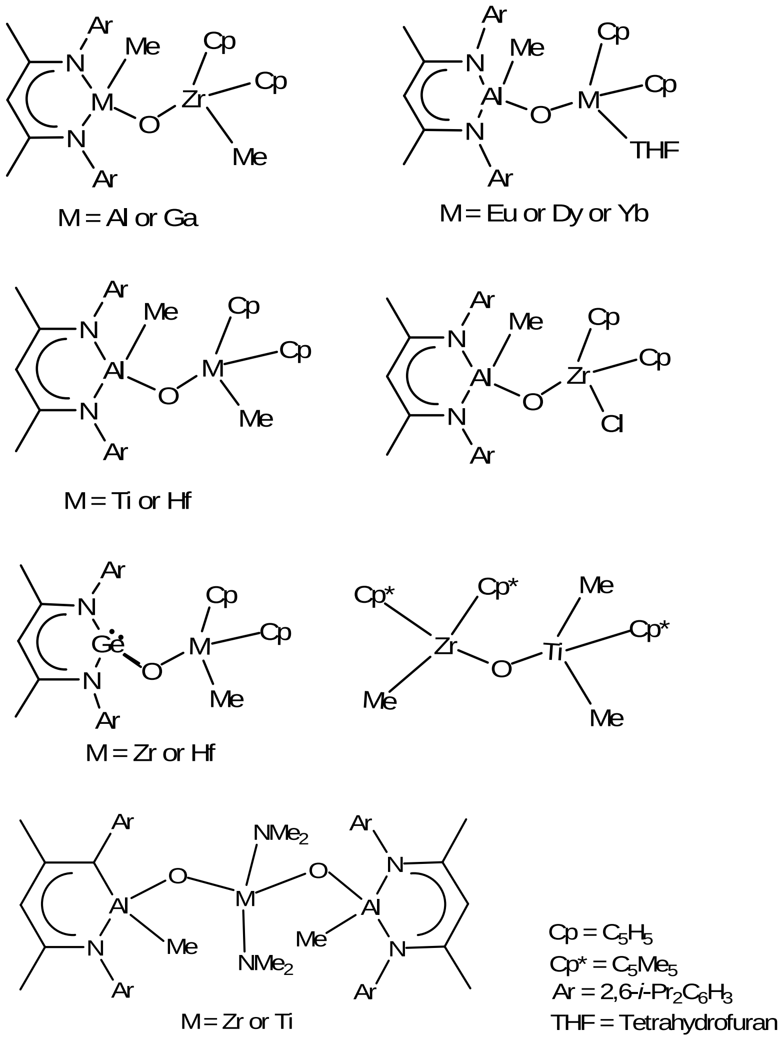

Chart 2. Heterobi- and trimetallic oxygen bridged complexes.

Therefore, it was planned to incorporate the group 2 metals into the heterobi- and trimetallic framework and study its properties.

1.5. Heterobi- and trimetallic compounds with the Mg–O–Al structural motif

Is it possible to construct soluble compounds with the Mg–O–Al structural motif? To address this issue, we became interested in developing soluble compounds with the Mg–O–Al structural motif.

Spinel is a very attractive and historically important gemstone and mineral. Spinel of composition $MgAl_2O_4$ is found in nature and it is prepared by reacting aluminum oxide with MgO at high temperatures. The structure of $MgAl_2O_4$ consists of cubic closest packed oxide ions. One eighth of the tetrahedral vacancies of this structure are occupied by Mg^{II} and half of the octahedral vacancies are filled with Al^{III} ions. A multitude of spinels using other elements has been reported.[76,94,95] These compounds have a variety of applications; for example, hot pressed $MgAl_2O_4$ is used as an optical window, and the ferrite spinels are an important family of magnetic materials. All spinels have in common that they are high melting inorganic solids and insoluble in organic solvents. Moreover, it was shown that SiO_2 as well as $MgCl_2$ function as supports for metallocene–methylaluminoxane (MAO) catalysts.[96] The magnesium supported system exhibits activity 2-fold higher in ethylene polymerization than the silica analogues. An explanation of this phenomenon has not been given.[97-100] Previous quantum chemical calculations have shown that adsorbed rhenium subcarbonyls on MgO surfaces form strong Re–O adsorption bonds justifying the inert MgO surface able to anchor organometallic fragments as a support.[101] Recently, an alkoxy bridged Mg–O(R)→Al compound has been reported.[102] However, the stability and bonding situation of this system is quite different from that of an oxide bridged Mg–O–Al motif.

1.6. Heterometallic oxides containing calcium

Calcium is an inexpensive and biocompatible metal. Calcium finds extensive application in the production of polyoxygenates such as poly(ethyleneoxide) PEO, and polypropylene oxide PPO. Ca^{2+} is a kinetically labile ion[103] and it is hard like the Mg^{2+} ion, but significantly larger than either Mg^{2+} or the softer Zn^{2+} ion.

The organo magnesium compounds are extensively and routinely employed in both organic and organometallic synthesis.[104-106] Nevertheless, the heavier group 2 metal complexes are highly labile and undergo Schlenk-type redistrubition processes in solution, in view of the increasing atomic radius and electropositive character. Unless polydentate and/or bulky and kinetically-stabilizing ligands are employed, there exists a tendency towards the formation of oligomeric or polymeric species.[107] Recently, several reports have described the synthesis of heavier alkaline earth metal complexes containing *β*−diketiminate ligands and their bis(phosphinimino)-methyl analogues.[108-116] Exploration of this field is driven by the potential use of these complexes in catalysis, organic synthesis, chemical vapor deposition (CVD), and film growth.[117,118] To date numerous homo and heteroleptic calcium alkoxides and aryloxides have been synthesized and structurally characterized.[119-121] In view of the increasing importance of heteroleptic complexes in polymerization reactions, heterobimetallic oxides containing the Ca−O−Al moiety may also catalyse various polymerization and organic tranformations.

1.7. Alkaline earth metal-zirconium oxide compounds

Inorganic oxides such as $MgZrO_3$, $CaZrO_3$, and Mg_2ZrO_4 contain both the alkaline earth and zirconium metal ion. Moreover, these compounds are high melting and insoluble in organic solvents. Due to the lack in appropriate synthetic strategies, it is always a challenge to construct soluble oxides containing both the alkaline earth and zirconium metal ion. Alkaline earth alkoxides are also highly polymeric in character and insolube in organic solvents. Mehrotra and coworkers have reported some soluble double alkoxides with alkaline earth metals.[122] Nevertheless, no example of an oxide compound containing M−O−Zr (M = Mg, Ca) moiety is known. By utilizing tailor made synthetic strategy and starting from zirconium hydroxide, we have demonstrated the facile route for the synthesis of compounds containing the M−O−Zr moiety (M = Mg, Ca).

Especially, there is a growing interest in calcium-zirconium based oxides for potential sensor/device applications at elevated temperatures. In particular, several studies have been reported on the use of calcium zirconate-based systems for monitoring oxygen,[123,124] humidity and hydrogen.[125-127] $CaZrO_3$ has also been studied for its potential use as high-temperature thermistor material.[128] The electrical response of calcium zirconate (prepared by the solid state firing of $CaCO_3$ and ZrO_2 powders at 1400 °C) was found to be sensitive to methane, but was practically unaffected by humidity and carbon monoxide.

1.8. Aluminum-tin oxide complexes

Naturally occurring mineral of tin is an oxide, SnO_2 commonly known as cassiterite or tin-stone. It is analogous to the naturally occurring form of their lighter element of the group silicon, which also exists as oxide, SiO_2 but different to the heavier element lead which exists as sulphide, PbS.[94] Silicates and silica are important substances and their utilities are well documented. The inorganic materials such as aluminosilicates and zeolites that contain Al−O−Si moieties find various applications such as ion exchanger resins, catalysts, catalyst supports, and molecular sieves.[129-136] However, the chemistry of related organoaluminum tin oxides is not much documented. The use of trialkylaluminum compounds to alkylate the organotin oxides to obtain asymmetrical tetraorganotin derivatives was reported. But no attempt was made to isolate the mixed aluminum and tin oxide derivatives.[137] Mehrotra and coworkers have reported some aluminum alkoxide compounds containing tin, where tin is in its oxidation state (IV).[138,139] In 1994 Oliver and coworkers reported the dimeric structure of $[Me_2Al(OSnPh_3)]_2$ formed by the reaction of Me_3Al with $[Ph_3Sn]_2O$.[140] However, in this thesis we have described aluminum-tin oxide compounds containing Al−O−Sn(IV) and Al−O−Sn(II) moieties

1.9. Heterotrimetallic oxygen bridged system with three different metal atoms

In previous sections we have discussed various heterobi- and trimetallic oxygen bridged systems. None of the systems contain three different metal atoms. In view of this, for the first time we have developed a well-defined heterotrimetallic oxygen bridged system with three different metal centers. To the best our knowledge no example is known for such a system. Interestingly, this oxygen bridged trimetallic system is stabilized by *β*−diketiminate and cyclopentadienyl ligands.

1.10. Aim and scope of the present work

The above discussion shows that two magnesium hydroxide complexes are known. One is stabilized by the scorpionate ligand and the other is anchored on a *β*−diketiminate ligand. But the latter compound lacks the direct synthetic route. It is clear that heavier analogues are not reported. Two Grignard analogues $LMg{\cdot}IOEt_2$ and L^IMgBr are known, but the former compound is coordinated with the solvent and the latter one lacks the direct synthetic route. Also stable soluble CaF_2 complexes are known, where the CaF_2 is trapped in a soluble organometallic matrix. Simple calcium monofluoride complexes are totally missing. In the literature various heterobi- and trimetallic oxygen bridged complexes are well documented, but the oxides with group 2 metals are not at all documented. The oxygen bridged trimetallic system with three different metal atoms is also unknown.

Based on these facts the objective of the present work is as follows:

1. to develop a new synthetic strategy for the preparation of β−diketiminate supported magnesium and calcium hydroxide complexes.
2. to synthesize a monomeric solvent free magnesium chloride complex and soluble calcium monofluoride complex and to study its utility in preparing CaF_2 surface coatings.
3. to develop various heterobi- and trimetallic oxygen bridged complexes with group 2 metals.
4. to develop a synthetic route to obtain heterotrimetallic oxygen bridged system with three different metal atoms.
5. to use the spectral techniques such as NMR, IR spectroscopy, and X-ray structural analysis methods to characterize the products obtained.

2. Results and Discussion

2.1. Hydrolysis of LMgN(SiMe$_3$)$_2$ and X-ray crystal structure of [LMg(OH)·THF]$_2$ (1)

Compound [LMg(OH)·THF]$_2$ (**1**) is prepared by the reaction of LMgN(SiMe$_3$)$_2$ [141] with a stoichiometric amount of water at –20 °C (Scheme 2). Compound **1** is a white solid soluble in toluene, THF and sparingly soluble in benzene. It was characterized by IR, ^{1}H NMR spectroscopy, EI mass spectrometry, elemental analysis, and X-ray structural analysis. In the IR spectrum a sharp absorption around 3741 cm^{-1} can be attributed to the O–H stretching frequency. The ^{1}H NMR spectrum of **1** exhibits a resonance at –0.46 ppm for MgO–H. The base peak in the EI mass spectrum of **1** at m/z 916 corresponds to molecular ion peak [M^+].

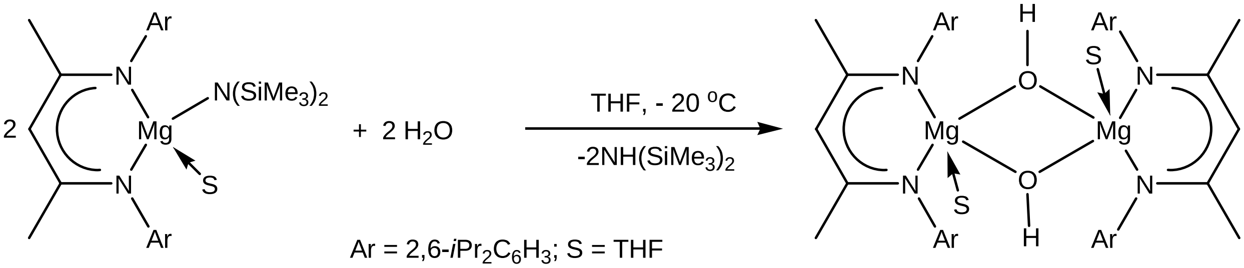

1

Scheme 2. Synthesis of β–diketiminate supported magnesium hydroxide.

The molecular structure of [LMg(OH)·THF]$_2$·toluene (**1**) has been determined by single crystal X-ray diffraction (Figure 2), demonstrating that the complex consists of a hydroxide bridged dimer in the solid state. Single crystals of **1** suitable for X-ray structural analysis were obtained from hot toluene and small amounts of THF solution at 0 °C within 24 h. Compound **1** crystallizes in the monoclinic space group $P2_1/n$, with one half dimer in the asymmetric unit. The coordination geometry around the metal center is a distorted square-pyramid, with the O atom of the THF moiety at the apex and N(1), N(2), O(1) and O(1A) forming the square base. The central Mg_2O_2 four-membered ring is planar with a center of symmetry. The Mg–O bond distances are in the range of 1.983(18) to 2.10(18) Å, and thus considerably shorter than the Ca–O bond distances observed in (*vide supra*) [LCa(OH)·THF]$_2$ (**2**) (2.210(6) Å). The Mg–N bond lengths 2.1688(18) Å 2.1708(18) Å are shorter than the Ca–N bond distances in **2** (2.419(2) and 2.422(3) Å).

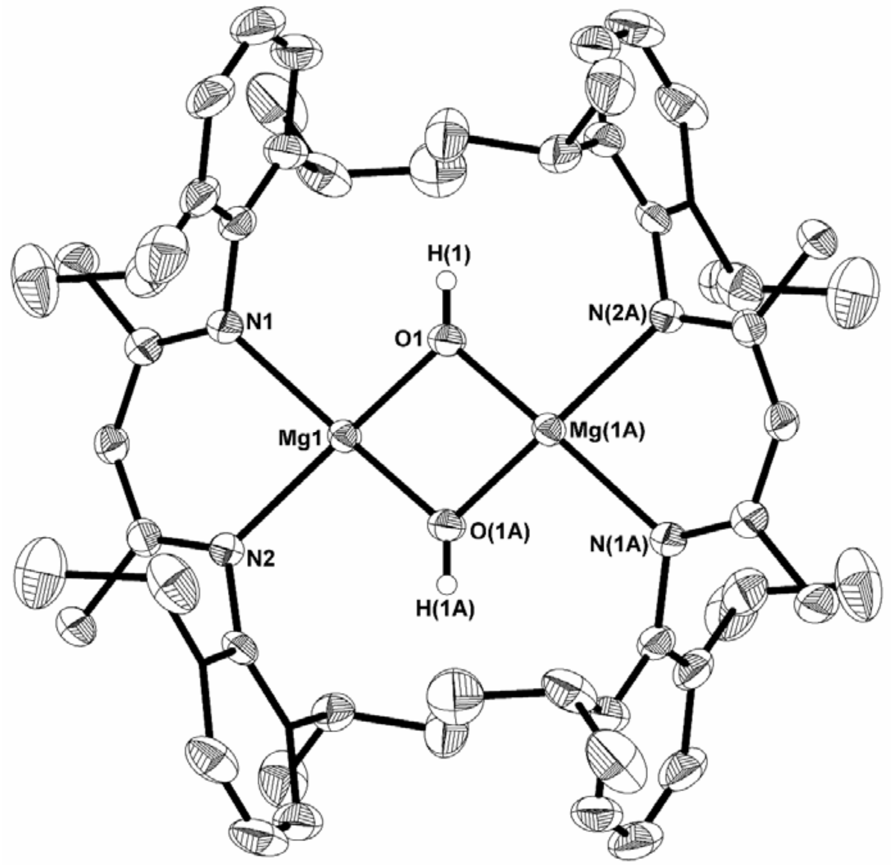

Figure 2. Molecular crystal structure of [LMg(OH)·THF]$_2$ (**1**). Thermal ellipsoids are shown with 40% probability. All hydrogen atoms (except Mg–OH) and two THF molecules are omitted for clarity. Selected bond lengths [Å] and bond angles [°]: Mg(1)–O(1) 1.983(18), Mg(1A)–O(1) 1.983(18), Mg(1)–Mg(1A) 3.112(14), Mg(1)–N(1) 2.167(2), Mg(1)–O(30) 2.095(18); O(1)–

Mg(1)–O(1A) 76.63(9), N(1)–Mg–N(2) 86.14(8), O(30)–Mg(1)–N(1) 96.36(8), Mg(1)–O(1)–Mg(1A) 103.37(9).

2.2. Hydrolysis of LCaN(SiMe$_3$)$_2$·THF and X-ray crystal structure of [LCa(OH)·THF]$_2$ (2)

A clean reaction of LCaN(SiMe$_3$)$_2$·THF[65] (L = CH{(CMe)(2,6-*i*Pr$_2$C$_6$H$_3$N)}$_2$) with water in THF results in the elimination of HN(SiMe$_3$)$_2$ and the formation of [LCa(OH)·THF]$_2$ (**2**) (Scheme 3). Compound **2** is a white solid soluble in benzene, toluene, and THF. It was characterized by IR, ^{1}H and ^{13}C NMR spectroscopy, EI mass spectrometry, elemental analysis, and X-ray structural analysis. In the IR spectrum a sharp absorption around 3698 cm^{-1} can be attributed to the O–H stretching frequency. The ^{1}H NMR spectrum of **2** exhibits a resonance at –0.79 ppm for the CaO–H. The chemical shifts of selected hydroxides with terminal and bridging OH functionalities are given in Table 1. Moreover, no molecular ion of **2** was detected in the EI mass spectrum; only small fragment ions are found.

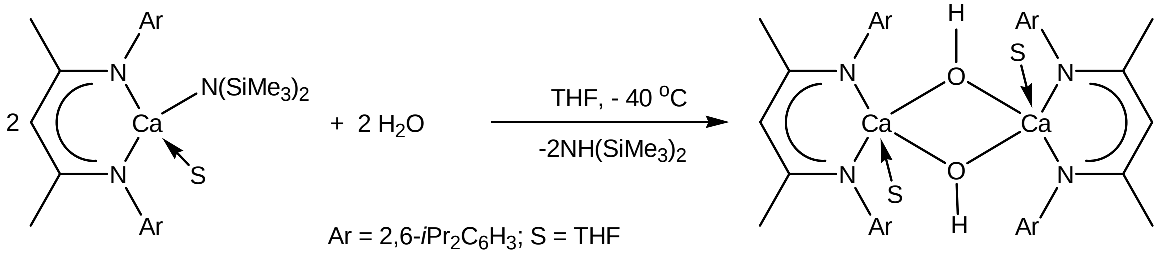

2

Scheme 3. Synthesis of β−diketiminate supported calcium hydroxide.

Metal hydroxide complexes	^{1}H NMR chemical shifts δ (ppm)
[LGe(OH)][16]	1.54
[LAlMe(OH)][30]	0.53
[LAl$(OH)_2$][44]	0.22
[LGaMe(OH)][46]	0.08
[LGa$(OH)_2$][45]	–0.27
[LMg(OH)·THF]	–0.46
[LCa(OH)·THF]	–0.78
[Cp^*_2ZrMe(OH)][92]	4.20

[a] L = CH{(CMe)(2,6-iPr$_2$C$_6$H$_3$N)}$_2$, Cp* = C_5Me_5

Table 1. ^{1}H NMR chemical shifts for the OH functionality in various metal hydroxide complexes.[a]

The molecular structure of [LCa(OH)·THF]$_2$ has been determined by single crystal X-ray diffraction (Figure 3), demonstrating that the complex consists of a hydroxide bridged dimer in the solid state. Single crystals of **2** suitable for X-ray structural analysis were obtained from hot toluene and small amounts of THF solution at 0 °C within 12 h. Compound **2** crystallizes in the triclinic space group $P\bar{1}$, with one half dimer in the asymmetric unit. The coordination geometry around the metal center is a distorted square-pyramid, with the O atom of the THF moiety at the apex and N(1), N(2), O(1) and O(1A) forming the square base. The central Ca_2O_2 four-membered ring is planar with a center of symmetry.

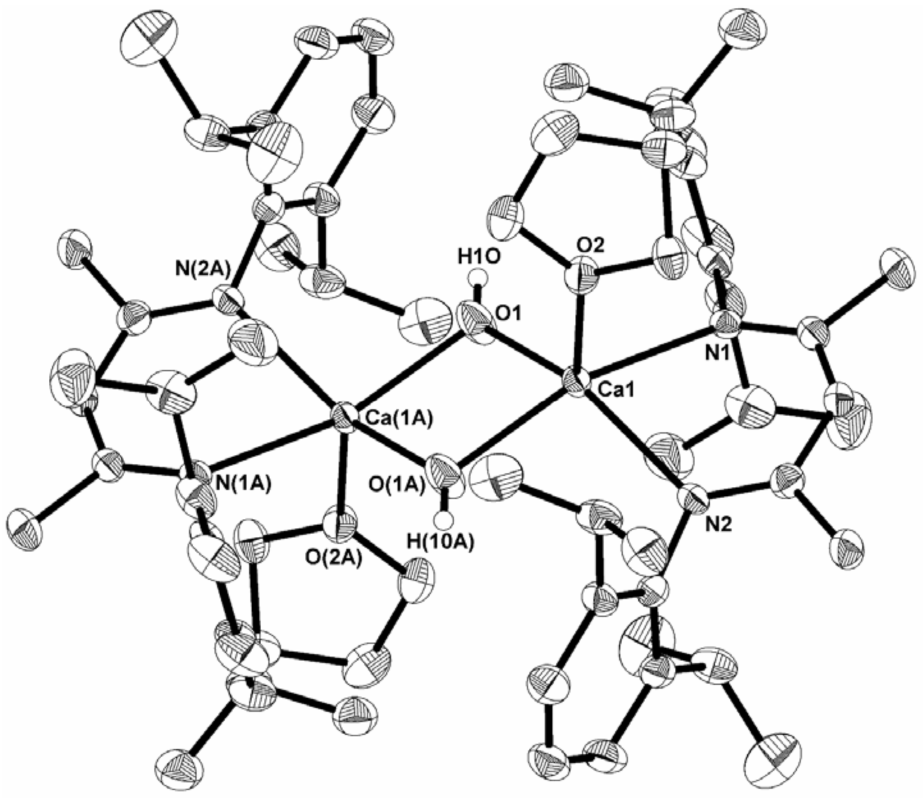

Figure 3. Molecular crystal structure of [LCa(OH)·THF]$_2$ (**2**). Thermal ellipsoids are shown with 50% probability. All hydrogen atoms are omitted for clarity (except Ca–OH). Selected bond lengths [Å] and bond angles [°]: H(1)–O(1) 0.741, Ca(1)–O(1) 2.221(3), Ca(1)–O(1A) 2.231(3), Ca(1A)–O(1) 2.231(3), Ca(1)–Ca(1A) 3.495(1), Ca(1)–N(1) 2.422(3), Ca(1)–O(2) 2.414(2); O(1)–Ca(1)–O(1A) 76.53(11), N(2)–Ca–N(1) 78.70(8), O(1)–Ca(1)–N(1) 96.03(9), O(2)–Ca(1)–N(1) 97.04(8), Ca(1)–O(1)–Ca(1A) 103.47(11), O(1)–Ca(1)–O(2) 111.15(10).

A noteworthy feature of compound **2** is the Ca–OH moiety (Ca–O 2.221(3), O–H 0.741 Å). The Ca–O bond distances are in the range of 2.221(3) to 2.231(3) Å, and thus considerably longer than the Mg–O bond distances observed in {[Tp $^{\mathrm{Ar,Me}}$]-Mg(μ-OH}$_2$ (Tp = tris (pyrazolyl)hydroborato, Ar = p-$_{t\mathrm{Bu}}$(C$_6$H$_4$))[47] 1.951(6) Å and [LMg(OH)·THF]$_2$·4THF **1**[48]

1.9878(17) Å. The Ca–N bond lengths (2.419(2) and 2.422(3) Å) are longer than the Mg–N bond distance of 2.1688(18) Å in **1** and the N(2)–Ca–N(1) bond angle of 78.70(8)° is sharper compared to the angle of N–Mg–N (86.11(10))°. However, the Ca–O and Ca–N bond distances 2.221(3) and 2.419(2) Å respectively are in good agreement with those in $\text{Tp}^{t\text{Bu}}\text{Ca(O-2,6-}i\text{Pr}_2\text{C}_6\text{H}_3)$ (2.106 (1), 2.412 (1) Å).[65]

2.3. Reaction of $\mathbf{L^IH}$ with MeMgCl and X-ray crystal structure of $\mathbf{[L^IMg(Cl)]}$ (3)

Monomeric $\text{L}^\text{I}\text{MgCl}$ can function as an interesting precursor for the preparation of a low valent metal complex. A clean reaction of $\text{L}^\text{I}\text{H}$[142] ($\text{L}^\text{I} = \text{CH\{Et}_2\text{NCH}_2\text{CH}_2\text{N(CMe)\}}_2$) with MeMgCl in diethlylether at –78 °C leads to the evolution of methane gas, and the formation of compound $\text{L}^\text{I}\text{MgCl}$ (**3**) (Scheme 4). Compound **3** is a white solid and melts at 158-162 °C. It was characterized by ^{1}H NMR spectroscopy, EI mass spectrometry, elemental analysis, and X-ray crystal structure analysis. The ^{1}H NMR spectrum of **3** exhibits a resonance at 4.74 ppm for the γ-H proton. The other chemical shifts are typical for the ligand L^I. Moreover, molecular ion of **3** was detected at *m/z* 354.

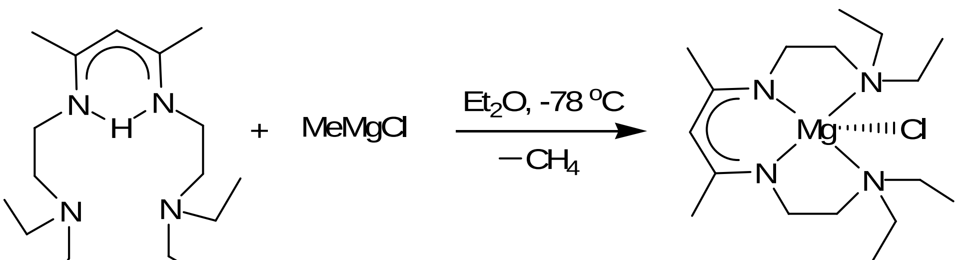

Scheme 4. Preparation of *β*-diketiminate magnesium chloride.

Single crystals of **3** suitable for X-ray structural analysis were obtained from toluene with a small amount of THF solution. The molecular structure of **3** is shown in Figure 4.

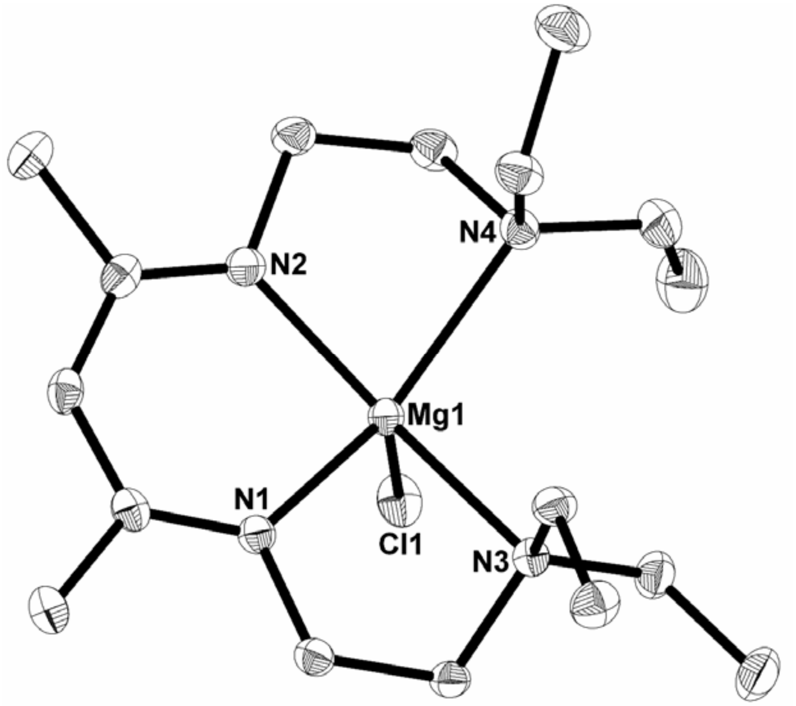

Figure 4. Molecular crystal structure of compound L^IMgCl (**3**); Thermal ellipsoids are shown with 50% probability. All hydrogen atoms are omitted for clarity. Selected bond lengths [Å] and bond angles [°]: Mg(1)–N(1) 2.0834(11), Mg(1)–N(2) 2.0815(11), Mg(1)–N(3) 2.2852(11), Mg(1)–N(4) 2.3295(11), Mg(1)–Cl(1) 2.3605(5); N(2)–Mg(1)–N(1) 88.16(4), N(2)–Mg(1)–Cl(1) 109.47(3), N(1)–Mg(1)–Cl(1) 109.19(3), N(4)–Mg(1)–Cl(1) 105.25(3), N(3)–Mg(1)–Cl(1) 99.52(3), N(3)–Mg(1)–N(4) 97.51(4), N(2)–Mg(1)–N(4) 78.47(4), N(1)–Mg(1)–N(3) 78.96(4).

Compound **3** crystallizes in the monoclinic space group $P2_1/c$ with one molecule in the asymmetric unit and half a molecule of disordered toluene located on a crystallographic inversion center. The central core of this structure is MgN_4Cl. The magnesium atom is surrounded by four nitrogen atoms of the monoanionic *β*-diketiminate ligand, and an axial chlorine atom. So, the magnesium atom is penta coordinate and the coordination geometry around the metal center is distorted square pyramidal.

The Mg–Cl bond distance 2.3605(5)Å is shorter than that found in LMgI·OEt_2 (2.6886(13) Å),[74] and [LFe(μ-$Cl)_2$]Mg$(THF)_4$ (2.5201(9)Å).[143] The N(1)–Mg(1)–N(2) bond angle is compressed to 88.16(4)° due to the rigid ligand backbone, while the N(2)–Mg(1)–Cl(1) angle opens up to 109.47°. The bond angle of N(2)–Mg(1)–N(1) is 88.16(4)°, which is sharper than the angle found in LMgI·OEt_2 (93.1°).

2.4. Reaction of LCaN$(SiMe_3)_2$·THF with Me_3SnF and X-ray crystal structure of [LCa(F)·THF]$_2$ (4)

The first example of a soluble calcium monofluoride [LCa(F)·THF]$_2$ (L = CH{(CMe)(2,6-$i$$Pr_2C_6H_3N$)}$_2$) (**4**) is obtained from the reaction of LCaN$(SiMe_3)_2$·THF[65] with Me_3SnF[144] (Scheme 5). Compound **4** is a white solid, soluble in benzene, toluene, and THF. It was thoroughly characterized by ^{1}H, ^{13}C, and ^{19}F NMR spectroscopy, EI mass spectrometry, elemental analysis and X-ray structural analysis. The ^{1}H NMR of compound **4** shows a singlet at 4.72 ppm for the *γ*-C*H* protons and one septet (3.14 ppm) corresponding to the C*H* protons of the *i*Pr moieties. Also, the complete disappearance of the $SiMe_3$ resonance (0.20 ppm) of LCaN$(SiMe_3)_2$·THF clearly indicates the formation of compound **4**. The ^{19}F NMR of **4** exhibits a singlet at –78 ppm. Moreover, no molecular ion peak of **4** was detected in the EI mass spectrum and only small fragment ions were found.

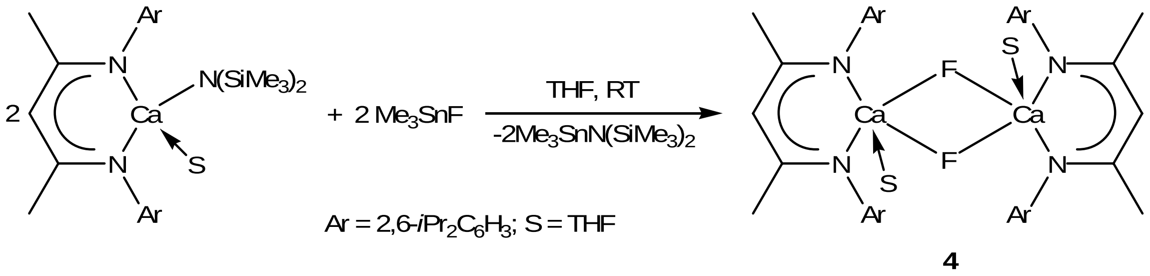

Scheme 5. Synthesis of a hydrocarbon-soluble calcium monofluoride.

The molecular structure of [LCa(F)·THF]$_2$ (**4**) has been determined by single crystal X-ray diffraction analysis (Figure 5) which demonstrates that the complex exists as a fluorine bridged dimer in the solid state. Single crystals of **4** suitable for X-ray structural analysis were obtained by slowly cooling the hot solution of **4** in toluene and THF (10:1) to 0 °C. Compound **4** crystallizes in the triclinic space group $P\bar{1}$, with one half dimer in the asymmetric unit. Each calcium atom is pentacoordinate and the coordination geometry around the metal center is distorted trigonalbipyramidal with the O atom of the THF molecule and one of the fluorine atoms occupying the axial positions. The equatorial sites are occupied by both the nitrogen atoms of the ligand L and also by the other fluorine atom. The dimeric nature of **4** results in the formation of three rings namely the central Ca_2F_2 four-membered ring and two adjacent C_3N_2Ca six-membered rings. The four-membered ring is perfectly planar, but the six-membered rings are puckered with a mean plane deviation of 0.191 Å (the deviation of the individual atoms from the mean plane defined by themselves are Ca1 0.033Å, N1 -0.305Å, C2 0.080Å, C3 0.346Å, C4 0.077Å, and N2 -0.305Å respectively). Also, the dihedral angle of 86.88° between the Ca_2F_2 four-membered ring and the C_3N_2Ca six-membered rings unequivocally indicates that the four- and six- membered rings are almost perpendicular to each other.

The average Ca–F bond distance of 2.170(2) Å is slightly shorter than the Ca–OH distance of 2.231 Å in [LCa(OH)·THF]$_2$·tol[145] (**2**) and considerably longer than the Mg–F distance of

1.9507(17) Å in the Mg-analogue of **4**.[146] The average Ca–N and Ca–O (THF) bond distances of 2.379 Å and 2.433 Å respectively, are longer than those of the Mg-analogue (ca. 2.147(2) Å and 2.078(2) Å). Finally the average Ca–F bond length of 2.170 Å is shorter than the Ca–F distance (2.366 Å) found in CaF_2.[147]

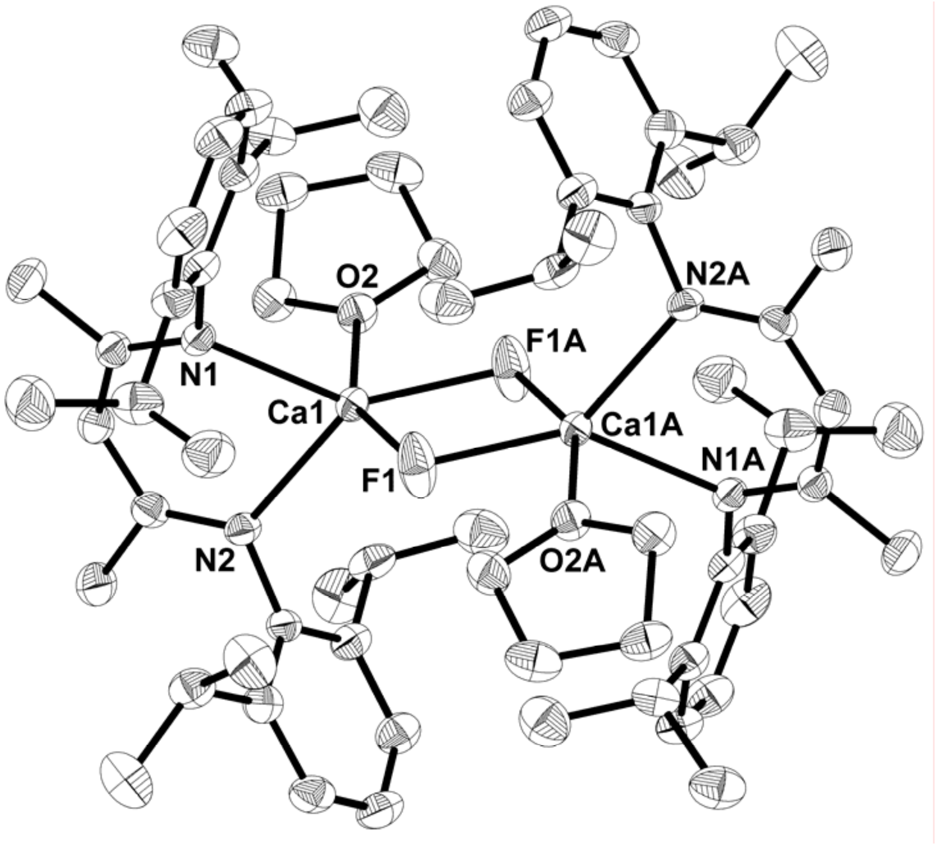

Figure 5. Molecular crystal structure of [LCa(F)·THF]$_2$ (**4**). Thermal ellipsoids are shown with 50% probability. All hydrogen atoms are omitted for clarity. Selected bond lengths [Å] and bond angles [°]: Ca(1)–F(1) 2.170(2), Ca(1)–F(1A) 2.189(2), Ca(1)–O(2) 2.433(2), Ca(1)–N(1) 2.379(2), Ca(1)–Ca(1A) 3.463(1); Ca(1)–F(1)–Ca(1A) 105.21(7), F(1)–Ca(1)–F(1A) 74.79(7), F(1)–Ca(1)–N(1) 102.45(7), F(1)–Ca(1)–O(2) 154.27(6).

2.5. The application of soluble calcium derivatives for surface coating

To test the feasibility of obtaining CaF_2 coatings *in situ* from **4** its reaction with a toluene solution of HF•pyridine on a pure unpolished silicon surface has been investigated (see dip-coating experiments) (Scheme 6, eq 1). A SEM micrograph of an unpolished pure silicon substrate before and after dip-coating with **3** is shown in Figure 6. The SEM micrograph after the dip-coating clearly reveals the formation of CaF_2 coatings. Furthermore, the Energy-Dispersive X-ray spectroscopic (EDX) analysis (Figure 6) confirms the existence of CaF_2 on the surface of the substrate by showing distinct lines for both Ca and F respectively. Apart from the peaks for Si, Ca, and F in the EDX spectra one can also see the peaks for C and O. This may be due to the presence of toluene insoluble organic impurities formed during the fluorination reaction and/or due to the presence of trapped THF even after overnight drying at room temperature of the CaF_2 coatings.

$$[LCaF\cdot THF]_2 + 2HF\cdot Py \longrightarrow 2CaF_2 + 2LH + 2Py + 2THF \quad (1)$$

$$[LCaN(SiMe_3)_2\cdot THF] + 2HF\cdot Py \longrightarrow CaF_2 + LH + NH(SiMe_3)_2 + 2Py \quad (2)$$

$$Ca[N(SiMe_3)_2]_2\cdot 2THF + 2HF\cdot Py \longrightarrow CaF_2 + 2NH(SiMe_3)_2 + 2Py + 2THF \quad (3)$$

$$LCaL + 2HF\cdot Py \longrightarrow CaF_2 + 2LH + 2Py \quad (4)$$

$$[LCaOH\cdot THF]_2 + 4HF\cdot Py \longrightarrow 2CaF_2 + 2LH + 2H_2O + 4Py + 2THF \quad (5)$$

$(L = CH\{(CMe)(2,6\text{-}i Pr_2C_6H_3N)\}_2)$

Scheme 6. Reactions of HF·pyridine with the soluble calcium derivatives.

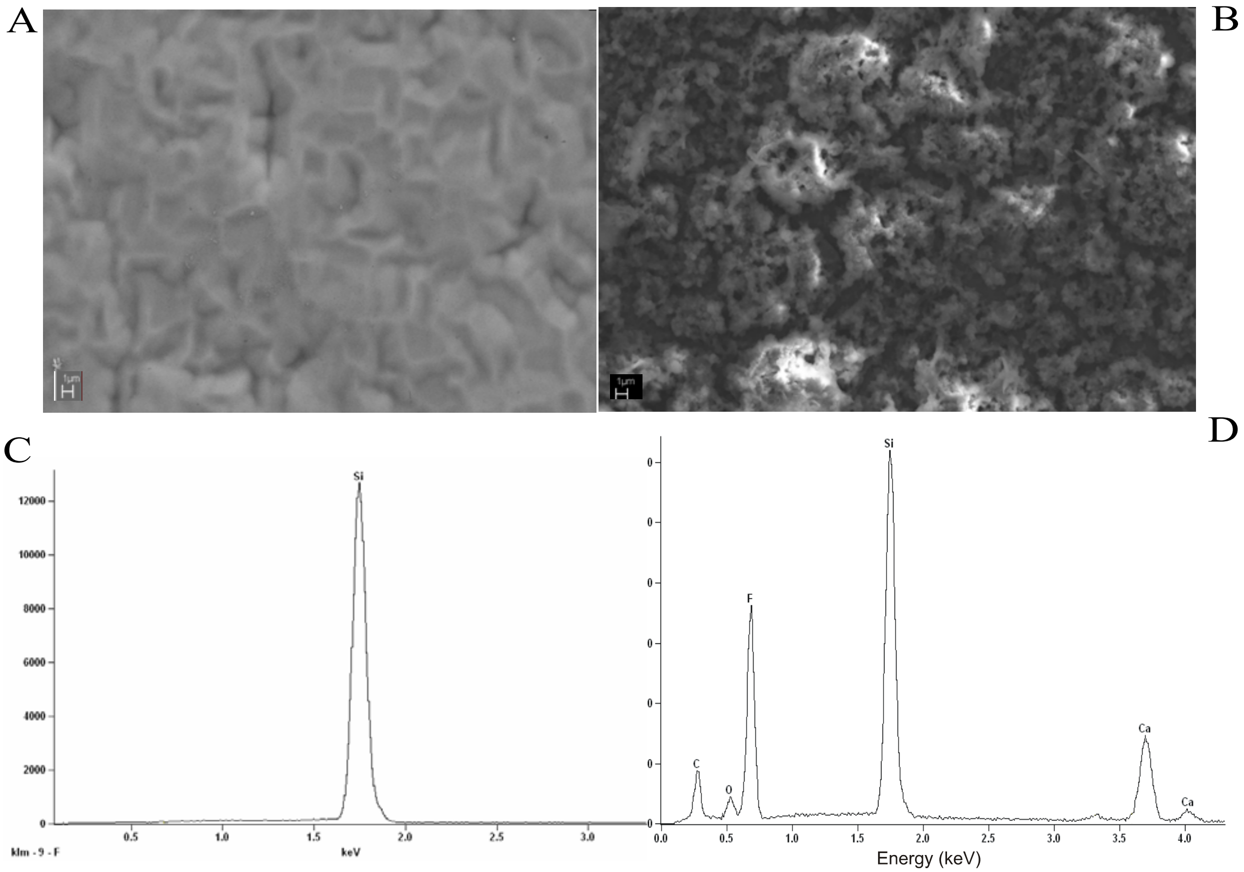

Figure 6. SEM micrograph for a pure silicon substrate before (**A**) and after (**B**) dip-coating with $[LCa(F){\cdot}THF]_2$ (**3**) and an EDX spectra of pure silicon substrate (**C**) and CaF_2 coating (**D**) obtained from **3**.

The scanning electron microscope (SEM) is a type of electron microscope capable of producing high-resolution images of a sample surface. A SEM is essentially a high magnification microscope, which uses a focussed scanned electron beam to produce images of the sample, both top-down and, with the necessary sample preparation, cross-sections. A basic knowledge of the principles of an EDX is useful for interpretation and evaluation of energy dispersive spectra. Electron-hole pairs are created by high eV incoming X-rays on semiconducting Si.

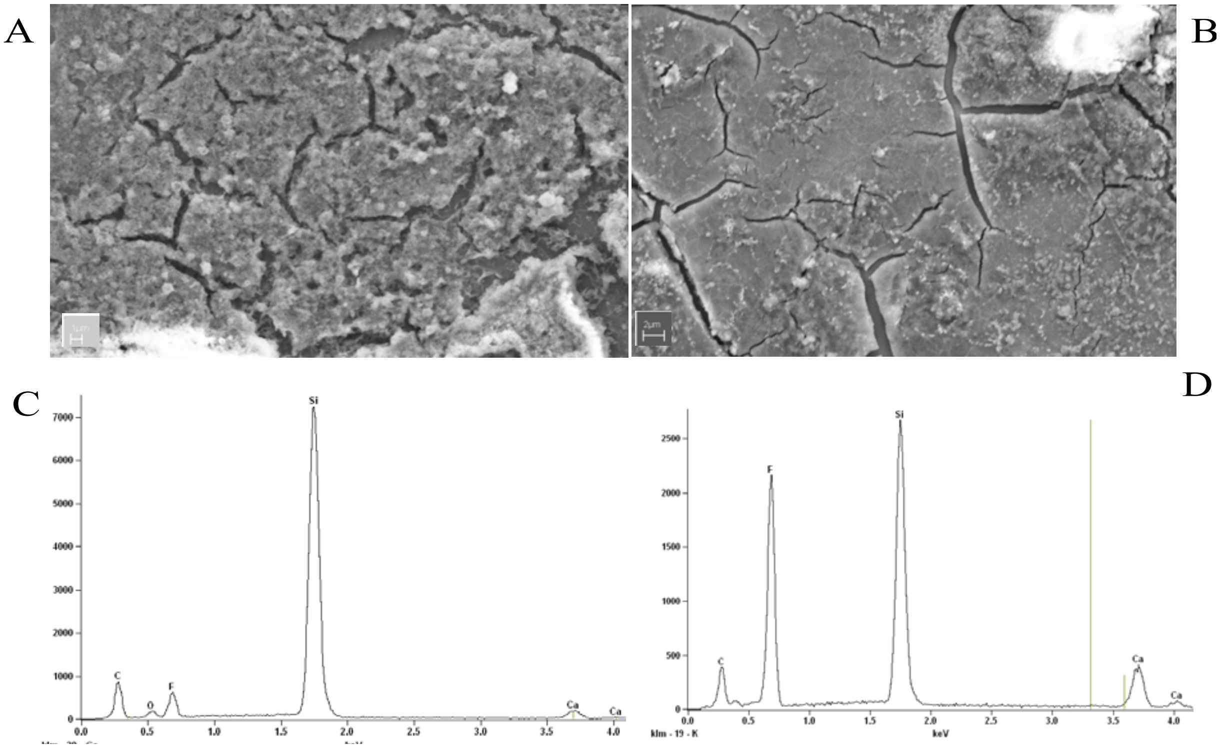

Figure 7. SEM micrograph (**A**) and an EDX (**C**) for the CaF_2 deposited on a pure silicon substrate starting from $LCaN(SiMe_3)_2·THF$ and SEM micrograph (**B**) and an EDX (**D**) for the CaF_2 deposited on a pure silicon substrate starting from $Ca\{N(SiMe_3)_2\}_2·2THF$.

In view of this interesting result, the utility has been further investigated other hydrocarbon-soluble calcium precursors such as $LCaN(SiMe_3)_2·THF$,[65] $Ca\{N(SiMe_3)_2\}_2·2THF$,[148] LCaL [149] and **2**[145] for obtaining CaF_2 coatings (Scheme 6; eq 2 – 5). The SEM and EDX analyses (Figures 7, 8) reveal that the above mentioned precursors are also amenable for the preparation of CaF_2 coatings. From these studies it appears that further soluble calcium precursors may lead to the formation of CaF_2 coatings when treated with a suitable fluoride source.

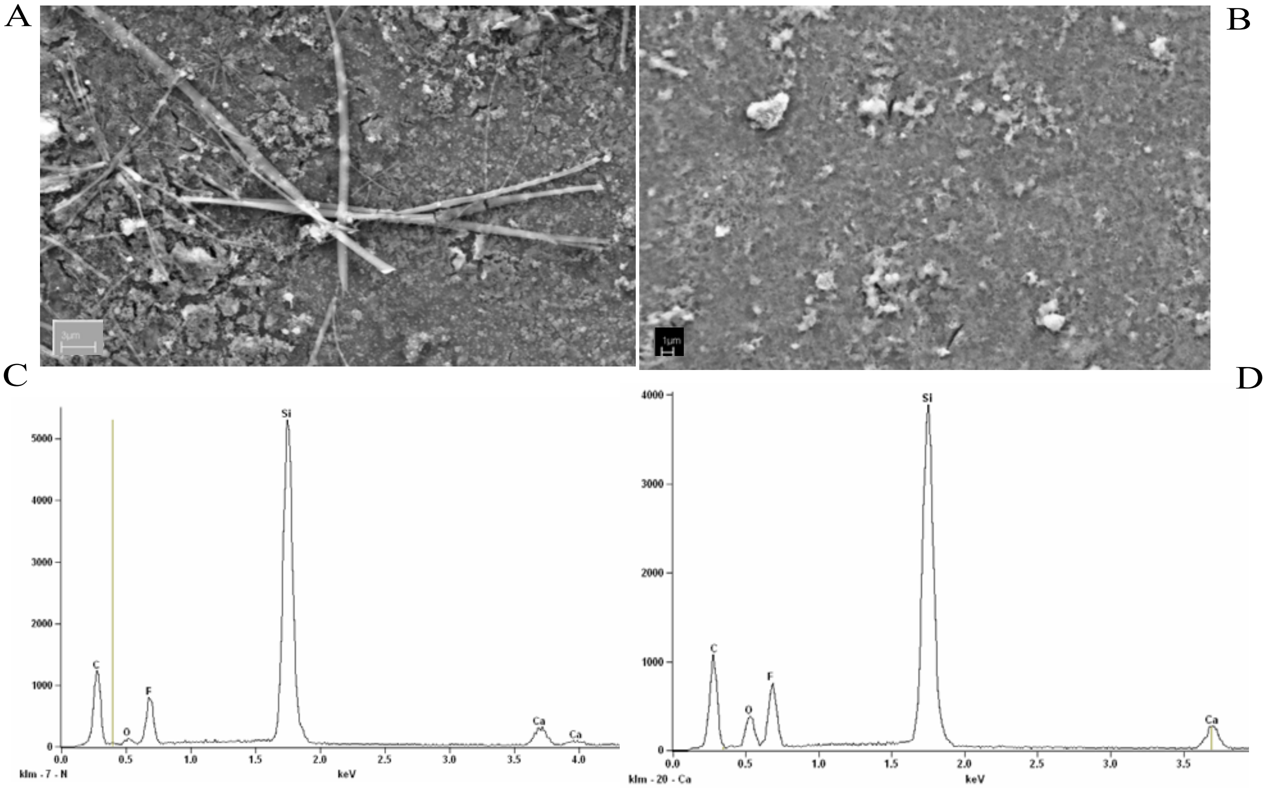

Figure 8. SEM micrograph (**A**) and an EDX (**C**) for the CaF_2 deposited on a pure silicon substrate starting from LCaL and SEM micrograph (**B**) and an EDX (**D**) for the CaF_2 deposited on a pure silicon substrate starting from $[LCa(OH)\cdot THF]_2$ (**2**).

2.6. Reaction of LAl(Me)OH with $Mg\{N(SiMe_3)_2\}_2$ and X-ray crystal structure of $[L(Me)Al–O–Mg(THF)_2–N(SiMe_3)_2]$ (5)

The reaction of $Mg\{N(SiMe_3)_2\}_2$[150-151] with a stoichiometric amount of LAl(Me)OH (L = $CH\{(CMe)(2,6\text{-}i Pr_2C_6H_3N)\}_2$[30] in THF/*n*-hexane (1:1) at 0 °C results in the elimination of $HN(SiMe_3)_2$ and the formation of the heterobimetallic compound $[L(Me)Al–O–Mg(THF)_2–O–N(SiMe_3)_2]$ (**5**) in high yield (Scheme 7). Compound **5** is soluble in pentane, hexane, benzene, toluene, and THF. It was characterized by ^1H, ^{13}C, and ^{29}Si NMR, IR spectroscopy, EI mass spectrometry, elemental analysis, and X-ray structural analysis. The ^{1}H NMR spectrum of **5** exhibits a resonance at –0.36 ppm for Al–*Me*, which by comparison with that of LAl(Me)OH (–0.88 ppm) clearly shows a downfield shift. The expected resonance for $SiMe_3$ is observed as a singlet (0.15 ppm). Finally no resonance was observed at 0.53 ppm which corresponds to AlO–H of the starting material LAl(Me)OH. The ^{29}Si NMR shows a signal at –9.8 ppm which is shifted to low field compared with that of $Mg\{N(SiMe_3)_2\}_2$ (–12.6 ppm).[152] Moreover, no molecular ion of **5** was detected in the EI mass spectrum. Only small fragment ions were found.

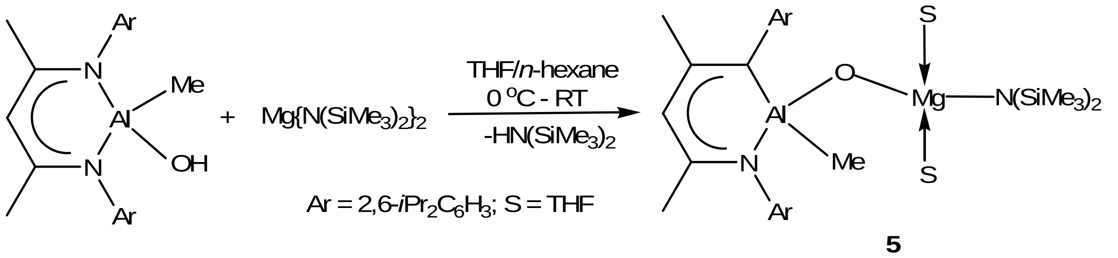

5

Scheme 7. Preparation of aluminum-magnesium oxide.

Crystals of **5** suitable for X-ray structural analysis were obtained from a *n*-pentane/THF solution at 0 °C. Compound **5** crystallizes in the monoclinic space group $P2_1/n$. The molecular structure is shown in Figure 9. The X-ray structural analysis of **5** revealed that the magnesium is bonded through a bridging oxygen atom to an aluminum atom. The geometry around the magnesium, as well as that of the aluminum, is tetrahedrally distorted. The Mg–O bond distances (1.850-2.095 Å) are consistent with the Mg–O bond lengths compiled by Holloway and Melnik for compounds of magnesium with the coordination number 4 at the magnesium (1.819-2.219 Å)[153] The Mg(1)–O(1)–Al(1) bond angle (157.1(1)°) is much wider compared to that in the alkoxy bridged $[Al_3Mg_3(\mu_3\text{-}O)(THFFO)_4Cl_4(Me)_5(THF)]$ (THFFO = 2-tetrahydrofurfuroxide) compound (Al–μ-$O_{(alkoxide)}$-Mg (128.2(2)°)).[102] The Al–C and Al–O bond distances are 1.975(2) and 1.682(2) Å respectively, which are in good agreement with those observed in $[OCMeCHCMeNAr]_2AlMe$

(Ar = 2,6-*i*$Pr_2C_6H_3$) (Al–C = 1.975(2)Å) and $[HC(CMeNMe)_2AlCl]_2(\mu\text{-}O)$ (Al–O = 1.677(2) Å).[154-155]

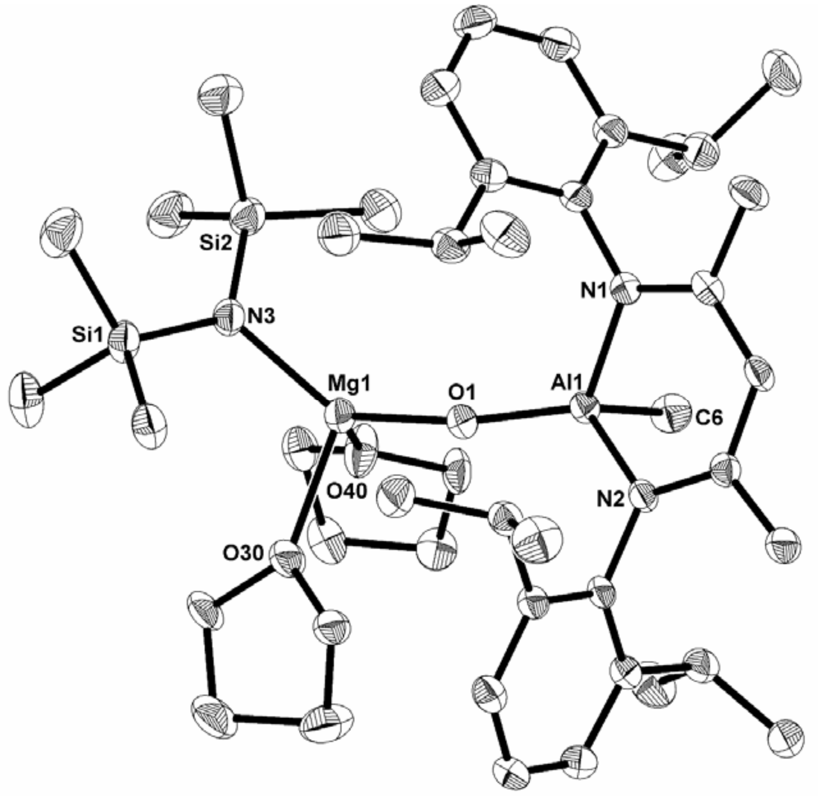

Figure 9. Molecular crystal structure of $[L(Me)Al–O–Mg(THF)_2–O–N(SiMe_3)_2]$ (**5**). Thermal ellipsoids are shown with 50% probability. All hydrogen atoms are omitted for clarity. Selected bond lengths [Å] and bond angles [°]: Mg(1)–O(1) 1.850(2), Mg(1)–O(30) 2.094(2), Mg(1)–O(40) 2.070(2), Mg(1)–N(3) 2.019(2), O(1)–Al(1) 1.682(2), Al(1)–C(6) 1.975(2); Mg(1)–O(1)–Al(1) 157.1(1), O(40)–Mg(1)–O(30) 88.4(1), O(1)–Al(1)–C(6) 120.6(1), Si(1)–N(3)–Si(2) 125.1(1).

2.7. Reaction of LAl(Me)OH (2 eqv) with Mg{N(SiMe$_3$)$_2$}$_2$ and X-ray crystal structure of [L(Me)Al–O–Mg(THF)$_2$–O–Al(Me)L] (6)

The reaction of one equivalent of Mg{N(SiMe$_3$)$_2$}$_2$[150-151] and two equivalents of LAl(Me)OH[30] in THF/*n*-hexane (1:1) at 0 °C results in the elimination of HN(SiMe$_3$)$_2$ and the formation of L(Me)Al–O–Mg(THF)$_2$–O–Al(Me)L (**6**) (Scheme 8). Compound **6** is soluble in hexane, benzene, toluene, and THF. It was characterized by ^{1}H, ^{13}C, and ^{27}Al NMR, IR spectroscopy, EI mass spectrometry, elemental analysis, and X-ray structural analysis. The ^{1}H NMR spectrum of **6** shows a single resonance for the Al–*Me* (–0.66 ppm). The proton resonances of the starting material Mg{N(SiMe$_3$)$_2$}$_2$ and AlO–H of LAl(Me)OH were not detected anymore. Moreover, the ^{27}Al NMR for **6** was silent, obviously due to the quadrupole moment of the aluminum atom.

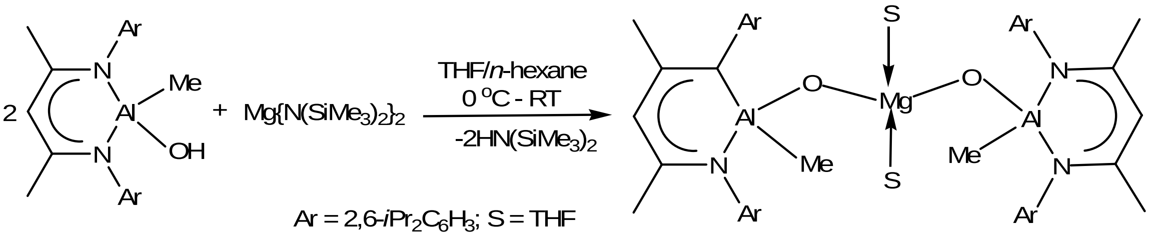

6

Scheme 8. Preparation of *β*-diketiminate aluminum-magnesium oxide.

Single crystals of **6** suitable for X-ray structural analysis were obtained from a *n*-hexane/THF solution at 0 °C. Compound **6** crystallizes in the monoclinic space group $P2_1/c$. The molecular structure is shown in Figure 10. The magnesium atom in **6** is four coordinate and surrounded by two THF molecules and two μ-O bonded oxygen resulting in a distorted tetrahedral environment. The bond distances of Mg–O (1.858-2.089 Å) are in agreement with those found in **5** (1.850-2.094 Å).

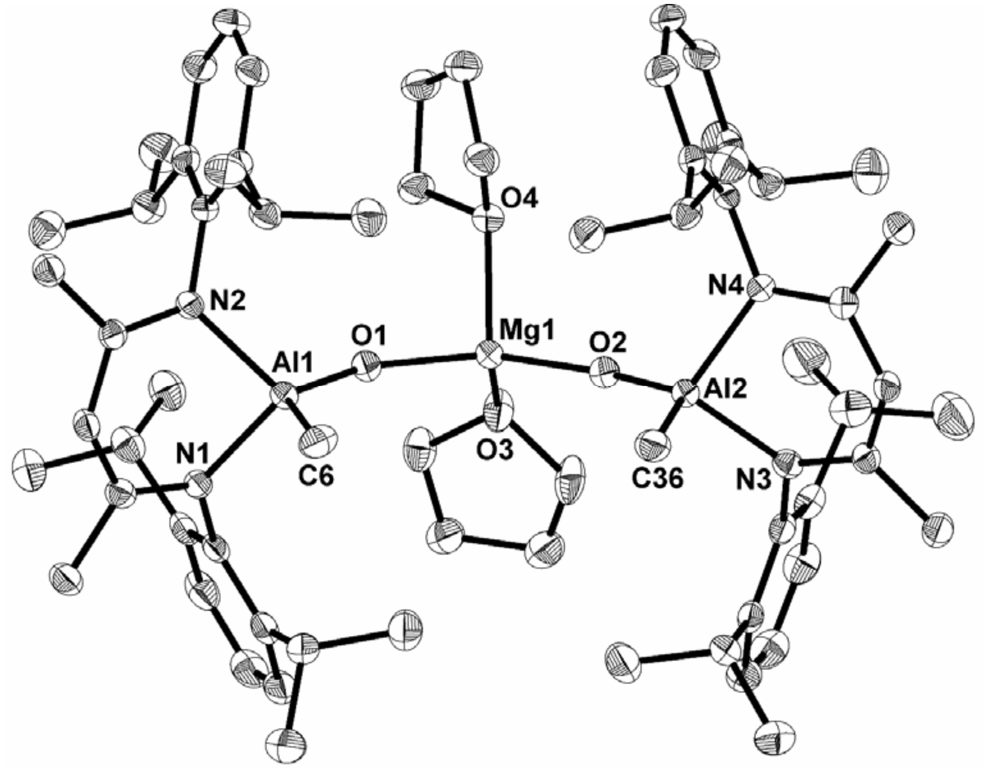

Figure 10. Molecular crystal structure of L(Me)Al–O–Mg(THF)$_2$–O–Al(Me)L (**6**). Thermal ellipsoids are shown with 50% probability. All hydrogen atoms are omitted for clarity. Selected bond lengths [Å] and bond angles [°]: Al(1)–O(1) 1.671(2), O(1)–Mg(1) 1.873(2), Mg(1)–O(2) 1.858(2), O(3)–Mg(1) 2.043(2), O(4)–Mg(1) 2.089(2), O(2)–Al(2) 1.671(2), Al(1)–C(6) 1.971(3), Al(2)–C(36) 1.980(3); Al(1)–O(1)–Mg(1) 150.2(1), Al(2)–O(2)–Mg(1) 159.6(1), O(2)–Mg(1)–O(1) 142.4(1), O(3)–Mg(1)–O(4) 99.8(1).

Compounds **5** and **6** were investigated by theoretical methods to obtain further information of their spectroscopic properties. The molecules were first fully optimized with the DFT-variant B3LYP[156,157] as implemented in the Gaussian G03[158] program-suite employing the 6-31G basis set.[159-162] Following this optimization the harmonic vibrational frequencies were calculated by using analytical second derivatives. The character of the vibrations was then determined through a normal mode analysis available in Gaussian G03. The resulting equilibrium structures agree very well with the experimental data available by X-ray crystallography. For compound **5** the calculated vibrations are clearly localized within the Mg–O–Al subunit. The calculated antisymmetric Mg–O–Al vibration (778.5 cm^{-1}) compares well with that found at 761 wave numbers in the IR spectrum. The deviation between the calculated and found values might be due to the coordination of two THF molecules in **5**. From the calculation of **6** three bands can be clearly assigned to isolated Mg–O–Al vibrations. The antisymmetric Mg–O–Al vibrations have calculated wavenumbers of 678.7 and 786.9 cm^{-1}. The symmetric Mg–O–Al vibration is calculated to 747.9 cm^{-1}. From the three modes (1015, 1030, and 1060 cm^{-1}) belonging to Mg–O vibrations, the band at 1030 cm^{-1} is the most intensive one and compares to that found in the IR spectrum (1021 cm^{-1}). The difference in wave numbers might be due to THF coordination.

2.8. Reaction of LAl(Me)OH with $LMgMe\cdot OEt_2$ or $LMgN(SiMe_3)_2$ and X-ray crystal structure of [LMg(THF)–O–Al(Me)L] (7·THF)

The synthesis of soluble molecular compounds with the Mg–O–Al moiety was further extended by using an unprecedented aluminum hydroxide LAl(Me)OH. The reaction of LAl(Me)OH[30] with a stoichiometric amount of $LMgMe\cdot OEt_2$[163-165] or $LMgN(SiMe_3)_2$[141] in toluene at reflux temperature, results in the formation of the compound LMg–O–Al(Me)L (**7**) in excellent yield (Scheme 9).

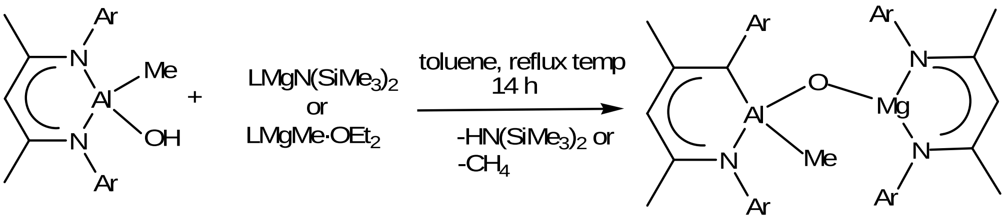

L= $CH(C(Me)NAr)_2$; Ar = 2,6-$iPr_2C_6H_3$

7

Scheme 9. Preparation of *β*-diketiminate aluminum-magnesium oxide.

Compound **7** is a colorless crystalline solid and melts in the range from 259 to 262 °C. It has been characterized by ^{1}H NMR, IR spectroscopy, elemental analysis, EI mass spectrometry, and X-ray structural analysis. The ^{1}H NMR spectrum of **7** exhibits the Al–*Me* to resonate at –1.42 ppm. The backbone protons of the ligand resonate at 4.82 and 4.92 ppm, respectively. Other resonances are typical for the *β*–diketiminate ligand. The EI mass spectrum of **7** revealed that the most intense peak appears at *m/z* 901 and corresponds to the loss of one methyl group from the molecular ion, [M^+ – Me].

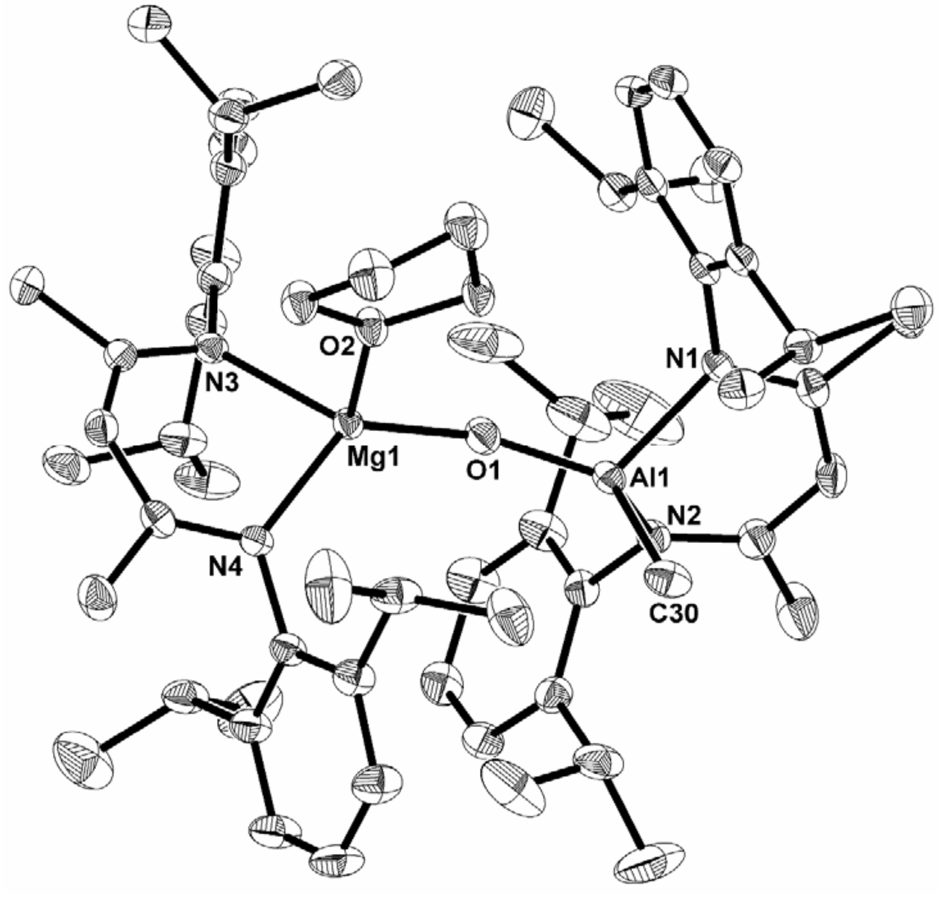

Figure 11. Molecular crystal structure of [L(Me)Al–O–Mg(THF)L] (**7·THF**). Thermal ellipsoids are shown with 50% probability. All hydrogen atoms are omitted for clarity. Selected bond

lengths [Å] and bond angles [°]: Mg(1)–O(1) 1.8572(14), Mg(1)–O(2) 2.0834(13), Mg(1)–N(3) 2.1033(16), Mg(1)–N(4) 2.0933(16), Al(1)–O(1) 1.6836(14), Al(1)–N(2) 1.9484(15), Al(1)–N(1) 1.9767(15), Al(1)–C(30) 1.982(2); Mg(1)–O(1)–Al(1) 157.62(9), O(1)–Al(1)–N(2) 117.64(7), O(1)–Al(1)–C(30) 120.46(8), N(1)–Al(1)–C(30) 102.35(7).

It was difficult to get X-ray quality crystals for compound **7·THF**, after several attempts crystals separated toluene and THF solution. The difficulty might be due to the close arrangement of the bulky *β*-diketiminate ligands. The asymmetric unit contains both the molecules **7·THF** and LAl(Me)OH. However, Crystals of **7·THF** suitable for X-ray structural analysis were obtained from toluene/THF solution at 0 °C. Compound **7·THF** crystallizes in the monoclinic space group *C2/c*. The X-ray crystal structure for compound **7·THF** is shown in Figure 11. The X-ray structural analysis of **7·THF** revealed that the magnesium is bonded through a bridging oxygen atom to an aluminum atom. Interestingly, the magnesium and aluminum atoms are each arranged in a C_3N_2M six-membered ring. The latter two six-membered rings are linked through an oxygen atom. The geometry around the magnesium, as well as that of the aluminum, is tetrahedrally distorted. The Mg–O bond distances (1.850-2.095 Å) are consistent with the Mg–O bond lengths in compounds **5** and **6** (1.854-2.085 Å).[166] The Mg(1)–O(1)–Al(1) bond angle (157.1(1)°) is almost the same as those found in compounds **5** and **6** (Mg–O–Al av bond angle (157.1°). The Al–C and Al–O bond distances are 1.982(2) and 1.6836(14) Å respectively, which are in good agreement with those observed in $[OCMeCHCMeNAr]_2AlMe$ (Ar = 2,6-iPr$_2$C$_6$H$_3$) (Al–C = 1.975(2)Å) and $[HC(CMeNMe)_2AlCl]_2(\mu\text{-}O)$ (Al–O = 1.677(2) Å).[154-155]

2.9. Reaction of LAl(Me)OH with Ca{N(SiMe$_3$)$_2$}$_2$·2THF and X-ray crystal structure of [{L^{II}Al(Me)}(μ-O)(Ca·THF)]$_2$ (8)

In this section the synthesis of a heteroalumoxane containing an oxide ion between the metal centers will be discussed. The synthesis of this unexpected molecule was achieved by the reaction of LAl(Me)OH[30] with a stoichiometric amount of Ca{N(SiMe$_3$)$_2$}$_2$·2THF[148], in THF/*n*-hexane solution at 0 °C, and results in compound [{L^{II}Al(Me)}(μ-O)(Ca·THF)]$_2$ [L^{II} = [HC{C(CH$_2$)}(CMe)(NAr)$_2$] (**8**) (Scheme 10). When LAl(Me)OH reacted with Ca{N(SiMe$_3$)$_2$}$_2$·2THF, compound [L(Me)Al–O–Ca(THF)$_2$–N(SiMe$_3$)$_2$] could be considered as intermediate. Then further deprotonation at one methyl group at the backbone of ligand **L** is occuring.

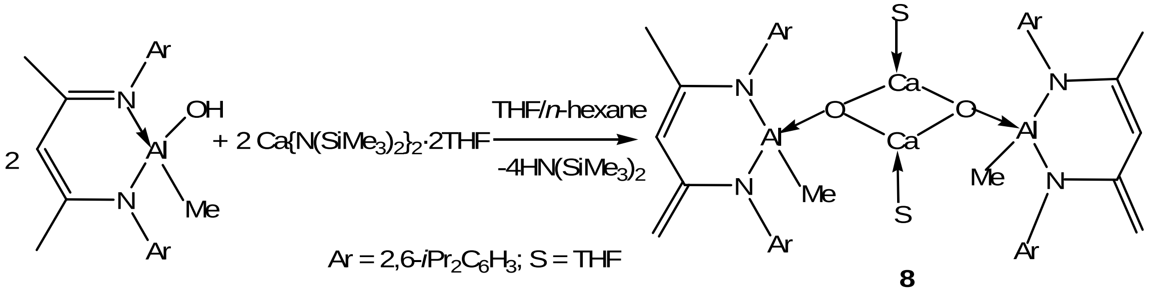

Scheme 10. Preparation of a calcium-aluminum oxide.

Compound **8** is a solid and melts under decomposition in the range from 228 to 230 °C. In the ^{1}H NMR spectrum of **8** the Al–*Me* resonates at –1.05 ppm. Also the proton resonance of the *β*-CH$_3$ group on the L^{II} ligand backbone (1.58 ppm) integrates for the six protons, while two other singlets are observed downfield (3.45 and 3.98 ppm) and integrate two protons each. The former corresponds to the normal CH$_3$-C group and the latter is assigned to the terminal CH$_2$=C group which gives rise to two nonequivalent protons due to the restricted rotation about the C=C double bond. The IR spectrum shows a band at 1619 cm^{-1} which can attributed to the C=C double bond. Moreover, no molecular ion of **8** was detected in the EI mass spectrum. Only small fragment ions were found.

Compound **8** represents the first example of a tetranuclear calcium oxide with a Ca_2O_2 core. Compound **8** was characterized by X-ray crystallographic analysis. The X-ray crystal structure along with selected bond distances and angles are shown in the Figures **12** and **13**.

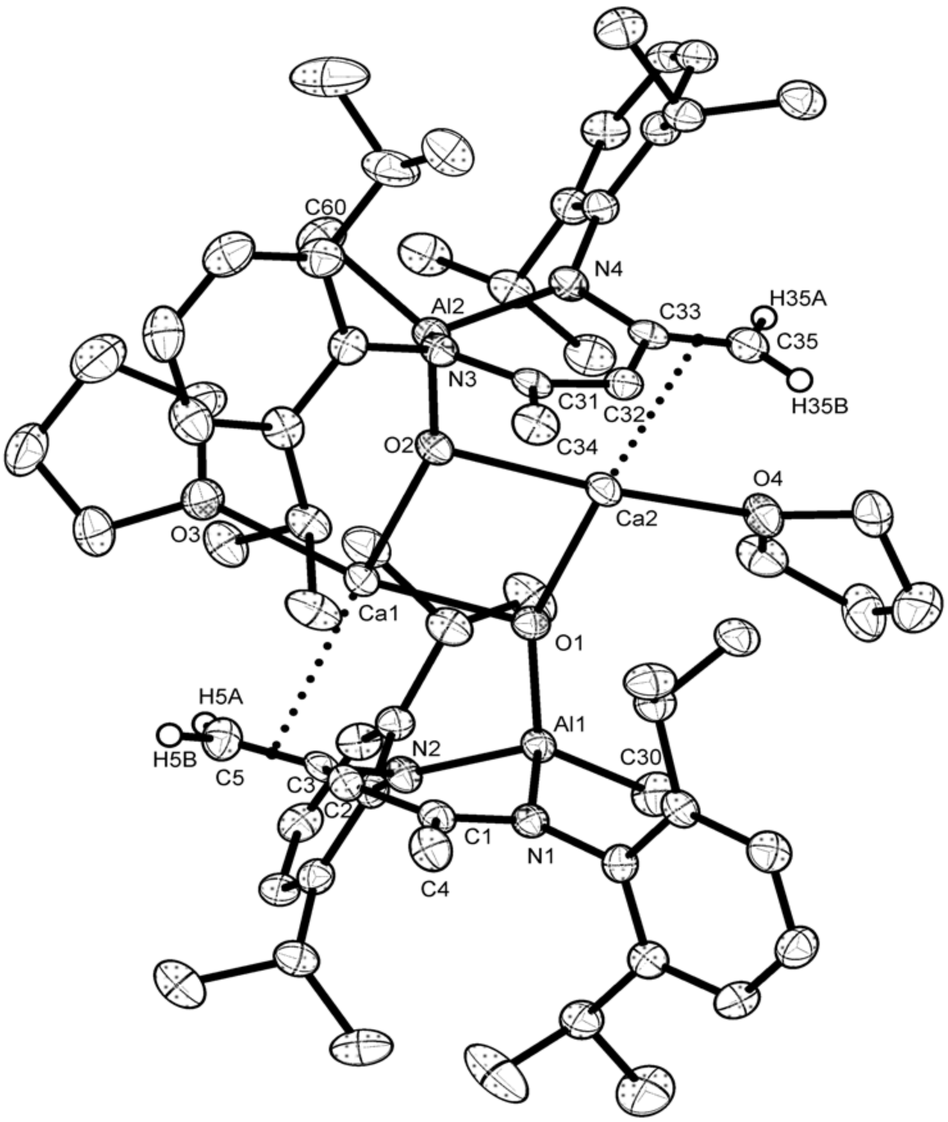

Figure 12. Molecular crystal structure of $[\{LAl(Me)\}(\mu\text{-}O)(Ca\cdot THF)]_2$ (**8**) Thermal ellipsoids are shown with 50% probability.

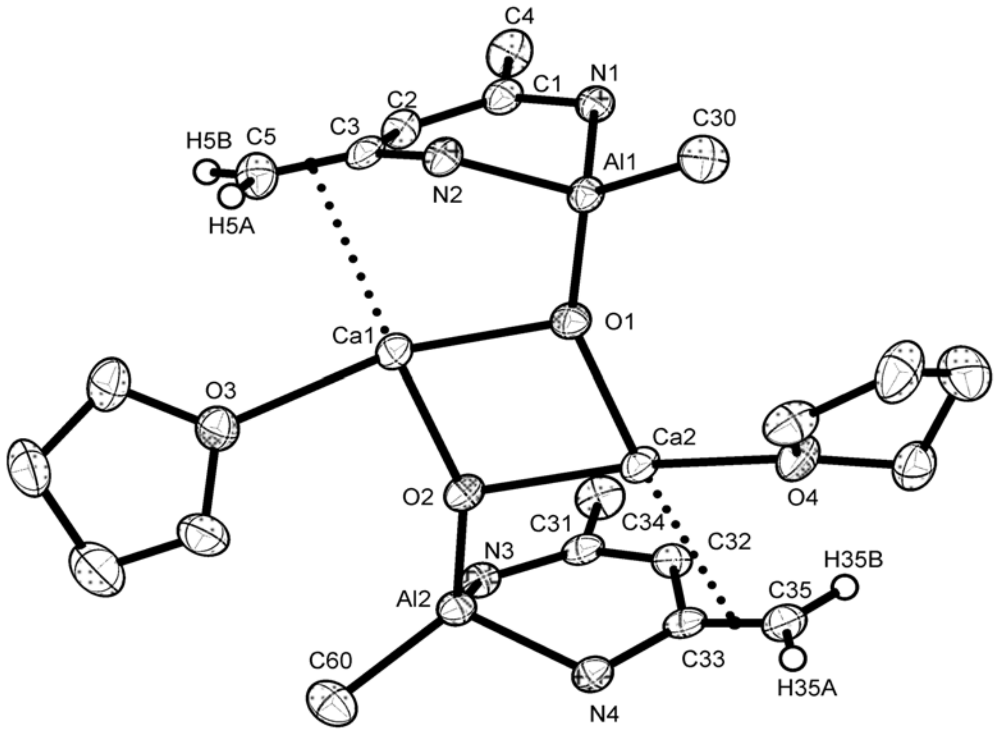

Figure 13. Core structure of compound [{LAl(Me)}(μ-O)(Ca·THF)]$_2$ (**8**); Thermal ellipsoids are shown with 50% probability. Selected bond lengths [Å] and bond angles [°]: Ca(1)–O(1) 2.255(2), Ca(1)–O(2) 2.179(2), Ca(1)–O(3) 2.414(3), Ca(2)–O(1) 2.170(2), Ca(2)–O(2) 2.262(2), Ca(2)–O(4) 2.436(3), Ca(2)–C(33) 2.696(3), Ca(2)–N(4) 2.991(3), Ca(1)–N(3) 2.679(3), Ca(1)–N(2) 3.103(3), Al(1)–O(1) 1.741(2), Al(1)–N(1) 1.898(3), Al(1)–N(2) 1.900(3), Al(1)–C(30) 1.959(4), Al(2)–O(2) 1.735(2), Al(2)–N(4) 1.899(3), Al(1)–C(60) 1.958(4), C(1)–C(4) 1.509(5), C(1)–C(2) 1.380(5), C(2)–C(3) 1.456(5), C(3)–C(5) 1.373(5), C(31)–C(34) 1.513(5), C(31)–C(32) 1.374(5), C(33)–C(35) 1.372(5), N(1)–C(1) 1.355(4), N(2)–C(3) 1.396(4); O(2)–Ca(1)–O(1) 82.45(9), O(2)–Ca(1)–O(3) 94.86(9), O(1)–Ca(2)–O(2) 82.47(9), O(1)–Ca(2)–O(4) 93.40(9), O(2)–Ca(2)–O(4) 157.85(9), O(1)–Ca(2)–C(33) 160.46(10), O(2)–Al(2)–N(4) 103.64(13), N(4)–Al(2)–N(3) 98.05(13), O(2)–Al(2)–C(60) 122.35(15), N(3)–Al(2)–C(60)

108.43(15), Al(1)–O(1)–Ca(2) 150.96(14), Al(1)–O(1)–Ca(1) 110.36(12), Ca(2)–O(1)–Ca(1) 97.73(9), Al(2)–O(2)–Ca(1) 153.27(14), Al(2)–O(2)–Ca(2) 109.47(12), Ca(1)–O(2)–Ca(2) 97.25(9).

Compound **8** crystallizes in the triclinic space group $P\bar{1}$ with two molecules in the asymmetric unit and two *n*-hexane molecules. The X-ray structure analysis reveals that **8** is a dimer of the [{LAl(Me)}(μ-O)(Ca·THF)] unit. The structure contains two terminal LAlMe units that are linked to a central [(Ca·THF)(μ-O)]$_2$ core. Both six-membered AlN_2C_3 rings are puckered and possess Al–N and Al–C bond distances shorter than those observed in compounds **5** and **6**. The alternative endocyclic C-C and C=C distances indicate little π conjugation. The aluminum atom is coordinated to a bridging oxygen atom, a methyl group, and two nitrogen atoms of the ligand. The geometry around the metal center is highly tetrahedrally distorted. Whereas the calcium atom is coordinated to two O, and one THF molecule. The geometry around the calcium atom is distorted square planar. In the ligand backbone, the terminal C–C bond lengths [C(2)–C(3) 1.456(5) Å, C(3)–C(5) 1.373(5) Å] are indicative of a single and double bond respectively, as are others within the backbone [C(1)–C(4) 1.509(5) Å, C(1)–C(2) 1.380(5) Å]. The adjacent N–C bond distances [N(1)–C(1) 1.355(4) Å, N(2)–C(3) 1.396(4) Å] are intermediate between N–C double and single bonds. The bond distance of Ca–O av 2.216 Å is in agreement with that found in [LCa(OH)·THF]$_2$[145] (**2**) (av 2.227 Å). The angle of O(1)–Ca(2)–O(2) 82.47(9)° is slightly wider than that observed in **2** (Ca(1)–O1(1A) 76.53 (9)°), Whereas the angle of Ca(2)–O(1)–Ca(1) 97.73(9)° is narrower than that found in **2** (Ca(1)–O(1)–Ca(1A) 103.47(11)°).

2.10. Reaction of LAl(Me)OH with LCaN(SiMe$_3$)$_2$·THF

The reaction of LAl(Me)OH[30] with a stoichiometric amount of LCaN(SiMe$_3$)$_2$·THF[65] in THF/*n*-hexane at –40 °C, results in the formation of compound LCa(THF)–O–Al(Me)L (**9**) in good yield (Scheme 11).

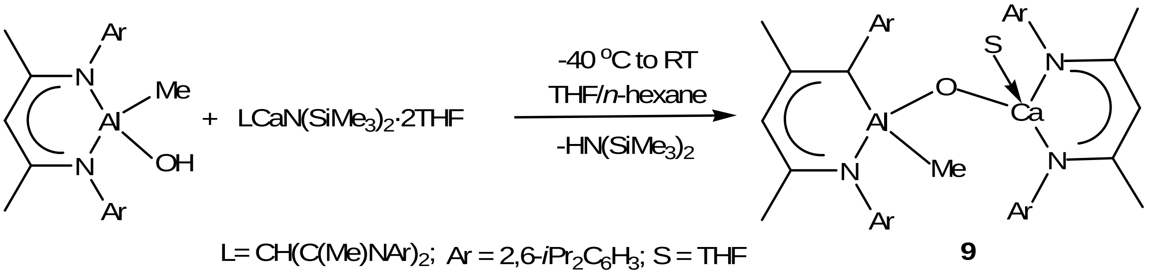

9

Scheme 11. Preparation of calcium-aluminum oxide.

Compound **9** is a colorless crystalline solid that melts in the range from 125 to 130 °C. It is highly soluble in a wide range of organic solvents. It has been characterized by ^{1}H NMR, IR spectroscopy, EI mass spectrometry, and elemental analysis. The ^{1}H NMR spectrum of **9** exhibits the Al–*Me* resonance at –1.09 ppm. The complete disappearance of the resonance at 0.53 ppm clearly indicates the deprotonation of Al–OH and the formation of compound **9**. Other resonances are typical for the *β*–diketiminate ligand. The EI mass spectrum of **9** exhibits peaks corresponding to the free ligand, L and its fragments.

2.11. Reaction of Cp*$_2$Zr(Me)OH (2 eqv) with Mg{N(SiMe$_3$)$_2$}$_2$ and X-ray crystal structure of [Cp*$_2$(Me)Zr–O–Mg(THF)$_2$–O–Zr(Me)Cp*$_2$] (10)

Two equivalents of Cp*$_2$Zr(Me)OH[92] reacted with one equivalent of Mg{N(SiMe$_3$)$_2$}$_2$[150,151] in toluene to result in the formation of compound [Cp*$_2$(Me)Zr–O–Mg(THF)$_2$–O–Zr(Me)Cp*$_2$] (**10**) (Scheme 12).

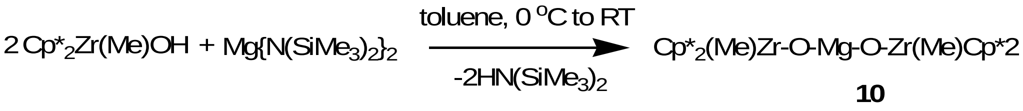

$$2\,Cp^*_2Zr(Me)OH + Mg\{N(SiMe_3)_2\}_2 \xrightarrow[-2HN(SiMe_3)_2]{\text{toluene, } 0\ ^oC \text{ to RT}} \underset{\mathbf{10}}{Cp^*_2(Me)Zr\text{-}O\text{-}Mg\text{-}O\text{-}Zr(Me)Cp^*2}$$

Scheme 12. Preparation of magnesium-zirconium oxide.

Compound **10** is a colorless crystalline solid and melts in the range of 162-165 °C. The ^{1}H NMR spectrum of **10** shows Zr–*Me* to resonate at –1.01 ppm and Cp**Me* at 1.89 ppm.The complete disappearance of the resonance at 4.2 ppm clearly indicates the deprotonation of Zr–OH and the formation of compound **10**.

The X-ray crystal structure along with selected bond distances and bond angles are shown in Figure 14.

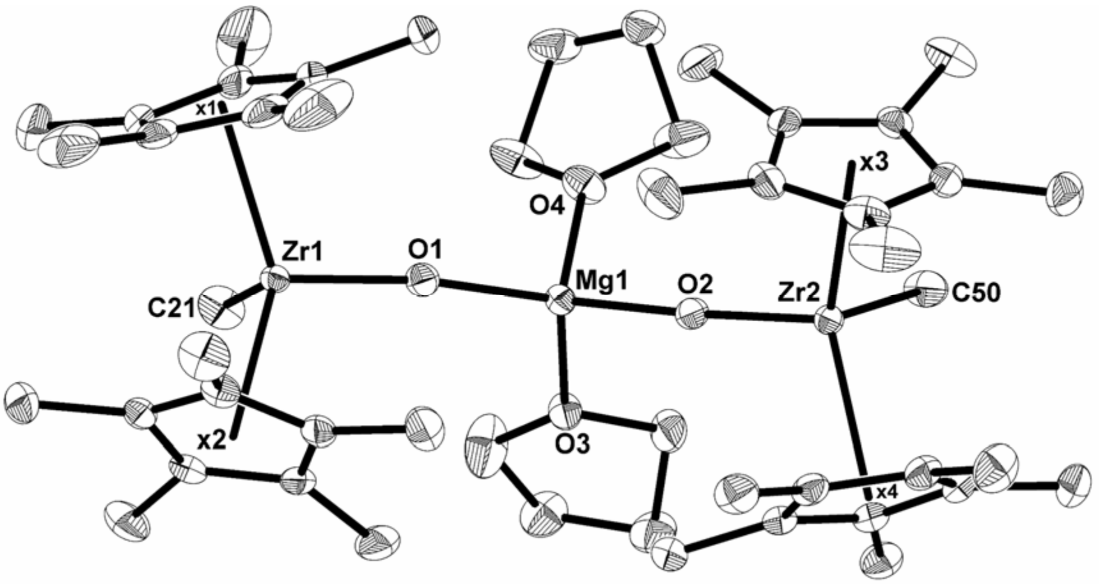

Figure 14. Molecular structure of compound [Cp*$_2$(Me)Zr–O–Mg(THF)$_2$–O–Zr(Me)Cp*$_2$] (**10**); Thermal ellipsoids are shown with 50% probability. All hydrogen atoms are omitted for clarity. Selected bond lengths [Å] and bond angles [°]: Mg(1)–O(1) 1.8837(14), Mg(1)–O(2) 1.8850(14), Mg(1)–O(3) 2.0633(13), Zr(1)–C(21) 2.3065(19), Zr(1)–C(50) 2.3109(19), x(1)–Zr(1) 2.326(1), x(2)–Zr(1) 2.319(1), x(3)–Zr(2) 2.316(1), x(4)–Zr(2) 2.330(1); O(1)–Zr(1)–C(21) 94.96(7), O(2)–Zr(2)–C(50) 97.27(7), Mg(1)–O(1)–Zr(1) 168.11(8), Mg(1)–O(2)–Zr(2) 175.35(8), O(1)–Mg(1)–O(2) 130.56(6), O(2)–Mg(1)–O(4) 105.30(6), O(1)–Mg(1)–O(3) 112.61(6), x(1)–Zr(1)–x(2) 132.04, x(1)–Zr(1)–O(1) 108.88, x(1)–Zr(1)–C(21) 103.22, x(4)–Zr(2)–x(3) 133.14, x(4)–Zr(2)–O(2) 108.5, x(4)–Zr(2)–C(50) 102.31; x = centroid of Cp* ring.

Single crystals suitable for X-ray measurement were grown in a toluene and THF solution at 0 °C. Compound **10** crystallizes with one molecule in the asymmetric unit. The central metal atom magnesium is coordinated to two THF molecules and two oxygen atoms. One THF molecule is disordered with a site occupation factor of 0.53. The geometry around the zirconium as well as around the magnesium is highly distorted tetrahedral. Interestingly, the bond distances of Mg(1)–O(1) and Mg(1)–O(2) (1.8837(14) Å and 1.8850(14) Å) respectively, are nearly the same, whereas the Mg(1)–O(1) and Mg(1)–O(2) bond lengths 1.8436(17) Å and 1.9005(17) Å are different in compound *vide supra* **14**. In the latter compound the bond distance Mg(1)–O(1) is shorter than Mg(1)–O(2), this might be due to the different radii of aluminum and zirconium. The bond angle of O(1)–Mg(1)–O(2) 130.56(6)° is slightly sharper than that observed in *vide supra* **14** (O(1)–Mg(1)–O(2) 137.10(8)°

2.12. Reaction of $Cp^*_2Zr(Me)OH$ with $Ca\{N(SiMe_3)_2\}_2\cdot 2THF$ and X-ray crystal structure of $[Cp^*_2(Me)Zr–O–Ca(THF)_3N(SiMe_3)_2]$ (11)

Compound **11** is a promising precursor for the preparation of heterotrimetallic oxygen bridged systems. It is formed by the reaction of $Cp^*_2Zr(Me)OH$[92] with a stiochiometric amount of $Ca\{N(SiMe_3)_2\}_2\cdot 2THF$[148] in *n*-hexane solution at room temperature. The reaction proceeds under elimination of $HN(SiMe_3)_2$ to $Cp^*_2Zr–O–CaN(SiMe_3)_2$ **(11)** (Scheme 13).

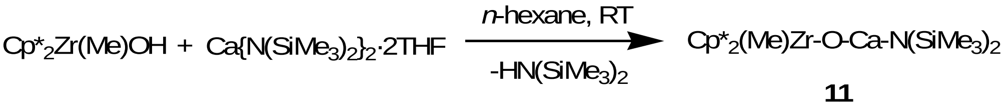

$$Cp^*_2Zr(Me)OH + Ca\{N(SiMe_3)_2\}_2\cdot 2THF \xrightarrow[-HN(SiMe_3)_2]{n\text{-hexane, RT}} Cp^*_2(Me)Zr\text{-}O\text{-}Ca\text{-}N(SiMe_3)_2$$

11

Scheme 13. Preparation of calcium-zirconium oxide.

Compound **11** was characterized by ^1H, ^{13}C, and ^{29}Si NMR spectroscopy, elemental analysis, EI mass spectrometry, and X-ray structural analysis. The ^1H NMR resonances (–0.36 and 0.51 ppm) for **11** correspond to $Zr–CH_3$ and $Ca–N(SiCH_3)_2$, respectively. The ^{13}C NMR reveals that the three resonances (117.34, 22.72, and 2.56 ppm) for **11** correspond to Cp* carbon, $Zr–CH_3$ and $N(SiCH_3)_2$, respectively. The ^{29}Si NMR exhibits a resonance at –13.50 ppm. The EI mass spectrum exhibit peaks at *m*/*z* (503) and (516) that correspond to $[M^+–Me_6]$, and $[M^+–Me_5]$ respectively.

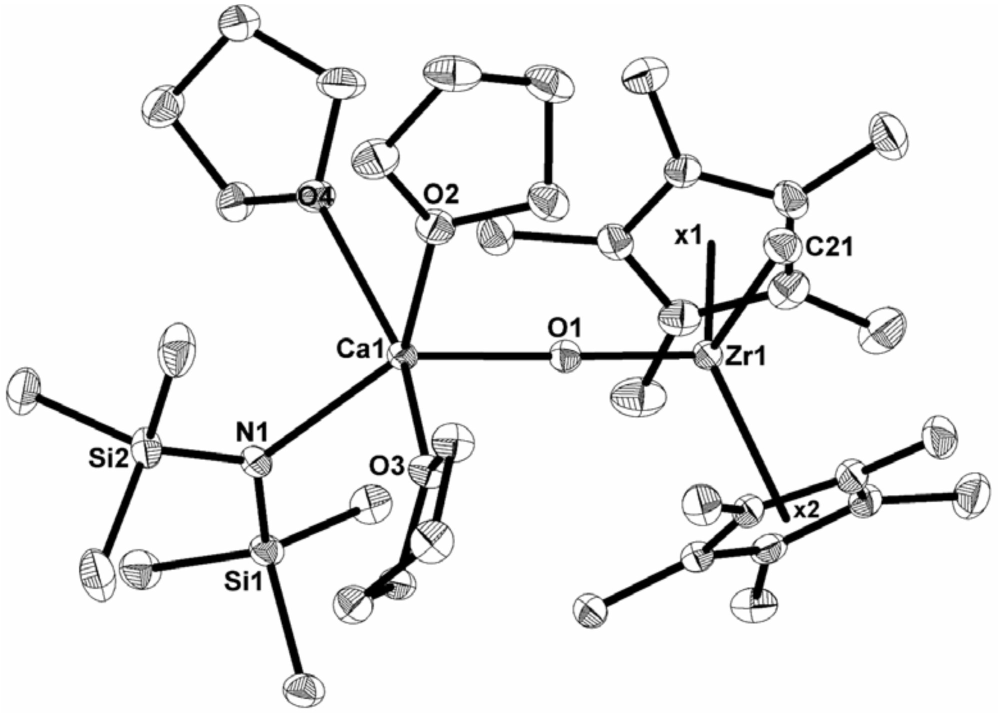

Figure 15. Molecular structure of compound [Cp*$_2$(Me)Zr–O–Ca(THF)$_3$N(SiMe$_3$)$_2$] (**11**); Thermal ellipsoids are shown with 50% probability. All hydrogen atoms are omitted for clarity.Selected bond lengths [Å] and bond angles [°]: Ca(1)–O(1) 2.2068(13), Ca(1)–O(2) 2.4165(14), Ca(1)–O(3) 2.4357(13), Ca(1)–O(4) 2.4625(13), Ca(1)–N(1) 2.3706(16), Zr(1)–O(1) 1.8879(16), Zr(1)–C(21) 2.326(2), x(1)–Zr(1) 2.330, x(2)–Zr(1) 2.333; Ca(1)–O(1)–Zr(1) 176.98(7), O(1)–Ca(1)–N(1) 126.27(5), O(1)–Ca(1)–O(2) 97.20(5), N(1)–Ca(1)–O(2) 136.49(5), O(1)–Ca(1)–O(4) 104.98(5), x(1)–Zr(1)–x(2) 134.17, x(1)–Zr(1)–O(1) 108.26, x(2)–Zr(1)–C(21) 100.8, x(1)–Zr(1)–C(21) 101.78; x = centroid of Cp* ring.

Single crystals suitable for X-ray measurement were grown in a toluene and THF solution at 0 ^{o}C. Compound **11·(3THF)** crystallizes with one molecule in the asymmetric unit. The interesting feature of this compound is the Ca–O–Zr moiety. The X-ray structural analysis of **11·(3THF)** revealed that the calcium is bonded through a bridging oxygen atom to a zirconium atom. The calcium atom is surrounded by an oxygen atom, and three THF molecules and a nitrogen atom of the amide group. The geometry around the calcium atom is trigonal bipyramidal, whereas the geometry around the zirconium atom is tetrahedral, when the Cp* ring is considered as one coordination site. The bond distance of Ca(1)–O(1) (2.2068(13) Å), is significantly longer than Mg–O bond distances found in compound **10** (1.8837(14) Å and 1.8850(14) Å). Interestingly, the bond angle of Ca–O–Zr is nearly linear 176° and it is nearly the same like that of Mg–O–Zr in **10** (175.35(8)°).

2.13. Reaction of [L(Me)Al–O–Mg(THF)$_2$–N(SiMe$_3$)$_2$] (5) with Ph$_3$SnOH and X-ray crystal structure of [L(Me)Al–O–SnPh$_3$] (12)

The reaction of [L(Me)Al–O–Mg(THF)$_2$–N(SiMe$_3$)$_2$][166] (**5**) with triphenyltinhydroxide in toluene solution at room temperature, unexpectedly results in the formation of [LAl(Me)(μ-O)SnPh$_3$] (**12**) (Scheme 14).

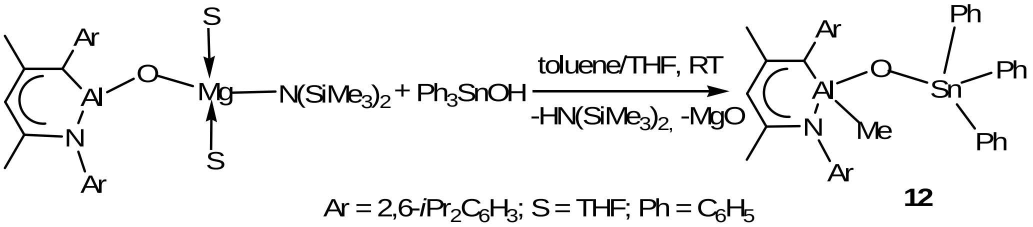

Scheme 14. Preparation of aluminum-tin oxide.

Compound **12** was characterized by ^{1}H, and ^{119}Sn NMR spectroscopy, elemental analysis, EI mass spectrometry, and X-ray structural analysis. Compound **12** is a colorless crystalline solid and melts in the range of 168 to 171 °C. The ^{1}H NMR resonance (–0.66 ppm) for **12** corresponds to Al–*Me*. The other resonances for **12** are characteristic for the *β*-diketiminate ligand and protons of the phenyl rings. The ^{119}Sn NMR exhibits a resonance at –110 ppm typical for Sn(IV) center bonded to three phenyl groups and a bridging oxygen. The EI mass spectrum of **12** revealed that the most intense peak appears at *m/z* 811 and corresponds to the loss of one methyl group from the molecular ion.

Single crystals of **12** suitable for X-ray structural analysis were obtained from a toluene/ THF solution. The molecular structure of **12** is shown in Figure 16 along with selected bond lengths and bond angles.

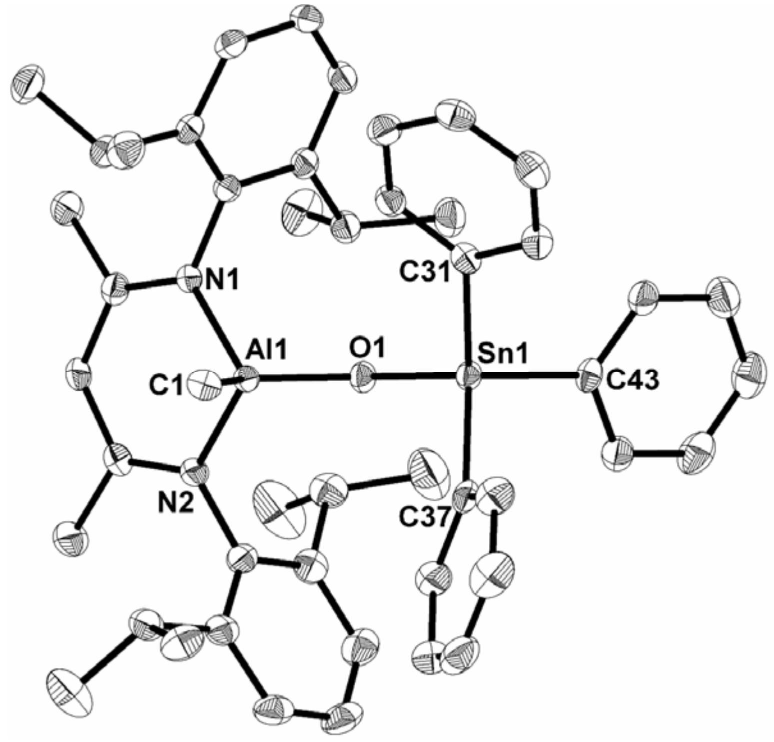

Figure 16. Molecular crystal structure of [LAl(Me)(μ-O)SnPh$_3$] (**12**). Thermal ellipsoids are shown with 50% probability. All hydrogen atoms are omitted for clarity. Selected bond lengths [Å] and bond angles [°]: Al(1)–O(1) 1.718(13), Sn(1)–O(1) 1.943(12), Al(1)–C(1) 1.944(2), Al(1)–N(1) 1.922(16), Al(1)–N(2) 1.909(16), Sn(1)–C(31) 2.136(19); Al(1)–O(1)–Sn(1)

136.90(8), O(1)–Al(1)–C(1) 114.50(8), O(1)–Sn(1)–C(31) 110.43(6), O(1)–Al(1)–N(2) 110.43(7), N(2)–Al(1)–N(1) 96.26(7).

Compound **12** crystallizes in the triclinic space group $P\bar{1}$ with one molecule in the asymmetric unit and solvent free. The X-ray structural analysis of **12** revealed that an aluminum atom is bonded through a bridging oxygen atom to the tin atom. The aluminum atom exhibits a highly distorted tetrahedral geometry with two nitrogen atoms of the *β*-diketiminate ligand, one methyl group and a bridging oxygen atom, whereas the tin atom shows a slightly distorted tetrahedral environment with three phenyl groups and an oxygen atom. The Sn(1)–O(1) bond length observed in **12 (**1.943(12) Å) is slightly shorter than that of the organoaluminum stannoxide Sn–O $[(Me_2Al)(\mu–OSnPh_3)]_2$ (1.984(4) Å).[140] The Al(1)–O(1)–Sn(1) core is bent with an angle of 136.90(8)° which is very slightly wider than that found in $[(Me_2Al)(\mu–OSnPh_3)]_2$ (131.3(2)°).

2.14. Reaction of LAl(Me)OH with (2 eqv) Sn{N(SiMe$_3$)}$_2$ and X-ray crystal structure of [L(Me)Al–O–Sn–O–Al(Me)L] (13)

When $Sn\{N(SiMe_3)_2\}_2$ is treated with 2 eqv. LAl(Me)OH[30] it affords compound **13** with a O–Sn(II)–O core (Scheme 15). Compound **13** is a light yellow solid that melts in the range of 210 to 212 °C. Formation of **13** was monitored by ^{1}H NMR spectroscopy. ^{1}H NMR spectra of **13** exhibits the Al–*Me* to resonate at –0.80 ppm and the complete disappearance of amide protons of $Sn\{N(SiMe_3)_2\}_2$. This indicates the complete conversion of the tin amide to the corresponding tin-aluminum oxide. Other resonances are typical for the *β*-diketiminate ligand.

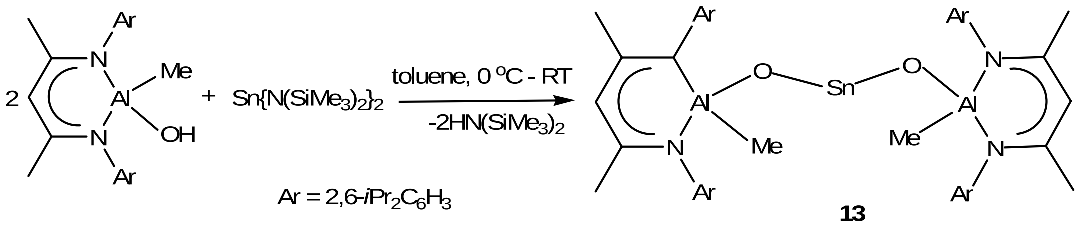

***Scheme* 15.** Aluminum-tin oxide complex with O–Sn(II)–O core.

The EI mass spectrum of **13** exhibits the molecular ion peak at *m/z* 1069 albeit in low intensity. The most intense peak appears at *m/z* 1055 and corresponds to the loss of one methyl group from the molecular ion. The ^{119}Sn NMR for **13** shows a resonance at 137 ppm which is consistent with the two coordinated Sn(II) centre. Compound **13** however exhibits very upfield chemical shift for the tin center compared to the Sn{N(SiMe$_3$)$_2$}$_2$ (734 ppm).

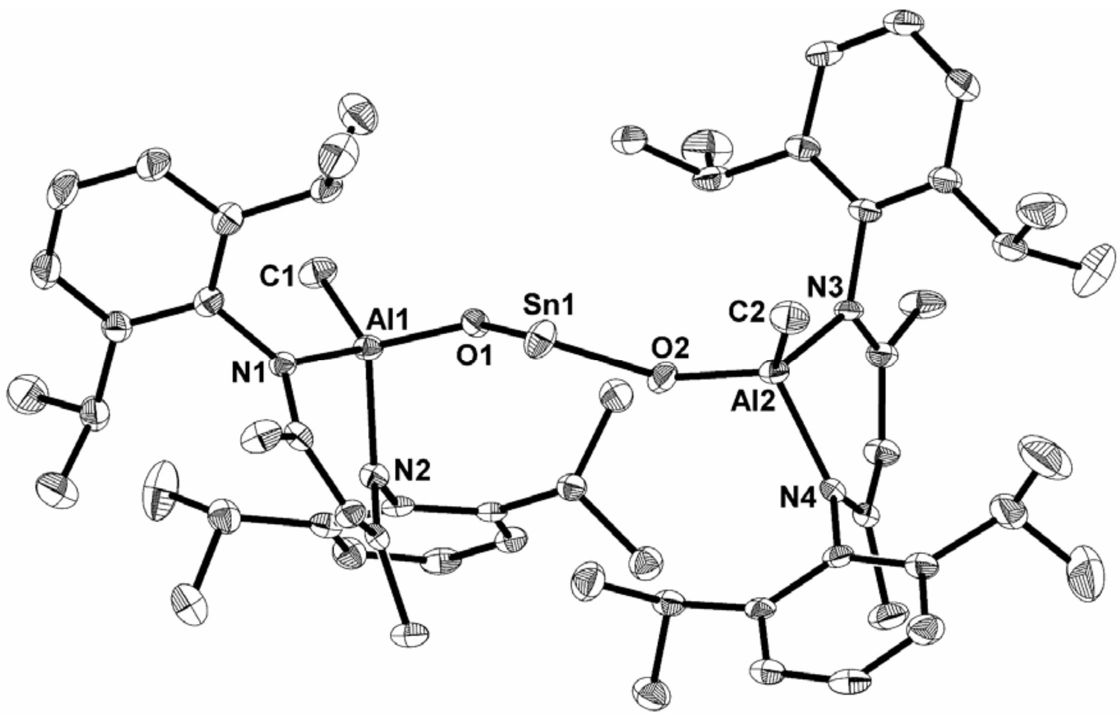

Figure 17. Molecular crystal structure of [L(Me)Al–O–Sn–O–Al(Me)L] (**13**). Thermal ellipsoids are shown with 50% probability. All hydrogen atoms are omitted for clarity. Selected bond lengths [Å] and bond angles [°]: Al(1)–O(1) 1.715(2), Sn(1)–O(1) 1.964(2), Sn(1)–O(2) 1.9656(19), Al(1)–N(1) 1.920(3), Al(1)–C(1) 1.947(3), Al(2)–O(2) 1.714(2), Al(1)–N(3) 1.907(3), Al(1)–C(2) 1.951(3); Al(1)–O(1)–Sn(1) 137.58(12), Al(2)–O(2)–Sn(1) 135.16(12), O(2)–Al(2)–C(2) 116.23(12), O(2)–Al(2)–N(3) 108.46(11), O(1)–Al(1)–C(1) 120.19(13), O(1)–Al(1)–N(2) 104.63(10), O(1)–Sn(1)–O(2) 99.64(8).

The molecular structure of **13** is shown in Figure 17 along with selected bond lengths and bond angles. Compound **13** crystallizes in the triclinic space group $P\bar{1}$ with one molecule in the asymmetric unit, and solvent free. The interesting feature of this compound is the central O–Sn(II)–O core, in turn it is linked to two six-membered AlC_3N_2 rings. The X-ray structural analysis of **13** revealed that an aluminum atom is bonded through a bridging oxygen atom to the tin atom. The aluminum atom exhibits a highly distorted tetrahedral geometry with two nitrogen atoms of the *β*-diketiminate ligand, one methyl group and a bridging oxygen atom. No Sn–Sn interaction was found in the solid stae for **13**. The Al–O bond distance in **13** (1.715 Å) is comparable to that in its parent compound LAl(Me)OH (1.731(3) Å).[30] The Sn(1)–O(1) bond length observed in **13** (1.964(12) Å) is slightly shorter than that of the organoaluminum stannoxide Sn–O $[(Me_2Al)(\mu\text{–}OSnPh_3)]_2$ (1.984(4) Å).[140] The Al(1)–O(1)–Sn(1) and Al(2)–O(2)–Sn(1) bond angle in **13** is 137.58(12) and 135.16(12) °, respectively. The O(1)–Sn(1)–O(2) bond angle 99.64(1) ° is comparable to that found in $(Me_3CN)_3(Me_3AlO)Sn_4$ (99.5-101.1°) [167] and wider that observed in $Sn(OC_6H_2\text{-4-Me-2,6-}_t\text{Bu})_2$ (88.8(2) °).[168]

2.15. Reaction of [L(Me)Al–O–Mg(THF)$_2$–N(SiMe$_3$)$_2$] (5) with LAl(Me)OH and X-ray crystal structure of [L(Me)Al–O–Mg(THF)$_2$–O–Zr(Me)Cp*$_2$] (14)

Very recently Roesky and co-workers reported the soluble molecular compound L(Me)Al–O–Mg(THF)$_2$–N(SiMe$_3$)$_2$] (**5**)[166], which can be considered to function as a precursor for heterotrimetallic oxygen bridged systems. By taking an advantage of the leaving amide group in compound **5**, the synthesis of a heterotrimetallic oxygen bridged system containing magnesium, aluminum and zirconium metal atoms succeeded. This system might endeavour very useful as catalyst in polymerization reactions. Treatment of L(Me)Al–O–Mg(THF)$_2$–N(SiMe$_3$)$_2$] (**5**) with a stoichiometric amount of a well-defined zirconium monohydroxide Cp*$_2$Zr(Me)OH[92] in THF/*n*-hexane solution at 0 °C leads to a heterotrimetallic oxygen bridged system [L(Me)Al–O–Mg(THF)$_2$–O–Zr(Me)Cp*$_2$] (**14**) (Scheme 16).

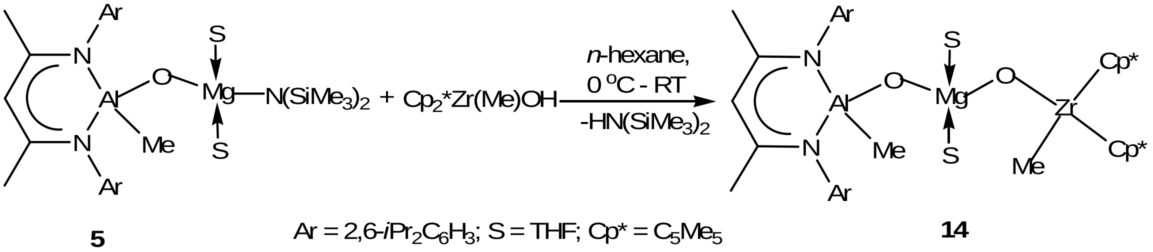

Scheme 16. Preparation of a heterotrimetallic oxygen bridged system.

Compound **14** was characterized by ^{1}H NMR spectroscopy, elemental analysis, and X–ray structural analysis. The ^{1}H NMR reveals the formation of compound **14** by complete disappearance of Zr–OH and N(SiMe$_3$)$_2$ resonances. The protonated amide moiety was removed *in vacuo*. The ^{1}H NMR spectrum exhibits two singlet resonances which can be attributed to the protons of Al–*Me* (–0.47 ppm) and Zr–*Me* groups (–0.39). Single crystals of **14** suitable for X-ray structural analysis were obtained from a *n*-hexane solution at 0 °C within one week. Compound

14 crystallizes in the monoclinic space group *P*2_1/*c* with one molecule in the asymmetric unit and one and a half molecules of *n*-hexane.

The X-ray crystal structure reveals that compound **14** contains a skeleton of Al–O–Mg–O–Zr (Figure 18).

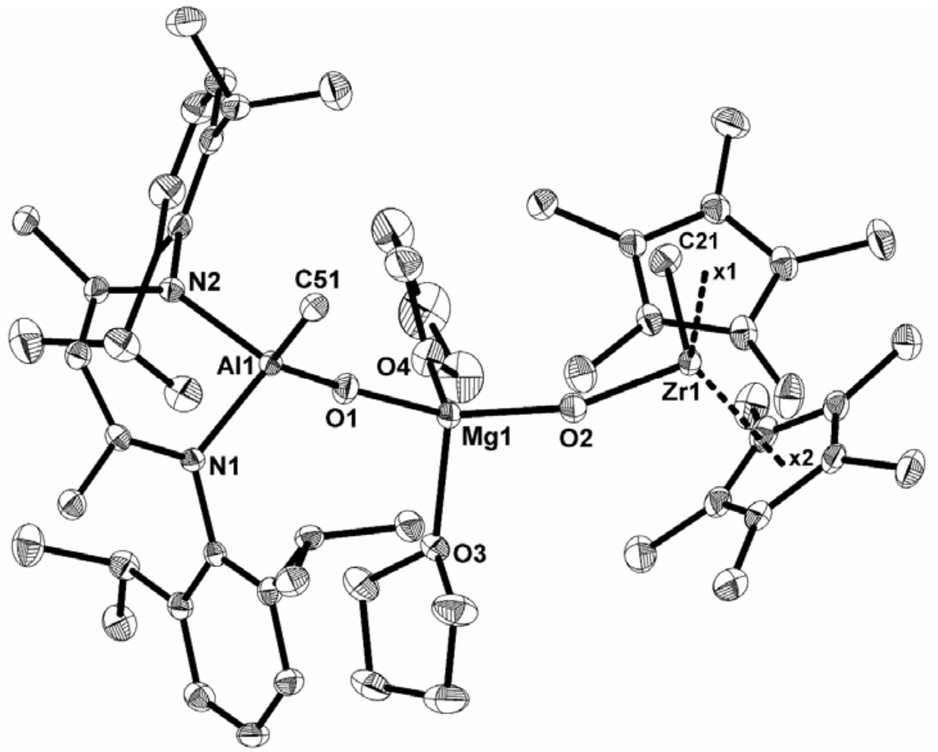

Figure 18. Molecular crystal structure of compound [L(Me)Al–O–Mg(THF)$_2$–O–Zr(Me)Cp*$_2$] (**14**); Thermal ellipsoids are shown with 50% probability. All hydrogen atoms are omitted for clarity. Selected bond lengths [Å] and bond angles [°]: Al(1)–O(1) 1.6699(17), Al(1)–C(51) 1.980(2), Al(1)–N(1) 1.9485(19), Al(1)–N(2) 1.9564(19), Mg(1)–O(1) 1.8436(17), Mg(1)–O(2) 1.9005(17), Mg(1)–O(4) 2.0381(18), Zr(1)–O(2) 1.8852(16), Zr(1)–C(21) 2.315(2), Zr(1)–x(1) 2.322, Zr(1)–x(2) 2.322; N(1)–Al(1)–N(2) 93.12(8), O(1)–Al(1)–N(1) 115.01(8), O(1)–Al(1)–

C(51) 117.87(10), Al(1)–O(1)–Mg(1) 164.14(11), O(1)–Mg(1)–O(3) 103.45(7), O(1)–Mg(1)–O(2) 137.10(8), O(2)–Mg(1)–O(4) 106.37(8), Zr(1)–O(2)–Mg(1) 158.94(10), O(2)–Zr(1)–C(21) 96.02(8), O(2)–Zr(1)–x(1) 107.35(7), O(2)–Zr(1)–x(2) 108.2(7), x(1)–Zr(1)–x(2) 133.74, x(1)–Zr(1)–C(21) 103.2, C(21)–Zr(1)–x(2) 101.5; x = centroid of Cp* ring.

The geometry around the zirconium as well as the magnesium metal atom is highly distorted tetrahedral. The central metal atom magnesium is coordinated by two THF molecules and two bridging oxygen atoms. One THF molecule shows disorder and could be refined anisotropically with a site occupation factor of 0.76. The geometry around the aluminum atom is also slightly tetrahedrally distorted.

In compound **14** the Mg(1)–O(1) bond distance (1.8436(17 Å) is shorter than the Mg(1)–O(2) bond distance (1.9005(17) Å). This could be due to the high oxophilicity of the zirconium atom which is bonded to an O(2) atom. The bond distances of Mg–O (1.8436-2.0492 Å) are in good agreement with those found in **5** and **6** (1.858-2.089 Å and 1.850-2.094 Å). Furthermore, the Mg–O bond lengths (1.8436-2.0492 Å) are consistent with the Mg–O bond lengths compiled by Holloway and Melnik for compounds of magnesium with the coordination number 4 at the magnesium atom (1.819-2.219 Å).[153] The Al–C and Al–O bond distances are 1.980(2) and 1.6669(17) Å respectively, which are in good agreement with those observed in **5** (1.975(2) and 1.682(2) Å) respectively. The Mg(1)–O(1)–Al(1) bond angle (164.14(11)°) is slightly wider than in compound **5** (157.1(1)°) and much wider compared to that in the alkoxy bridged $[Al_3Mg_3(\mu_3\text{-}O)(THFFO)_4Cl_4(Me)_5(THF)]$ (THFFO = 2-tetrahydrofurfuroxide) compound ($Al–\mu\text{-}O_{(alkoxide)}\text{-}Mg$ (128.2(2)°)).[102]

3. Summary and Future Directions

In recent years *β*−diketiminate ligand supported alkaline earth metal complexes found significant applications in polymerization reactions, catalysis, and organic transformations. In view of this we have prepared *β*−diketiminate ligand supported group 2 hydroxide, halide, oxygen bridged heterobi- and trimetallic complexes.

Controlled hydrolysis of the *β*−diketiminate ligand supported alkaline earth metal amides afforded the corresponding hydroxides as air and moisture sensitive compounds. The presence of sterically bulky ligands prevent self-condensation reaction in these hydroxides. Structural studies show that they are dimeric in the solid state. By using more bulky ligands one could stabilize the hydroxide compounds in their monomeric form.

Access to well-defined magnesium and calcium hydroxide complexes of the general formula $[LM(OH)\cdot THF]_2$ (M = Mg(**1**), Ca(**2**)) that are soluble in organic solvents has given the possibility to study the reactivity of the OH group on a molecular level.

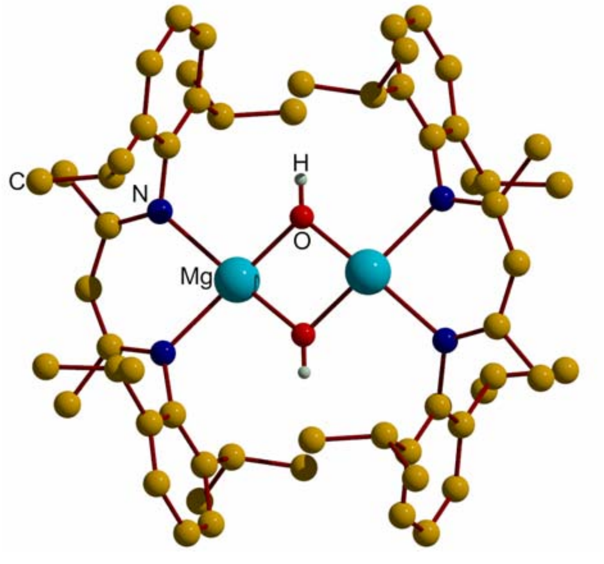

1

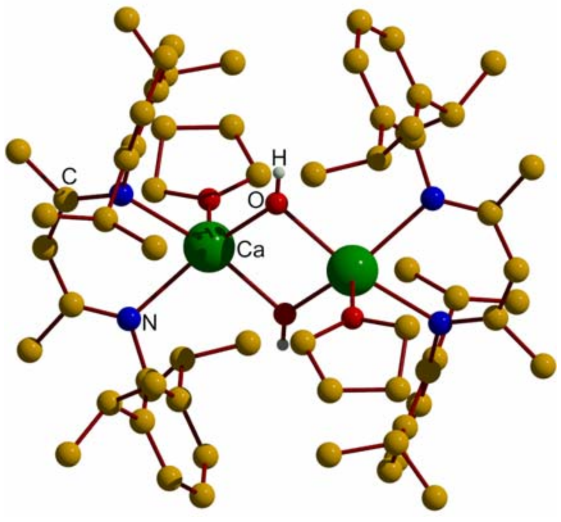

2

These hydroxides could also be of interest in sol-gel coatings, and as polymerization catalysts. These group 2 metal hydroxides might also be envisaged as synthons for assembling novel heterobimetallic systems.

The β−diketiminate ligand supported magnesium chloride has been prepared by using the free ligand and methylmagnesium chloride. Compound $L^{I}MgCl$ (**3**) is monomeric, solvent free, and an analogue of a Grignard reagent. It could be a very useful precursor for the preparation of a low valent magnesium complex.

By using the $LCaN(SiMe_3)_2\cdot THF$ and trimethyltin fluoride, we have prepared calcium monofluoride $[LCa(F)\cdot THF]_2$ (**4**). Compound **4** is the first example of a hydrocarbon-soluble calcium monofluoride that shows exceptional solubility in organic solvents. Furthermore, the dip-coating experiments reveal the feasibility of CaF_2 coating on a given substrate. Moreover, dip-coatings were studied with other soluble calcium precursors such as $LCaN(SiMe_3)_2\cdot THF$, $Ca\{N(SiMe_3)_2\}_2\cdot 2THF$, LCaL, and **2** for the preparation of thin layers of CaF_2. Based on these results, a broad application of CaF_2 coatings can be expected.

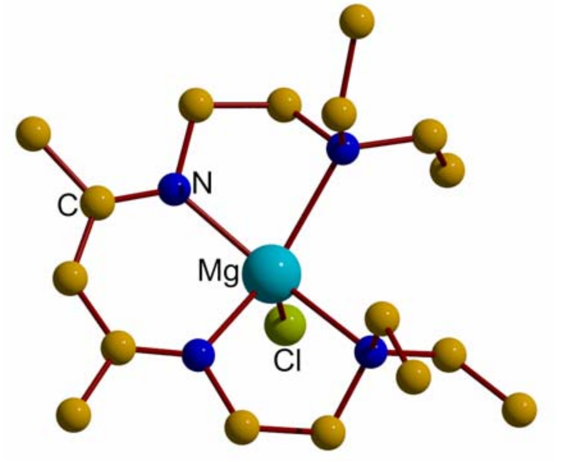

3

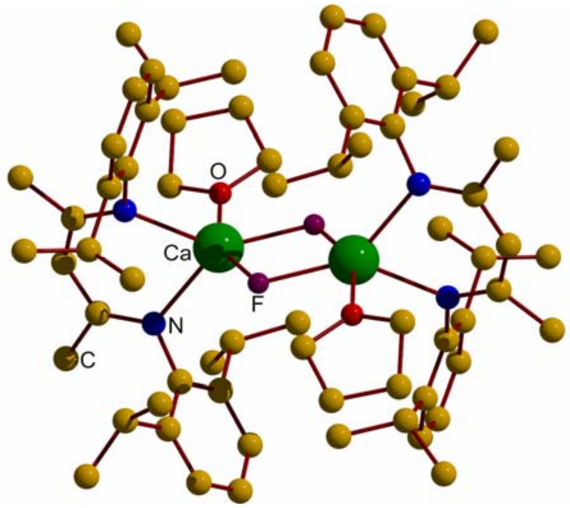

4

A clean reaction of aluminium hydroxide and magnesium amide afforded the soluble molecular compound with a Mg–O–Al structural motif. Compound **5** proved to be a right precursor for the preparation of a heterotrimetallic system. Moreover, L(Me)Al–O–Mg(THF)$_2$–O–Al(Me)L (**6**) might be a useful precursor for spin-coated spinel surfaces and may function as a molecular model for surface fixation of the organometallic species.

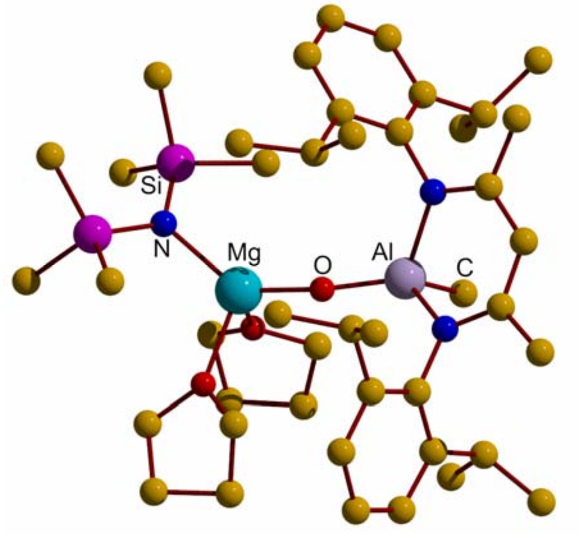

5

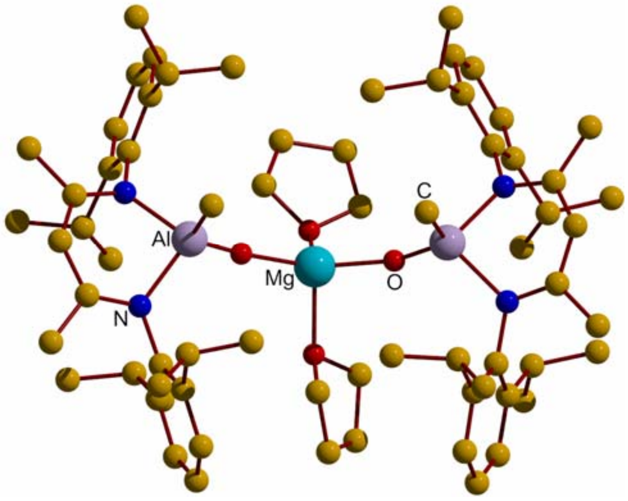

6

Furthermore, the heterobimetallic compound LMg(THF)–O–Al(Me)L (**7·THF**) has been prepared by the reaction of LMgN(SiMe$_3$)$_2$ or LMgMe·OEt$_2$ with LAl(Me)OH, in which the oxygen atom is linked to two six- membered MC$_3$N$_2$ (M = Mg, Al) rings.

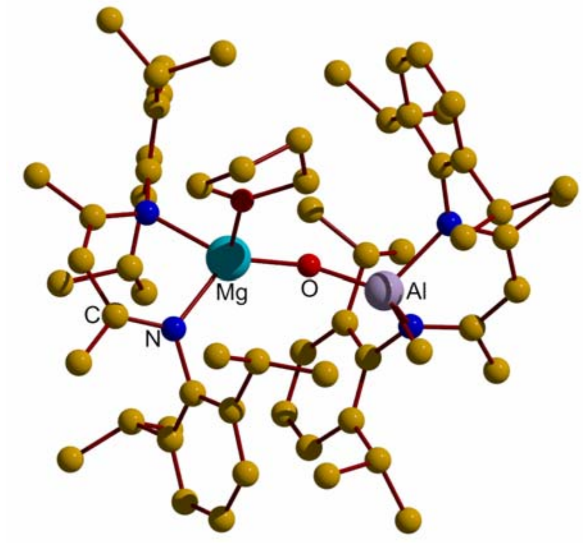

7

Heterobimetallic calcium-aluminum oxide compounds have been synthesized and one of them was structurally characterized. Compound **8** is formed by the reaction of aluminum hydroxide and calcium amide. Interestingly, this compound comprises three rings, the central Ca_2O_2 ring is linked to two six-membered AlC_3N_2 rings. These compounds might be useful in catalysis, organic synthesis, and chemical vapor deposition (CVD).

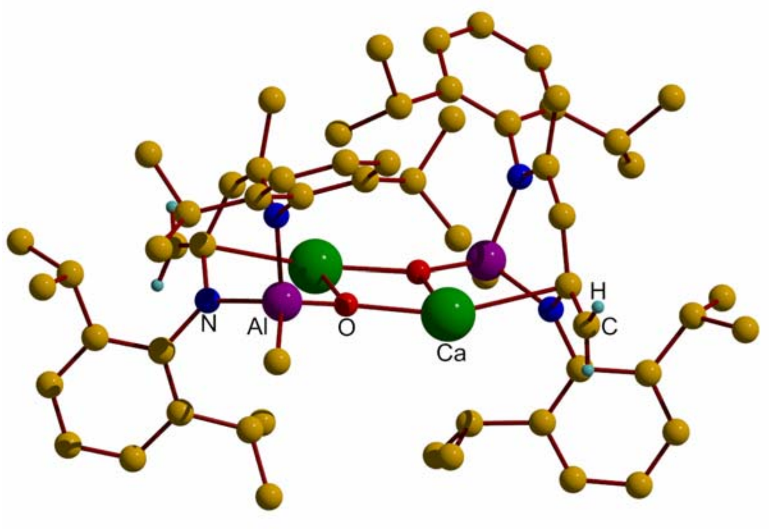

8

The reaction of $Cp^*_2Zr(Me)OH$ with $Mg\{N(SiMe_3)_2\}_2$ afforded the trimetallic compound **10** with a $(ZrO)_2Mg$ core. Furthermore, these studies were extended to heavier analogues of magnesium. Thus, the reaction of $Cp^*_2Zr(Me)OH$ with $Ca\{N(SiMe_3)_2\}_2$ afforded the heterobimetallic compound **11** with a Ca–O–Zr core. This calcium-zirconium oxide compound has a labile amide group on the calcium atom and in view of that it could be used as catalyst in hydroamination, [169-173] hydrophosphination,[174] and organic tranformations reactions [175-177] e.g. Tishenko reactions etc.

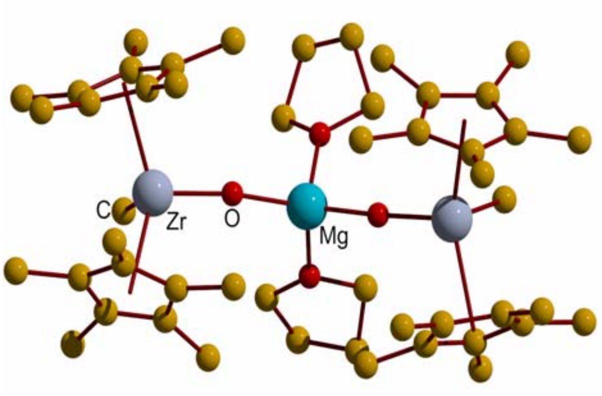

10

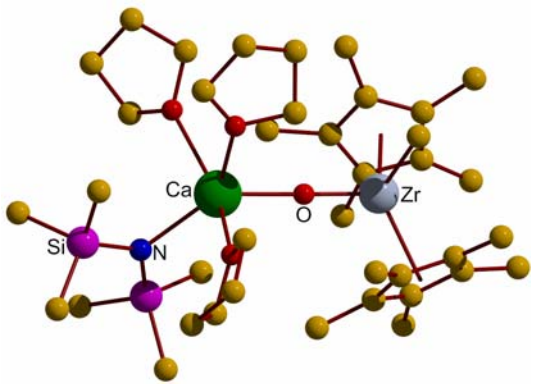

11

As organometallic complexes of the heavier alkaline- earth metals (Ca, Sr, and Ba) show similarities with early d and f-block metal complexes,[108, 173,178-183] and are increasingly used in catalysis, they could be potencial candidates for early main-group metal hydrosilylation catalysts.[184]

The reaction of **5** with Ph_3SnOH, leads unexpectedly to a bimetallic compound with an Al–O–Sn(IV) (**12)** core, while the reaction of LAl(Me)OH with $Sn\{N(SiMe_3)_2\}_2$ gave compound with a central O–Sn(II)–O core (**13**), in which the oxidation state of tin is +2.

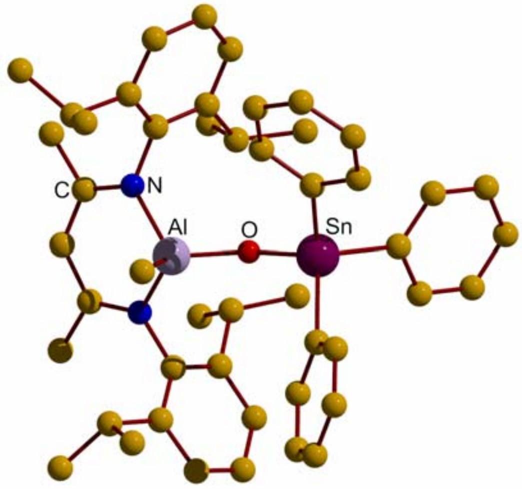

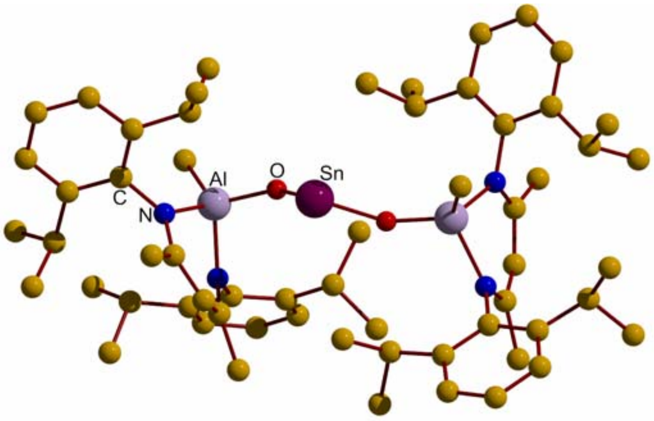

13

12

Finally, the reaction of the heterobimetallic compound **5** with Cp*$_2$Zr(Me)OH afforded the first heterotrimetallic oxygen bridged system, with three different metal atoms (magnesium, aluminum, and zirconium). This compound (**14**) might be useful in polymerization reactions.

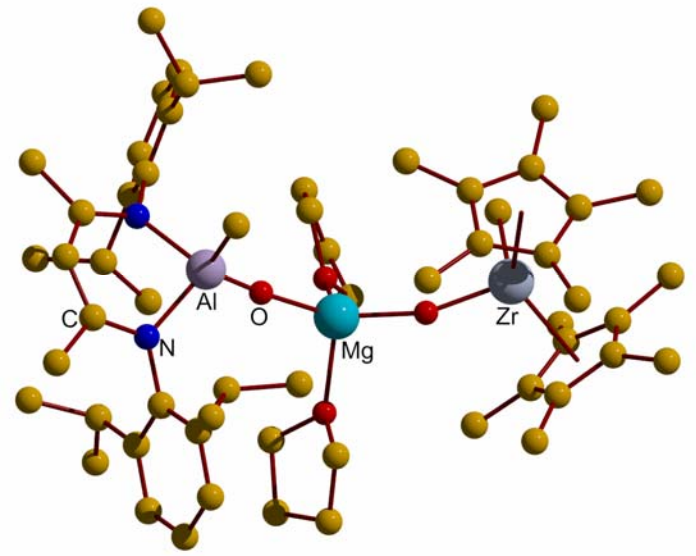

14

4. Experimental Section

4.1. General procedures

All manipulations and handling of reagents were carried out under an atmosphere of purified nitrogen or argon using standard Schlenk techniques or a glove box where O_2 and H_2O level is maintained usually below 1 ppm. All glassware was dried at 150 °C in an oven for at least 20 h and assembled hot and cooled *in vacuo* prior to use. Toluene (Na/benzophenone ketyl), tetrahydrofuran (Na/benzophenone ketyl), diethylether (Na/benzophenone ketyl), *n*hexane (Na/benzophenone ketyl and diphenyl ether), pentane (Na/benzophenone ketyl and diphenyl ether), dichloromethane (calcium dihydride) were dried and distilled under nitrogen and degassed prior to use.

4.2. Physical measurements

NMR spectra were recorded on Bruker Avance 200, Bruker Avance 300, Bruker Avance 500 spectrometers with $SiMe_4$ as external standard (for ^1H, ^{13}C, and ^{29}Si), C_6F_6 for ^{19}F nucleus, $SnMe_4$ for ^{119}Sn nucleus, and chemical shifts are reported in ppm. Downfield shifts relative to the reference are quoted positive; up field shifts are assigned negative values. Deuterated NMR solvents C_6D_6, and THF-D_8 were dried by stirring for 2 days over Na/K alloy followed by distillation under *vacuo* and degassed. Mass spectra were recorded on a Finnegan MAT 8230 or a Varian MAT CH5 spectrometer (70 eV) by EI-MS method. The most intense peak of an isotopic distribution is tabulated. IR spectra were recorded on a Bio-Rad Digilab FTS-7 spectrometer as nujol mull between KBr plates. The absorptions of characteristic functional groups (M-OH,) are assigned and other absorptions (moderate to very strong) are only listed. Melting points were obtained in sealed capillaries on a Büchi B-540 melting point instrument. Elemental analyses were performed at the Analytical Laboratory of the Institute of Inorganic Chemistry, University of Göttingen. The surface investigations and the EDX measurements were accomplished with a Leo Supra 35 scanning electron microscope equipped with a Noran EDX-system. The microscope was operated at an accelerating voltage of 10 kV (Institut für Materialphysik, Universität Gottingen).

Crystal structure determination: For compounds **1-3** and **5,** data were collected on an STOE-IPDS 2 instrument using Mo-Kα radiation. Diffraction data for compound **6** was measured on a Bruker three-circle diffractometer equipped with a SMART 6000 CCD detector using mirror monochromated Cu-Kα radiation (λ = 1.54178 Å). Data for compounds **4**, **7**, **8**, **10**, **11**, **12**, **13**, and **14** were collected on Bruker Smart Apex II with D8 goniometer. Data for all compounds were collected at low temperature. The structures were solved by direct methods (SHELXS-97)[185] and refined with SHELXL-97[186] on F^2. The crystal data for all compounds along with the final residuals and other pertaining details are tabulated in Section 6, Tables 2-14.

4.3. Starting materials

Hydrogen fluoride pyridine (hydrogen fluoride ~70 %, pyridine ~30 %), triphenyltinhydroxide, and MeMgCl were purchased from Aldrich and used as such. Compounds L,[36] L^I,[142] $LMgN(SiMe_3)_2$,[141] $Sn\{N(SiMe_3)_2\}_2$,[187] $LCaN(SiMe_3)_2\cdot THF$,[65] Me_3SnF,[96] $Ca\{N(SiMe_3)_2\}_2\cdot 2THF$,[148] $Mg\{N(SiMe_3)_2\}_2$,[150,151] $LMgMe\cdot OEt_2$,[120-121] $Cp^*_2Zr(Me)OH$,[92] and LAl(Me)OH[30] were prepared by literature procedures. Demineralized, degassed H_2O was used for hydrolysis experiments.

4.4. Syntheses of compounds 1-14

4.4.1. Synthesis of [LMg(OH)·THF]$_2$ (1)

Degassed and distilled water (46 μL, 2.55 mmol) was added to a solution of LMgN(SiMe$_3$)$_2$ (1.52 g, 2.53 mmol) in THF (30 mL) at –20 °C, and then allowed to warm to room temperature. After having been stirred at room temperature for 15 min, the slurry was dried *in vacuo*. The resulting solid of **1** was washed with *n*-hexane (10 mL) and finally dried *in vacuo*. Yield: (0.810 g, 1.528 mmol, 60%). Mp: 336-340 °C. Anal. Calcd for $C_{58}H_{84}Mg_2N_4O_2$ (916): C 75.89, H 9.22, N 6.10; found: C 75.50, H 9.19, N 6.14. ^{1}H NMR (200 MHz, C_6D_6,): δ –0.46 (s, 2H, Mg–O*H*), 0.88 (d, *J* = 6.9 Hz, 24H, CH(C*H*$_3$)$_2$), 1.11 (d, *J* = 6.8 Hz, 24H, CH(C*H*$_3$)$_2$), 1.30 (m, 8H, O-CH$_2$-C*H*$_2$), 1.54 (s, 12H, C*H*$_3$), 3.14 (sept, *J* = 6.8 Hz, 8H, C*H*(CH$_3$)$_2$), 3.57 (m, 8H, O-C*H*$_2$-CH$_2$), 4.81 (s, 2H, γ-C*H*), 7.11 (s, 12H, *m-, p*-Ar-*H*). ^{1}H NMR (500 MHz, THF-*d*$_8$): δ –1.41 (s, 2H, Mg–O*H*), 0.89 (d, *J* = 6.9 Hz, 24H, CH(C*H*$_3$)$_2$), 1.01 (d, *J* = 6.8 Hz, 24H, CH(C*H*$_3$)$_2$), 1.43 (s, 12H, C*H*$_3$), 1.80 (m, 8H, O-CH$_2$-C*H*$_2$), 2.97 (sept, 8H, *J* = 6.9 Hz, C*H*(CH$_3$)$_2$), 3.70 (m, 8H, O-C*H*$_2$-CH$_2$), 4.63 (s, 2H, γ-C*H*), 7.11 (s, 12H, *m-, p*-Ar-*H*). ^{13}C {1H} NMR (125 MHz, C_6D_6): δ 19-23, 26, 28.2, 29.5, 96, 70, 127-145. X-ray analysis of the crystals revealed that the complex exists as a μ-hydroxide bridged dimer in the solid state. EI-MS (70 eV): *m*/*z* (%): 916 (100) [*M*$^+$]. IR (Nujol, cm$^-$) $\tilde{\nu}$: 3741 (MgO–H), 3669, 1624, 1552, 1315, 1176, 1100, 1022, 931, 794, 759, 703.

4.4.2. Synthesis of [LCa(OH)·THF]$_2$ (2)

Degassed and distilled water (40 μL, 2.22 mmol) was added to a solution of LCaN(SiMe$_3$)$_2$·THF (1.5 g, 2.18 mmol) in THF at –40 °C, and then allowed to warm to room temperature. After having been stirred at room temperature for 30 min, the slurry was dried *in vacuo*. The resulting solid of **2** was washed with *n*-hexane (8 mL) and finally dried *in vacuo*. The product can be recrystallized by cooling a saturated hot toluene solution to 0 °C. Yield: (1.06 g, 1.94 mmol 89%). Mp: 277-280 °C. Anal. Calcd for $C_{66}H_{100}Ca_2N_4O_4$ (1093.68): C 72.48, H 9.22, N 5.12; found: C 72.82, H 8.87, N 4.90. ^{1}H NMR (400 MHz, C_6D_6,): δ –0.78 (s, 2H, Ca–O*H*), 1.05 (d, *J* = 6.9 Hz, 24H, CH(C*H*$_3$)$_2$), 1.22 (d, *J* = 6.8 Hz, 24H, CH(C*H*$_3$)$_2$), 1.41 (m, 8H, O-CH$_2$-C*H*$_2$), 1.69 (s, 12H, C*H*$_3$), 3.15 (sept, *J* = 6.9 Hz, 8H, C*H*(CH$_3$)$_2$), 3.48 (m, 8H, O-C*H*$_2$-CH$_2$), 4.74 (s, 2H, γ-C*H*), 7.06 (s, 12H, *m-, p*-Ar-*H*). ^{1}H NMR (300 MHz, THF-d_8,): δ –1.09 (s, 2H, Ca-O*H*), 0.87 (d, *J* = 6.9 Hz, 24H, CH(C*H*$_3$)$_2$), 1.01 (d, *J* = 6.8 Hz, 24H, CH(C*H*$_3$)$_2$), 1.44 (s, 12H, C*H*$_3$), 1.73 (m, 8H, O-CH$_2$-C*H*$_2$), 2.96 (sept, *J* = 6.9 Hz, 8H, C*H*(CH$_3$)$_2$), 3.58 (m, 8H, O-C*H*$_2$-CH$_2$), 4.44 (s, 2H, γ-C*H*), 6.87 (s, 12H, *m-, p*-Ar-*H*).^{13}C {1H} NMR (125.77 MHz, C_6D_6): δ 24.2, 24.3, 25.0, 25.3, 27.8, 68.4, 93.0, 123.2, 123.4, 141.3, 147.6, 164.4. X-ray analysis of the crystals revealed that the complex exists as a μ-hydroxide bridged dimer in the solid state. EI-MS (70 eV): *m*/*z* (%): 202 (100) [DippNCCH$_3$]$^+$. IR (Nujol, cm^{-1}) $\tilde{\nu}$: 3698 (CaO–H), 3647, 1623, 1552, 1314, 1169, 1100, 1019, 936, 883, 785, 758, 723.

4.4.3. Synthesis of [L^{I}Mg(Cl)] (3)

To a solution of L^{I}H (1.04 g, 3.3 mmol) in diethyl ether (15 mL) was slowly added drop by drop a solution of MeMgCl (3M in THF, 1.04 ml, 3.3 mmol) in diethyl ether (20 mL) at −78 °C. The stirring was continued for 1 h at this temperature. When allowed to warm to room temperature, an evolution of methane gas was noticed, and the stirring was continued at ambient temperature for 12 h. The solvent was removed and the residue washed with *n*-pentane (15 mL). The solid was dissolved in *n*-hexane (20 mL) and overnight storage of this solution at −32 °C resulted in colorless crystals of **3**. Yield: 1.20 g (63.5 %). Mp 158 -162 °C. Anal. Calcd for $C_{20.5}H_{39}ClMgN_4$ (401.32): C 61.35, H 9.79, N 13.96; found: C 60.89, H 9.56, N 13.75. ^{1}H NMR (200 MHz, C_6D_6, 25 °C, TMS): δ 0.8 (t, 12H, $CH_2C\mathit{H}_3$), 1.81 (s, 6H, $C\mathit{H}_3$), 2.61 (t, 4H, $C\mathit{H}_2CH_2N$),), 2.62–2.68 (q, 8H, $CH_3C\mathit{H}_2N$), 3.01 (t, 4H, $CH_2C\mathit{H}_2N$), 4.74 (s, 1H, γ-C*H*). EI-MS (70 eV): *m*/*z* (%): 355 (5) $[M]^+$, 319 (15) $[M-Cl]^+$, 86 (100) $[C_5H_{12}N]^+$

4.4.4. Synthesis of [LCa(F)·THF]$_2$ (4)

To a suspension of Me_3SnF (0.368 g, 2.00 mmol) in THF (10 mL), a clear solution of $LCaN(SiMe_3)_2\cdot THF$ (1.38 g, 2.00 mmol) in THF (30 mL) was added. The stirring was continued at room temperature for 16 h and dissolution of Me_3SnF indicated completion of the fluorination. This was followed by removal of all the volatiles *in vacuo* and extraction with *n*-hexane (60 mL). The solution afforded the title compound **4** as a white solid. An analytically pure sample of **4** was obtained by crystallizing from hot toluene and THF. Yield: (0.65 g, 60%). Mp: 277-280 °C. Anal. Calcd for $C_{66}H_{98}Ca_2F_2N_4O_2$ (1093.68): C 72.26, H 8.94, N 5.11; found: C 72.45, H 8.84, N 4.65. ^{1}H NMR (500 MHz, C_6D_6,): δ 1.01-1.02 (d, 24H, $CH(C\mathit{H}_3)_2$), 1.22-1.24 (d, 24H, $CH(C\mathit{H}_3)_2$), 1.42 (m, 8H, O-CH_2-$C\mathit{H}_2$), 1.64 (s, 12H, $C\mathit{H}_3$), 3.14 (sept, 8H, $C\mathit{H}(CH_3)_2$), 3.54 (m, 8H, O-$C\mathit{H}_2$-CH_2), 4.72 (s, 2H, γ-C*H*), 7.09 (s, 12H, *m*-, *p*-Ar-*H*). ^{13}C {1H} NMR (125.77 MHz, C_6D_6): δ 165.1, 147.2, 141.8, 123.8, 123.4, 93.4, 69.0, 27.9, 25.4, 25.3, 24.5. ^{19}F NMR (188.77 MHz, C_6D_6): δ –78 (s, Ca*F*). EI-MS (70 eV): *m*/*z* (%): 202 (100) $[DippNCCH_3]^+$.

Dip-coating experiments: Calcium difluoride coatings were prepared according to the following procedure: The pure unpolished silicon substrate was dipped into the toluene (20 mL) solution of [LCa(F)·THF]$_2$ (**4**) (1.00 g, 0.84 mmol) and dried. This was then further dipped into a moderate excess of the fluorinating agent HF·pyridine (0.063 g, 2.18 mmol) in toluene (20 mL).

These two processes were carried out alternatively for 10–12 times. Finally, the silicon substrate was washed with toluene to remove all the soluble side products. After drying at room temperature for 30 minutes a white solid remained on the substrate. This was subjected to the SEM and EDX analyses. The same procedure was applied to the $\mathrm{CaF_2}$ coatings using precursors such as $\mathrm{LCaN(SiMe_3)_2{\cdot}THF}$, $\mathrm{Ca\{N(SiMe_3)_2\}_2{\cdot}2THF}$, LCaL, and **2**

4.4.5. Synthesis of $\mathbf{[L(Me)Al{-}O{-}Mg(THF)_2{-}N(SiMe_3)_2]}$ (5)

LAl(Me)OH (0.476 g, 1mmol) dissolved in THF/*n*-hexane (20 mL) was added drop wise at 0 °C to a stirred solution of $\mathrm{Mg\{N(SiMe_3)_2\}_2}$ (0.345 g, 1 mmol) in THF/*n*-hexane (20 mL). The solution was allowed to warm to room temperature and stirred for 48 h. After removal of all the volatiles *in vacuo* compound **5** remained. Yield: (0.70 g, 87% with respect to LAl(Me)OH. Mp: 127-132 °C. Anal. Calcd for $\mathrm{C_{44}H_{78}AlMgN_3O_3Si_2}$ (804.56): C 65.68, H 9.77, N 5.22; found: C 64.21, H 9.71, N 5.02. ^{1}H NMR (300 MHz, $\mathrm{C_6D_6}$, 25 °C, TMS): δ –0.36 (s, 3H, Al-C*H*$_3$), 0.15 (s, 18H, (Si*Me*$_3$)$_2$, 1.17 (d, 12H, CH(C*H*$_3$)$_2$, 1.23 (d, 12H, CH(C*H*$_3$)$_2$, 1.35 (m, 8H, O-CH$_2$-C*H*$_2$), 1.53 (s, 6H, C*H*$_3$), 3.34 (m, 8H, O-C*H*$_2$-CH$_2$), 3.52 (sept, 2H, C*H*(CH$_3$)$_2$), 3.72 (sept, 2H, C*H*(CH$_3$)$_2$), 4.94 (s, 1H, γ-C*H*), 7.08-7.17 (m, 6H, *m-, p*-Ar-*H*). ^{13}C {H} NMR (75.475 MHz, $\mathrm{C_6D_6}$, 25 ºC, TMS): δ 168.6 (*C*N), 144.7, 144.4, 143.4, 126.2, 124.3, 124.2 (*i*-, *o*-, *m*-, *p-Ar*), 97.0 (γ-*C*H), 68.7 (O-*C*H$_2$-CH$_2$) 28.7 (*C*H$_3$), 27.6 (*C*H(CH$_3$)$_2$, 26.7 (O-CH$_2$-*C*H$_2$), 25.2 (*C*H(CH$_3$) 25.1 (CH(*C*H$_3$)$_2$, 24.8 (CH(*C*H$_3$)$_2$, 24.5 (CH(*C*H$_3$)$_2$, 23.7 (CH(*C*H$_3$)$_2$, 6.7 Si(*Me*$_3$)$_2$, 1.4 (Al-*C*H$_3$). ^{29}Si NMR (59.627 MHz, $\mathrm{C_6D_6}$, TMS): δ –9.8 (*Si*Me$_3$). EI-MS (70 eV): *m*/*z* (%): 202 (100) $\mathrm{[DippNCCH_3]^+}$. IR (Nujol, cm^{-1}) $\tilde{\nu}$: 1931, 1864, 1799, 1624, 1319, 1257, 1178, 1100, 1016, 936, 824, 799, 761, 723, 663, 606.

4.4.6. Synthesis of [L(Me)Al–O–Mg(THF)$_2$–O–Al(Me)L] (6)

Two equivalents of LAl(Me)OH (0.952 g, 2mmol) in THF/*n*-hexane (40 mL) were added dropwise to a solution of Mg{N(SiMe$_3$)$_2$}$_2$ (0.345 g, 1 mmol) in THF/*n*-hexane (20 mL) at 0 °C, allowed to warm to room temperature, and stirred for 48 h. After removal of the solvent *in vacuo* and washing the residue with pentane (10 mL) compound **6** was obtained. Yield: (0.96 g, 85% with respect to LAl(Me)OH). Mp: 162-165 °C. Anal. Calcd for $C_{68}H_{104}Al_2MgN_4O_4$ (1119.82): C 72.93, H 9.36, N 5.00; found: C 71.42, H 9.23, N 4.99. ^{1}H NMR (300 MHz, C_6D_6, 25 °C, TMS): δ –0.66 (s, 6H, Al-C*H*$_3$), 1.20 (d, 24H, CH(C*H*$_3$)$_2$, 1.22 (d, 24H, CH(C*H*$_3$)$_2$, 1.41 (m, 8H, O-CH$_2$-C*H*$_2$), 1.65 (s, 12H, C*H*$_3$), 3.19 (m, 8H, O-C*H*$_2$-CH$_2$), 3.46 (sept, 4H, C*H*(CH$_3$)$_2$), 3.90 (sept, 4H, C*H*(CH$_3$)$_2$), 4.99 (s, 2H, γ-C*H*), 7.08-7.16 (m, 12H, *m-, p*-Ar-*H*). ^{13}C {H}NMR (75.475 MHz, C_6D_6, 25 ºC, TMS): δ 167.9 (*C*N), 145.4, 144.2, 143.0, 128.3, 127.3, 125.4 (*i*-, *o*-, *m*-, *p-Ar*), 96.6 (γ-*C*H), 68.4 (O-*C*H$_2$-CH$_2$), 28.3 (*C*H$_3$), 28.1 (*C*H(CH$_3$)$_2$, 25.7 (O-CH$_2$-*C*H$_2$), 25.5 (*C*H(CH$_3$)$_2$, 25.3 (CH(*C*H$_3$)$_2$, 24.9 (CH(*C*H$_3$)$_2$, 24.6 (CH(*C*H$_3$)$_2$, 23.7 (CH(*C*H$_3$)$_2$, 1.4 (Al-*C*H$_3$). EI-MS (70 eV): *m*/*z* (%): 202 (100) [DippNCCH$_3$]$^+$. IR (Nujol, cm^{-1}) $\tilde{\nu}$: 2177, 1927, 1862, 1799, 1624, 1257, 1178, 1106, 1021, 962, 890, 799, 763, 642, 609.

4.4.7. Synthesis of LMg–O–Al(Me)L (7)

LAl(Me)OH (0.476 g, 1mmol) dissolved in toluene (20 mL) was added drop wise at room temperature to a stirred solution of LMgN(SiMe$_3$)$_2$ (0.601 g, 1.00 mmol) or LMgMe·Et$_2$O (0.530 g, 1.0 mmol) in toluene (20 mL). The solution was allowed to warm to reflux temperature and stirred for 14 h. After removal of all the volatiles *in vacuo* compound **7** remained. Yield (0.82 g, 89%). Mp: 260-263 °C. Anal. Calcd for $C_{59}H_{85}AlMgN_4O$ (916): C 77.29, H 9.28, N 6.11; found: C 76.77, H 9.13, N 6.06. ^{1}H NMR (200 MHz, C_6D_6, 25 °C, TMS): δ –1.43 (s, 3H, Al-C*H*$_3$), 1.08

(d, 12H, CH(C*H*$_3$)$_2$, 1.22 (d, 24H, CH(C*H*$_3$)$_2$, 1.31 (d, 12H, CH(C*H*$_3$)$_2$, 1.52 (s, 6H, C*H*$_3$), 1.64 (s, 6H, C*H*$_3$), 3.25 (sept, 6H, C*H*(CH$_3$)$_2$), 3.75 (sept, 2H, C*H*(CH$_3$)$_2$), 4.82 (s, 1H, γ-C*H*), 4.88 (s, 1H, γ-C*H*), 7.08-7.16 (m, 12H, *m-, p*-Ar-*H*). MS (70 eV): *m*/*z* (%): 901 (100) [M^+-Me], 916 (6) [M^+]. IR (Nujol, cm^{-1}) $\tilde{\nu}$: 1860, 1795, 1733, 1619, 1530, 1440, 1318, 1261, 1176, 1100, 1021, 955, 798, 760, 722, 623.

4.4.8. Synthesis of [{L$^{\mathrm{II}}$Al(Me)}(μ-O)(Ca·THF)]$_2$ (8)

LAl(Me)OH (0.476 g, 1mmol) dissolved in THF/*n*-hexane (20 mL) was added dropwise at room temperature to a stirred solution of Ca{N(SiMe$_3$)$_2$}$_2$·2THF (0.501 g, 1 mmol) in THF/*n*-hexane (20 mL). The solution was allowed to warm to room temperature and stirred for 48 h. After removal of all the volatiles *in vacuo* compound **8** remained. Yield: (0.44 g, 70% with respect to LAl(Me)OH), Mp: 228-230 °C decomp. Anal. Calcd for $C_{74}H_{116}Al_2Ca_2N_4O_4$ (1259.83): C 70.49, H 9.21, N 4.45; found: C 69.21, H 9.14, N 4.38. ^{1}H NMR (200 MHz, C_6D_6, 25 °C, TMS): δ –1.05 (s, 6H, Al-C*H*$_3$), 1.18 (d, 12H, CH(C*H*$_3$)$_2$), 1.27 (d, 12H, CH(C*H*$_3$)$_2$), 1.33 (d, 12H, CH(C*H*$_3$)$_2$), 1.38 (d, 12H, CH(C*H*$_3$)$_2$), 1.58 (s, 6H, CH$_3$), 3.45 (s, 2H, NCC*H*$_2$), 3.59 (sept, , 4 H, C*H*Me$_2$), 3.76 (sept, 4 H, C*H*Me$_2$), 3.98 (s, 2H, NCC*H*$_2$), 4.98 (s, 1H, γ-C*H*), 5.00 (s, 1H, γ-C*H*), 7.05-7.16 (m, 12H, *m-, p*-Ar-*H*). EI-MS (70 eV): *m*/*z* (%): 202 (100) [DippNCCH$_3$]$^+$. IR (Nujol, cm^{-1}) $\tilde{\nu}$: 1855, 1619, 1535, 1400, 1318, 1260, 1169, 1090, 1020, 936, 894, 810, 766.

4.4.9. Synthesis of LCa(THF)–O–Al(Me)L (9)

LAl(Me)OH (0.476 g, 1mmol) dissolved in THF/*n*-hexane (1:1, 20 mL) was added drop by drop to a solution of LCaN(SiMe$_3$)$_2$·THF (0.689 g, 1.0 mmol) in THF/*n*-hexane (1:1, 10 mL) at –40 °C, and then allowed to warm to room temperature. The stirring was continued at room temperature for 16 h. After removal of all the volatiles *in vacuo* compound **9** remained. Yield (0.80 g, 65%). Mp: 153-156 °C. Anal.Calcd for $C_{63}H_{93}AlCaN_4O_2$ (1004): C 75.30, H 9.26, N 5.58; found: C 75.47, H 9.19, N 5.51. ^{1}H NMR (200 MHz, C_6D_6, 25 °C, TMS): δ –0.96 (s, 3H, Al-C*H*$_3$), 1.12 (m, 4H, O-CH$_2$-C*H*$_2$), 1.15-1.27 (d, 48H, CH(C*H*$_3$)$_2$, 1.60 (s, 6H, C*H*$_3$), 1.70 (s, 6H, C*H*$_3$), 3.2-3.42 (m, 8H, C*H*(CH$_3$)$_2$), 3.8 (m, 4H, O-C*H*$_2$-CH$_2$), 4.81 (s, 2H, γ-C*H*), 7.08-7.16 (m, 12H, *m-, p*-Ar-*H*). MS (70 eV): *m*/*z* (%): 202 (100) [DippNCCH$_3$]$^+$. IR (Nujol, cm^{-1}) $\tilde{\nu}$: 1859, 1623, 1532, 1408, 1318, 1260, 1170, 1100, 1021, 936, 894, 797, 759, 603.

4.4.10. Synthesis of [Cp*$_2$(Me)Zr–O–Mg(THF)$_2$–O–Zr(Me)Cp*$_2$] (10)

Two equivalents of Cp*$_2$Zr(Me)OH (0.788 g, 2 mmol) in diethylether (40 mL) were added dropwise to a solution of Mg{N(SiMe$_3$)$_2$}$_2$ (0.345 g, 1 mmol) in THF/*n*-hexane (20 mL) at 0 °C and allowed to warm to room temperature, and stirred for 48 h. After removal of the solvent *in vacuo* and washing the residue with pentane (10 mL) compound **10** was obtained. Yield: (0.96 g, 85% with respect to Cp*$_2$Zr(Me)OH. Mp: 162-165 °C. Anal. Calcd for $C_{50}H_{82}MgO_4Zr_2$ (953.91): C 62.90, H 8.59; found: C 62.21, H 8.48. ^{1}H NMR (200 MHz, C_6D_6, 25 °C, TMS): δ –1.01 (s, 6H, Zr-C*H*$_3$), 1.35 (m, 8H, O-CH$_2$-C*H*$_2$), 3.34 (m, 8H, O-C*H*$_2$-CH$_2$), 1.89 (s, 60H, Cp**Me*). ^{13}C NMR (75.475 MHz, 25 ºC, TMS): δ 117.35 (s, Cp*$_2$, *C*10), 22.71 (s, Zr–*C*H$_3$).

4.4.11. Synthesis of [Cp*$_2$Zr–O–Ca(THF)$_3$N(SiMe$_3$)$_2$] (11)

Cp*$_2$Zr(Me)OH (0.393 g, 1 mmol) dissolved in *n*-hexane (20 mL) was added dropwise at 0 °C to a stirred solution of Ca{N(SiMe$_3$)$_2$}$_2$·2THF (0.505 g, 1 mmol) in *n*-hexane (20 mL). The solution was allowed to warm to room temperature and stirred for 24 h. After removal of all the volatiles *in vacuo* compound **11** remained. Yield (0.4 g, 68%). Mp: 226-230 °C. Anal. Calcd for $C_{39}H_{75}CaNO_4Si_2Zr$ (809.48): C 57.81, H 9.27, N 1.73; found: C 58.11, H 9.18, N 1.67. ^{1}H NMR (500 MHz, C_6D_6, 25 °C, TMS): δ –0.36 (s, 3H, Zr–CH_3), 0.51 (s, 18H, (SiMe_3)$_2$), 1.90 (s, 30H, Cp**Me*). ^{13}C NMR (75.475 MHz, 25 ºC, TMS): δ 117.35 (s, Cp*$_2$, *C*10), 22.72 (s, Zr–*C*H$_3$), 2.56 (s, (Si*C*H$_3$)$_2$). ^{29}Si NMR (99.36 MHz, C_6D_6, TMS): δ –13.50 (*Si*Me$_3$). MS (70 eV): *m*/*z* (%): 377 (100) [M^+–Me$_6$], 516 (30) [M^+–Me$_5$]

4.4.12. Synthesis of [L(Me)Al–O–SnPh$_3$] (12)

To a Ph_3SnOH (0.367 g, 1.0 mmol) suspension in THF/toluene (30 mL) was added a clear solution of **5** (0.804 g, 1mmol) at room temperature and stirred for 2 days. The solvent was removed and the residue recrystallized from THF/toluene solution (20 mL). The solution was kept at –32 °C for two days to give colorless crystals. The crystals were collected by filtration and the filtrate was concentrated (ca 8 mL) and kept at the same temperature to give another crop. Total yield: (0.50 g, 61 %). Mp: 168-171 °C Anal. Calcd. for $C_{48}H_{59}AlN_2OSn$ (825.64): C 69.76, H 7.15, N 3.39; found C 68.87, H 7.11, N 3.33. ^{1}H NMR (500 MHz, C_6D_6, 25 °C, TMS): δ –0.66 (s, 3H, Al-CH_3), 1.08 (d, 12H, CH(CH_3)$_2$), 1.15 (d, 6H, CH(CH_3)$_2$), 1.25 (d, 12H, CH(CH_3)$_2$), 1.58 (s, 6H, CH$_3$), 3.22 (sept, , 2 H, C*H*Me$_2$), 3.70 (sept, 2 H, C*H*Me$_2$), 5.00 (s, 1H, *γ*-C*H*), 7.48-7.69 (m, 15H, *Ph*), 7.6-7.16 (m, 6H, *m*-, *p*-Ar-*H*), ^{119}Sn NMR (186 MHz, C_6D_6, 25 °C, TMS): δ –110. EI-MS (70 eV): *m*/*z* (%): 826 (3) [M^+], 811 (100) [M^+-*Me*].

4.4.13. Synthesis of [L(Me)Al–O–Sn–O–Al(Me)L] (13)

LAl(Me)OH (0.95 g, 2.00 mmol) dissolved in toluene (30 mL) was added dropwise at –40 °C to a stirring solution of Sn{N(SiMe$_3$)$_2$}$_2$ (0.44 g, 1.00 mmol) in toluene (15 mL). The solution was allowed to warm to room temperature and stirred overnight. The color of the solution changes from orange to yellow, after removal of all the volatiles *in vaccuo* the residue was extracted with *n*-hexane (50 mL). Partial removal of the solvent and storage the solution at room temperature for 2 days afforded colorless crystals of **13**. Yield (0.76 g, 71 %). Mp: 210-212 °C. Anal. Calcd for $C_{60}H_{88}Al_2N_4O_2Sn$ (1070.04): C 67.35, H 8.29, N 5.24; found C 67.33, H 8.31, N 5.28. ^{1}H NMR (200 MHz, C_6D_6): δ –0.80 (s, 6 H, Al*Me*), 1.13 (d, *J* = 6.8 Hz, 12 H, CH*Me*$_2$), 1.23 (d, *J* = 6.8 Hz, 12 H, CH*Me*$_2$), 1.32 (d, *J* = 6.8Hz, 12 H, CH*Me*$_2$), 1.40 (d, *J* = 6.8Hz, 12 H, CH*Me*$_2$), 1.64 (s, 12 H, C*Me*), 3.27 (sept, *J* = 6.8 Hz, 4 H, C*H*Me$_2$), 3.95 (sept, *J* = 6.8 Hz, 4 H, C*H*Me$_2$), 5.10 (s, 2 H, *γ*-C*H*), 7.07-7.12 (m, *Ar*). EI-MS (70 eV): *m*/*z* (%): 1069 (6) [M^+], 1039 (21) [M^+-Me_2], 1055 (100) [M^+-*Me*]. IR (Nujol, Cm^{-1}) $\tilde{\nu}$: 1532, 1383, 1320, 1255, 1193, 1172, 1106, 1043, 938, 876, 770, 689, 543, 456.

4.4.14. Synthesis of [L(Me)Al–O–Mg(THF)$_2$–O–Zr(Me)Cp*$_2$] (14)

One equivalent of **5** (0.804 g, 1mmol) in THF/*n*-hexane (40 mL) was added dropwise to a solution of Cp*$_2$Zr(Me)OH (0.345 g, 1 mmol) in THF/*n*-hexane (20 mL) at 0 °C and allowed to warm to room temperature, and stirring was continued for 48 h. After removal of the solvent *in vacuo* and washing the residue with pentane (15 mL) compound **14** was obtained. Yield (0.96 g, 85%). Mp: 162-165 °C; Anal. Calcd for $C_{68}H_{114}AlMgN_2O_4Zr$ (1166.12): C 69.80, H 9.78, N 2.40; found: C 68.91, H 9.71, N 2.32. ^{1}H NMR (300 MHz, C_6D_6, 25 °C, TMS): δ –0.39 (s, 3H, Zr-C*H*$_3$), –0.41 (s, 3H, Al-C*H*$_3$), 1.22 (d, 12H, CH(C*H*$_3$)$_2$, 1.32 (d, 12H, CH(C*H*$_3$)$_2$, 1.41 (m, 8H, O-CH$_2$-C*H*$_2$), 1.69 (s, 6H, C*H*$_3$), 1.96 (s, 30H, Cp**Me*), 3.19 (m, 8H, O-C*H*$_2$-CH$_2$), 3.46 (sept, 4H, C*H*(CH$_3$)$_2$), 3.90 (sept, 4H, C*H*(CH$_3$)$_2$), 4.99 (s, 1H, *γ*-C*H*), 7.08-7.16 (m, 12H; *m*-, *p*-Ar-*H*).

MS (70 eV): *m*/*z* (%): 202 (100) [DippNCCH$_3$]$^+$. IR (Nujol, cm^{-1}) $\widetilde{\nu}$: 2170, 1930, 1872, 1810, 1620, 1245, 1180, 1116, 1020, 972, 880, 790, 760, 609.

5. Handling and Disposal of Solvents and Residual Wastes

1. The recovered solvents were condensed into a liquid nitrogen cold-trap under *vacuo* and collected in halogen-free or halogen-containing solvent containers, and stored for disposal.
2. Used NMR solvents were classified into halogen-free or halogen-containing solvents and disposed accordingly.
3. The acid-bath used for cleaning glassware was neutralized with Na_2CO_3 and the resulting NaCl solution was washed off in the communal water drainage.
4. The residue of the base-bath used for cleaning glassware was poured into a container for waste disposal.
5. Sodium metal used for drying solvents was collected and reacted carefully with *iso*-propanol and poured into the base-bath for cleaning glassware.
6. Ethanol and acetone used for low temperature reactions for cold-baths (with solid CO_2 or liquid N_2) were subsequently used for cleaning glassware.

Amounts of various types of disposable wastes generated during the work:

Halogen-containing solvent waste	4 L
Halogen-free solvent waste	15 L
Acid waste	12 L
Basic waste	18 L

6. Crystal Data and Refinement Details

Table 2. Crystal data and structure refinement details for [LMg(OH)·THF]$_2$·toluene (**1**).

Empirical formula	$C_{73}H_{108}Mg_2N_4O_4$ incl. toluene
Formula weight	1154.25
Temperature	133(2) K
Wavelength	0.71073 Å
Crystal system	Monoclinic
Space group	$P2_1/n$
Unit cell dimensions	a = 12.648(8) Å
	b = 14.068(6) Å β = 93.905(5)°
	c = 19.167(12) Å
Volume	3402.5(3) Å^3
Z	2
Density (calculated)	1.127 Mg/m^3
Absorption coefficient	0.085 mm^{-1}
F(000)	1260
Crystal size	0.30 x 0.30 x 0.20 mm^3
θ range for data collection	1.80 to 24.86°
Index ranges	$14 \le h \le 14$, $-16 \le k \le 16$, $-22 \le l \le 22$
Reflections collected	50405
Independent reflections	5872 (R_{int} = 0.1282)
Completeness to θ = 24.86°	99.4 %
Max. and min. transmission	0.9832 and 0.9750
Refinement method	Full-matrix least-squares on F^2
Data / restrains / parameters	5872 / 0 / 405
Goodness-of-fit on F^2	0.768
Final R indices (I>2sigma (I))	$R1$ = 0.0489, $wR2$ = 0.1242
R indices (all data)	$R1$ = 0.0952, $wR2$ = 0.1452
Largest difference peak and hole	0.384 and -0.299 e.Å^{-3}

Table 3. Crystal data and structure refinement details for $[LCa(OH)\cdot THF]_2$ (**2**).

Empirical formula	$C_{66}H_{100}Ca_2N_4O_4$ x C_7 H_8
Formula weight	1185.79
Temperature	133(2) K
Wavelength	0.71073 Å
Crystal system	Triclinic
Space group	$P\bar{1}$
Unit cell dimensions	a = 12.666(9) Å α = 98.423(6)°
	b = 12.708(9) Å β = 113.730(5)°
	c = 13.298(10) Å γ = 110.982(6)°
Volume	1720.6(2) Å^3
Z	1
Density (calculated)	1.144 Mg/ m^3
Absorption coefficient	0.215 mm^{-1}
F(000)	646
Crystal size	0.40 x 0.30 x 0.25 mm^3
θ range for data collection	1.78 to 24.00 deg.
Index ranges	$-14 \leq h \leq 14$, $-13 \leq k \leq 14$, $-15 \leq l \leq 15$
Reflections collected	23691
Independent reflections	5409 (R_{int} = 0.1115)
Completeness to θ = 24.00°	100.0%
Refinement method	Full-matrix least-squares on F^2
Data / restrains / parameters	5409 / 0 / 371
Goodness-of-fit on F^2	0.942
Final R indices (I>2sigma (I))	$R1$ = 0.0561, $wR2$ = 0.0802
R indices (all data)	$R1$ = 0.1152, $wR2$ = 0.0890
Largest difference peak and hole	0.527 and -0.301 e. Å^{-3}

Table 4. Crystal data and structure refinement details for [L^{I}Mg(Cl)] (**3**).

Empirical formula	$C_{20.50}H_{39}ClMgN_4$
Formula weight	401.32
Temperature	100(2) K
Wavelength	0.71073 Å
Crystal system	Monoclinic
Space group	$P2_1/c$
Unit cell dimensions	a = 17.1111(8) Å
	b = 7.1331(3) Å β = 110.703(10)°
	c = 19.7089(9) Å
Volume	2250.2(17) Å^3
Z	4
Density (calculated)	1.185 Mg/m^3
Absorption coefficient	0.210 mm^{-1}
F(000)	876
Crystal size	0.4 x 0.25 x 0.1 mm^3
θ range for data collection	2.12 to 25.69°
Index ranges	$-20 \le h \le 19$, $0 \le k \le 8$, $0 \le l \le 24$
Reflections collected	36297
Independent reflections	4273 (R_{int}= 0.0235)
Completeness to θ = 25.69°	99.9 %
Refinement method	Full-matrix least-squares on F^2
Data / restrains / parameters	4273 / 0 / 266
Goodness-of-fit on F^2	1.049
Final R indices (I>2sigma (I))	$R1$ = 0.0303, $wR2$ = 0.0796
R indices (all data)	$R1$ = 0.0329, $wR2$ = 0.0812
Largest difference peak and hole	0.575 and -0.257 e.Å^{-3}

Table 5. Crystal data and structure refinement details for [LCa(F)·THF]$_2$ (**4**).

Empirical formula	$C_{66}H_{98}Ca_2F_2N_4O_2$ x C_7H_8
Formula weight	1189.78
Temperature	133(2) K
Wavelength	0.71073 Å
Crystal system	Triclinic
Space group	$P\bar{1}$
Unit cell dimensions	a = 12.454(10) Å α = 101.349(6)°
	b = 13.124(10) Å β = 112.188(6)°
	c = 13.308(11) Å γ = 111.489(6)°
Volume	1726.4(2) Å^3
Z	1
Density (calculated)	1.144 Mg/m^3
Absorption coefficient	0.216 mm^{-1}
F(000)	646
θ range for data collection	1.79 to 24.82°
Index ranges	$-14 \leq h \leq 14$, $-15 \leq k \leq 15$, $-15 \leq l \leq 15$
Reflections collected	25302
Independent reflections	5909 (R_{int} = 0.1045)
Completeness to θ = 24.82°	99.4%
Refinement method	Full-matrix least-squares on F^2
Data / restrains / parameters	5909 / 0 / 367
Goodness-of-fit on F^2	0.979
Final R indices (I>2sigma(I))	$R1$ = 0.0516, $wR2$ = 0.0737
R indices (all data)	$R1$ = 0.1083, $wR2$ = 0.0825
Largest difference peak and hole	0.542 and -0.344 e.A^{-3}

Table 6. Crystal data and structure refinement details for [L(Me)Al–O–Mg(THF)$_2$–N(SiMe$_3$)$_2$] (**5**).

Empirical formula	$C_{44}H_{78}AlMgN_3O_3Si_2$	
Formula weight	804.56	
Temperature	133(2) K	
Wavelength	0.71073 Å	
Crystal system	Monoclinic	
Space group	$P2_1/n$	
Unit cell dimensions	a = 11.746(2) Å	
	b = 21.439(3) Å	β = 101.66(2)°
	c = 19.870(3) Å	
Volume	4900.5(13) Å^3	
Z	4	
Density (calculated)	1.091 Mg/m^3	
Absorption coefficient	0.141 mm^{-1}	
F(000)	1760	
Crystal size	0.30 x 0.20 x 0.20 mm^3	
θ range for data collection	1.90 to 24.84°	
Index ranges	$-14 \leq h \leq 14, -17 \leq k \leq 17, -18 \leq l \leq 18$	
Reflections collected	72419	
Independent reflections	8441 (R_{int} = 0.1283)	
Completeness to θ = 24.84°	99.4 %	
Refinement method	Full-matrix least-squares on F^2	
Data / restrains / parameters	8441 / 405 / 582	
Goodness-of-fit on F^2	0.848	
Final R indices (I>2sigma(I))	$R1$ = 0.0394, $wR2$ = 0.0772	
R indices (all data)	$R1$ = 0.0802, $wR2$ = 0.0855	
Largest difference peak and hole	0.208 and -0.207 e.Å^{-3}	

Table 7. Crystal data and structure refinement details for [L(Me)Al–O–Mg(THF)$_2$–O–Al(Me)L] (**6**).

Empirical formula	$C_{68}H_{104}Al_2MgN_4O_4$
Formula weight	1119.82
Temperature	100(2) K
Wavelength	1.54178 Å
Crystal system	Monoclinic
Space group	$P2_1/c$
Unit cell dimensions	a = 16.067(2) Å
	b = 23.113(2) Å β = 102.06(2)°
	c = 18.001(2) Å
Volume	6537.3(12) Å^3
Z	4
Density (calculated)	1.138 Mg/m^3
Absorption coefficient	0.865 mm^{-1}
F(000)	2440
Crystal size	0.1 x 0.12 x 0.15 mm^3
θ range for data collection	2.81 to 59.16°
Index ranges	$-17 \le h \le 16$, $-25 \le k \le 25$, $-9 \le l \le 18$
Reflections collected	45629
Independent reflections	9220 (R_{int} = 0.0641)
Completeness to θ = 59.16°	97.4 %
Refinement method	Full-matrix least-squares on F^2
Data / restrains / parameters	9220 / 173 / 777
Goodness-of-fit on F^2	1.007
Final R indices (I>2sigma (I))	$R1$ = 0.0422, $wR2$ = 0.0941
R indices (all data)	$R1$ = 0.0679, $wR2$ = 0.1057
Largest difference peak and hole	0.245 and -0.257 e.Å^{-3}

Table 8. Crystal data and structure refinement details for [L(Me)Al–OMg(THF)L] (**7·THF**). (Contains 50% LAl(Me)OH)

Empirical formula	$C_{93}H_{138}Al_2MgO_3N_6$
Formula weight	1466.36
Temperature	100(2) K
Wavelength	0.71073 Å
Crystal system	Monoclinic
Space group	*C*2/*c*
Unit cell dimensions	a = 20.4616(12) Å b = 18.1842(10) Å β = 100.9780(10)° c = 47.396(3) Å
Volume	17312.2(17) Å^3
Z	8
Density (calculated)	1.125 Mg/m^3
Absorption coefficient	0.092 mm^{-1}
F(000)	6400
Crystal size	0.2 x 0.13 x 0.1 mm^3
θ range for data collection	1.51 to 25.35°
Index ranges	$0 \le h \le 24$, $0 \le k \le 21$, $-57 \le l \le 56$
Reflections collected	52737
Independent reflections	15817 (R_{int}= 0.0278)
Completeness to θ = 25.35°	99.7 %
Refinement method	Full-matrix least-squares on F^2
Data / restrains / parameters	15817 / 2 / 999
Goodness-of-fit on F^2	1.028
Final *R* indices (*I*>2sigma (*I*))	$R1 = 0.0481$, $wR2 = 0.1149$
R indices (all data)	$R1 = 0.0593$, $wR2 = 0.1208$
Largest difference peak and hole	0.595 and -0.348 e.Å^{-3}

Table 9. Crystal data and structure refinement details for $[\{L^{II}Al(Me)\}(\mu\text{-}O)(Ca\cdot THF)]_2$ (**8**).

Empirical formula	$C_{74}H_{118}Al_2Ca_2N_4O_4$
Formula weight	1259.83
Temperature	100(2) K
Wavelength	0.71073 Å
Crystal system	Triclinic
Space group	$P\bar{1}$
Unit cell dimensions	a = 17.771(14) Å α = 103.393(2)° b = 17.8154(14) Å β = 106.785(2)° c = 25.285(2) Å γ = 90.117(2)°
Volume	7435.3(10) $Å^3$
Z	4
Density (calculated)	1.127 Mg/m^3
Absorption coefficient	0.224 mm^{-1}
$F(000)$	2752
Crystal size	0.1 x 0.08 x 0.06 mm^3
θ range for data collection	0.87 to 25.03°
Index ranges	$-21 \leq h \leq 20$, $-21 \leq k \leq 20$, $0 \leq l \leq 30$
Reflections collected	94970
Independent reflections	26248 (R_{int}= 0.0593)
Completeness to θ = 25.03°	99.9 %
Refinement method	Full-matrix least-squares on F^2
Data / restrains / parameters	26248 / 29 / 1553
Goodness-of-fit on F^2	1.033
Final R indices (I>2sigma (I))	$R1$ = 0.0651, $wR2$ = 0.1638
R indices (all data)	$R1$ = 0.0910, $wR2$ = 0.1758
Largest difference peak and hole	1.013 and -0.579 e.$Å^{-3}$

Table 10. Crystal data and structure refinement details for [Cp*$_2$(Me)Zr–O–Mg(THF)$_2$–O–Zr(Me)Cp*$_2$] (**10**)

Empirical formula	$C_{50}H_{82}MgO_4Zr_2$
Formula weight	953.91
Temperature	100(2) K
Wavelength	71.073 pm
Crystal system	Monoclinic
Space group	$P2_1/c$
Unit cell dimensions	$a = 17.111(8)$ Å
	$b = 7.133(3)$ Å $\beta = 93.5650(10)°$
	$c = 19.709(9)$ Å
Volume	4788.5(4) Å^3
Z	4
Density (calculated)	1.323 Mg/m^3
Absorption coefficient	0.490 mm^{-1}
F(000)	2024
Crystal size	0.4 x 0.3 x 0.2 mm^3
θ range for data collection	2.19 to 26.03°
Index ranges	$0 \leq h \leq 15$
	$0 \leq k \leq 21$
	$-26 \leq l \leq 26$
Reflections collected	49392
Independent reflections	9361 (R_{int}= 0.0252)
Completeness to $\theta = 26.03°$	99.1 %
Refinement method	Full-matrix least-squares on F^2
Data / restrains / parameters	9361 / 8 / 555
Goodness-of-fit on F^2	1.061
Final *R* indices (*I*>2sigma (*I*))	$R1 = 0.0264$, $wR2 = 0.0668$
R indices (all data)	$R1 = 0.0298$, $wR2 = 0.0688$
Largest difference peak and hole	0.446 and -0.437 e.Å^{-3}

Table 11. Crystal data and structure refinement details for [Cp*$_2$(Me)Zr–O–Ca(THF)$_3$N(SiMe$_3$)$_2$] (**11**).

Empirical formula	$C_{39}H_{75}CaNO_4Si_2Zr$
Formula weight	809.48
Temperature	100(2) K
Wavelength	0.71073 Å
Crystal system	Monoclinic
Space group	$P2_1/n$
Unit cell dimensions	a = 14.4608(12) Å
	b = 19.4611(16) Å β = 109.4660(10)°
	c = 16.7106(15) Å
Volume	2171.72(3) Å^3
Z	4
Density (calculated)	1.213 Mg/m^3
Absorption coefficient	0.453 mm^{-1}
F(000)	1744
Crystal size	0.4 x 0.26 x 0.2 mm^3
θ range for data collection	3.02 to 26.03°
Index ranges	$0 \leq h \leq 17$, $0 \leq k \leq 24$, $-20 \leq l \leq 19$
Reflections collected	37016
Independent reflections	8592 (R_{int}= 0.0355)
Completeness to θ = 26.03°	98.3 %
Refinement method	Full-matrix least-squares on F^2
Data / restrains / parameters	8592 / 0 / 450
Goodness-of-fit on F^2	1.048
Final R indices (I>2sigma (I))	$R1$ = 0.0306, $wR2$ = 0.0680
R indices (all data)	$R1$ = 0.0404, $wR2$ = 0.0715
Largest difference peak and hole	0.320 and -0.320 e.Å^{-3}

Table 12. Crystal data and structure refinement details for [LAl(Me)–O–SnPh$_3$] (**12**).

Empirical formula	$C_{48}H_{59}AlOSnN_2$
Formula weight	825.64
Temperature	100(2) K
Wavelength	0.71073 Å
Crystal system	Triclinic
Space group	$P\bar{1}$
Unit cell dimensions	a = 11.460(8) Å α = 84.520(10)°
	b = 11.5128(8) Å β = 84.951(10)°
	c = 16.7507(12) Å γ = 81.884(10)°
Volume	2171.72(3) Å^3
Z	2
Density (calculated)	1.263 Mg/m^3
Absorption coefficient	0.645 mm^{-1}
F(000)	864
Crystal size	0.13 x 0.09 x 0.04 mm^3
θ range for data collection	2.25 to 25.36°
Index ranges	$-13 \leq h \leq 13$, $-13 \leq k \leq 13$, $0 \leq l \leq 20$
Reflections collected	34307
Independent reflections	7961 (R_{int}= 0.0338)
Completeness to θ = 25.36°	99.9 %
Refinement method	Full-matrix least-squares on F^2
Data / restrains / parameters	7961 / 0 / 489
Goodness-of-fit on F^2	1.053
Final R indices (I>2sigma (I))	$R1$ = 0.0238, $wR2$ = 0.0543
R indices (all data)	$R1$ = 0.0278, $wR2$ = 0.0558
Largest difference peak and hole	0.416 and -0.309 e.Å^{-3}

Table 13. Crystal data and structure refinement details for [L(Me)Al–O–Sn–O–Al(Me)L] (**13**).

Empirical formula	$C_{63}H_{95}Al_2O_2SnN_4$	
Formula weight	1113.08	
Temperature	100(2) K	
Wavelength	0.71073 Å	
Crystal system	Triclinic	
Space group	$P\bar{1}$	
Unit cell dimensions	a = 8.9774(7) Å	α = 74.8150(10)°
	b = 18.0738(14) Å	β = 82.5050(10)°
	c = 20.4139(16) Å	γ = 79.1890(10)°
Volume	3128.3(4) $Å^3$	
Z	2	
Density (calculated)	1.182 Mg/m^3	
Absorption coefficient	0.479 mm^{-1}	
F(000)	1186	
Crystal size	0.4 x 0.18 x 0.05 mm^3	
θ range for data collection	2.32 to 25.03°	
Index ranges	$-10 \le h \le 10$, $-20 \le k \le 21$, $0 \le l \le 24$	
Reflections collected	38089	
Independent reflections	10077 (R_{int}= 0.0322)	
Completeness to θ = 25.03°	91.0 %	
Refinement method	Full-matrix least-squares on F^2	
Data / restrains / parameters	10077 / 0 / 672	
Goodness-of-fit on F^2	0.918	
Final R indices (I>2sigma (I))	$R1$ = 0.0381, $wR2$ = 0.0803	
R indices (all data)	$R1$ = 0.0573, $wR2$ = 0.0840	
Largest difference peak and hole	0.702 and -0.641 e.$Å^{-3}$	

Table 14. Crystal data and structure refinement details for [L(Me)Al–O–Mg(THF)$_2$–O–Zr(Me)Cp*$_2$] (**14**).

Empirical formula	$C_{68}H_{114}AlMgN_2O_4Zr$
Formula weight	1166.12
Temperature	100(2) K
Wavelength	0.71073 Å
Crystal system	Monoclinic
Space group	$P2_1/c$
Unit cell dimensions	a = 10.2257(5) Å
	b = 36.888(2) Å β = 100.954(10)°
	c = 17.8324(9) Å
Volume	6604.0(6) Å^3
Z	4
Density (calculated)	1.173 Mg/m^3
Absorption coefficient	0.235 mm^{-1}
F(000)	2532
Crystal size	0.1 x 0.06 x 0.03 mm^3
θ range for data collection	2.03 to 25.37°
Index ranges	$-12 \leq h \leq 12$, $0 \leq k \leq 44$, $0 \leq l \leq 21$
Reflections collected	48462
Independent reflections	12104 (R_{int} = 0.0558)
Completeness to θ = 25.37°	99.8 %
Refinement method	Full-matrix least-squares on F^2
Data / restrains / parameters	12104 / 40 / 732
Goodness-of-fit on F^2	1.053
Final R indices (I>2sigma(I))	$R1$ = 0.0402, $wR2$ = 0.0859
R indices (all data)	$R1$ = 0.0620, $wR2$ = 0.0921
Largest difference peak and hole	0.329 and -0.369 e.Å^{-3}

7. References

[1] L. Bourget-Merle, M. F. Lappert, J. R. Severn, *Chem. Rev.* **2002**, *102*, 3031-3065.

[2] R. H. Holm, G. W. Everett Jr., A. Chakravorty, *Prog. Inorg. Chem.* **1966**, *7*, 83-214.

[3] S. G. McGeachin, *Can. J. Chem.* **1968**, *46*, 1903-1912.

[4] L. C. Dorman, *Tetrahedron Lett.* **1966**, *4*, 459-464.

[5] W. J. Barry, I. L. Finar, E. F. Mooney, *Spectrochim. Acta* **1965**, *21*, 1095-1099.

[6] R. Bonnett, D. C. Bradley, K. J. Fisher, *J. Chem. Soc. Chem. Commun.* **1968**, 886-887.

[7] R. Bonnett, D. C. Bradley, K. J. Fisher, I. F. Rendall, *J. Chem. Soc. (A)* **1971**, 1622-1627.

[8] J. E. Parks, R. H. Holm, *Inorg. Chem.* **1968**, *7*, 1408-1416.

[9] C. P. Richards, G. A. Webb, *J. Inorg. Nucl. Chem.* **1969**, *31*, 3459-3464.

[10] F. A. Cotton, B. G. DeBoer, J. R. Pipal, *Inorg. Chem.* **1970**, *9*, 783-788.

[11] M. Elder, B. R. Penfold, *J. Chem. Soc. (A)* **1969**, 2556-2559.

[12] C. L. Honeybourne, G. A. Webb, *Mol. Phys.* **1969**, *17*, 17-31.

[13] C. L. Honeybourne, G. A. Webb, *Chem. Phys. Lett.* **1968**, *2*, 426-428.

[14] P. B. Hitchcock, M. F. Lappert, D.-S. Liu, *J. Chem. Soc. Chem. Commun.* **1994**, 1699-1700.

[15] C. Cui, H. W. Roesky, H.-G. Schmidt, M. Noltemeyer, H. Hao, F. Cimpoesu, *Angew. Chem.* **2000**, *112*, 4444-4446; *Angew. Chem. Int. Ed.* **2000**, *39*, 4274-4276.

[16] L. W. Pineda, V. Jancik, H. W. Roesky, D. Neculai, A. M. Neculai, *Angew. Chem.* **2004**, *116*, 1443-1445; *Angew. Chem. Int. Ed.* **2004**, *43*, 1419-1421.

[17] V. C. Gibson, J. A. Segal, A. J. P. White, D. J. Williams, *J. Am. Chem. Soc.* **2000**, *122*, 7120-7121.

[18] M. H. Chisholm, J. C. Huffman, K. Phomphrai, *J. Chem. Soc. Dalton Trans.* **2001**, 222-224.

[19] P. J. Bailey, R. A. Coxall, C. M. Dick, S. Fabre, S. Parsons, *Organometallics* **2001**, *20*, 798-801.

[20] M. H. Chisholm, J. Gallucci, K. Phomphrai, *Inorg. Chem.* **2002**, *41*, 2785-2794.

[21] M. H. Chisholm, K. Phomphrai, *Inorg. Chim. Acta* **2003**, *350*, 121-125.

[22] A. P. Dove, V. C. Gibson, E. L. Marshall, A. J. P. White, D. J. Williams, *Dalton Trans.* **2004**, 570-578.

[23] P. J. Bailey, R. A. Coxall, C. M. Dick, S. Fabre, L. C. Henderson, C. Herber, S. T. Liddle, D. Loroño-González, A. Parkin, S. Parsons, *Chem. Eur. J.* **2003**, *9*, 4820-4828.

[24] J. Chai, H. Zhu, H. W. Roesky, C. He, H.-G. Schmidt, M. Noltemeyer, *Organometallics* **2004**, *23*, 3284-3289.

[25] J. Chai, H. Zhu, K. Most, H. W. Roesky, D. Vidovic, H.-G. Schmidt, M. Noltemeyer, *Eur. J. Inorg. Chem.* **2003**, 4332-4337.

[26] L. W. M. Lee, W. E. Piers, M. R. J. Elsegood, W. Clegg, M. Parvez, *Organometallics* **1999**, *18*, 2947-2949.

[27] D. Drees, J. Magull, *Z. Anorg. Allg. Chem.* **1995**, *621*, 948-952.

[28] P. B. Hitchcock, M. F. Lappert, S. Tian, *J. Chem. Soc. Dalton Trans.* **1997**, 1945-1952.

[29] D. Drees, J. Magull, *Z. Anorg. Allg. Chem.* **1994**, *620*, 814-818.

[30] G. Bai, S. Singh, H. W. Roesky, M. Noltemeyer, H.-G. Schmidt, *J. Am. Chem. Soc.* **2005***, 127,* 3449-3455.

[31] V. C. Gibson, P. J. Maddox, C. Newton, C. Redshaw, G. A. Solan, A. J. P. White, D. J. Williams, *J. Chem. Soc. Chem. Commun.* **1998**, 1651-1652.

[32] D. S. Richeson, J. F. Mitchell, K. H. Theopold, *Organometallics* **1989**, *8*, 2570-2577.

[33] A. C. Filippou, C. Völkl, R. D. Rogers, *J. Organomet. Chem.* **1993**, *463*, 135-142.

[34] V. C. Gibson, C. Newton, C. Redshaw, G. A. Solan, A. J. P. White, D. J. Williams, *Eur. J. Inorg. Chem.* **2001**, 1895-1903.

[35] B. J. O'Keefe, M. A. Hillmyer, W. B. Tolman, *J. Chem. Soc. Dalton Trans.* **2001**, 2215-2224.

[36] J. Feldman, S. J. McLain, A. Parthasarathy. W. J. Marshall, C. J. Calabrese, S. D. Arthur, *Organometallics* **1997**, *16*, 1514-1516.

[37] P. H. M. Budzelaar, A. B. van Oort, A. G. Orpen, *Eur. J. Inorg. Chem.* **1998**, 1485-1494.

[38] M. Rahim, N. J. Taylor, S. Xin, S. Collins, *Organometallics* **1998**, *17*, 1315-1323.

[39] P. L. Holland, W. B. Tolman, *J. Am. Chem. Soc.* **1999**, *121*, 7270-7271.

[40] D. W. Randall, S. D. George, P. L. Holland, B. Hedman, K. O. Hodgson, W. B. Tolman, E. I. Solomon, *J. Am. Chem. Soc.* **2000**, *122*, 11632-11648.

[41] M. Fujiwara, H. Wessel, P. Hyung-Suh, H. W. Roesky, *Tetrahedron* **2002**, *58*, 239-243.

[42] N. Winkhofer, A. Voigt, H. Dorn, H. W. Roesky, A. Steiner, D. Stalke, A. Reller, *Angew. Chem.* **1994**, *106*, 1414-1416; *Angew. Chem. Int. Ed.* **1994**, *33*, 1352-1354.

[43] R. Murugavel, V. Chandrasekhar, A. Voigt, H. W. Roesky, H.-G. Schmidt, M. Noltemeyer, *Organometallics* **1995**, *14*, 5298-5301.

[44] V. Jancik, L. W. Pineda, J. Pinkas, H. W. Roesky, D. Neculai, A. M. Neculai, R. Herbst-Irmer, *Angew. Chem.* **2004**, *116*, 5650-5652; *Angew. Chem. Int. Ed.* **2004**, *43*, 2142-2145.

[45] V. Jancik, L. W. Pineda, A. C. Stückl, H. W. Roesky, R. Herbst-Irmer, *Organometallics* **2005**, *24*, 1511-1515.

[46] S. Singh, V. Jancik, H. W. Roesky, R. Herbst-Irmer, *Inorg. Chem.* **2006**, *45*, 949-951.

[47] P. Ghosh, G. Parkin, *Inorg. Chem.* **1996**, *35*, 1429-1430.

[48] L. F. Sánchez-Barba, D. L. Hughes, S. M. Humphrey, M. Bochmann, *Organometallics* **2006**, *25*, 1012-1020.

[49] T. P. Hanusa, *Coord. Chem. Rev.* **2000**, *210*, 329-367.

[50] M. Westerhausen, *Angew. Chem.* **2001**, *113*, 3063-3065; *Angew. Chem. Int. Ed.* **2001**, *40*, 2975-2977.

[51] J. S. Alexander, K. Ruhlandt-Senge, *Eur. J. Inorg. Chem.* **2002**, 2761-2774.

[52] B. G. Gowenlock, W. E. Lindsell, B. Singh, *J. Chem. Soc. Dalton Trans.* **1978**, 657-664.

[53] T. P. Hanusa, *Polyhedron* **1990**, *9*, 1345-1362.

[54] F. G. N. Cloke, P. B. Hitchcock, M. F. Lappert, G. A. Lawless, B. Royo, *J. Chem. Soc. Chem. Commun.* **1991**, 724-726.

[55] C. Eaborn, S. A. Hawkes, P. B. Hitchcock, J. D. Smith, *J. Chem. Soc. Chem. Commun.* **1997**, 1961-1962.

[56] M. J. Harvey, T. P. Hanusa, V. G. Young Jr., *Angew. Chem.* **1999**, *111,* 241-242; *Angew. Chem. Int. Ed.* **1999**, *38*, 217-219.

[57] S. Harder, S. Müller, E. Hübner, *Organometallics* **2004**, *23*, 178-183.

[58] S.-O. Hauber, F. Lissner, G. B. Deacon, M. Niemeyer, *Angew. Chem.* **2005**, *117*, 6021-6025; *Angew. Chem. Int. Ed.* **2005**, *44*, 5871-5875.

[59] C. Ruspic, S. Harder, *Organometallics* **2005**, *24*, 5506-5508.

[60] R. Fischer, H. Görls, M. Westerhausen, *Inorg. Chem. Commun.* **2005**, *8*, 1159-1161.

[61] R. Fischer, M. Gärtner, H. Görls, M. Westerhausen, *Angew. Chem.* **2006**, *118*, 624-627; *Angew. Chem. Int. Ed.* **2006**, *45*, 609-612.

[62] S. Harder, J. Brettar, *Angew. Chem.* **2006**, *118*, 3554-3558; *Angew. Chem. Int. Ed.* **2006**, *45*, 3474-3478.

[63] K. M. Fromm, E. D. Gueneau, A. Y. Robin, W. Maudez, J. Sague, R. Bergougnant, *Z. Anorg. Allg. Chem.* **2005**, *631*, 1725-1740.

[64] G. Xu, N. Yao, I. A. Aksay, J. T. Groves, *J. Am. Chem. Soc.* **1998**, *120*, 11977-11985.

[65] M. H. Chisholm, J. C. Gallucci, K. Phomphrai, *Inorg. Chem.* **2004**, *43*, 6717-6725.

[66] H. M. El-Kaderi, M. J. Heeg, C. H. Winter, *Polyhedron* **2006**, *25*, 224-234.

[67] W. Maudez, D. Häussinger, K. M. Fromm, *Z. Anorg. Allg. Chem.* **2006**, *632*, 2295-2298.

[68] Y. Xie, H. F. Schaefer III, E. D. Jemmis, *Chem. Phys. Lett.* **2005**, *402*, 414-421.

[69] M. Westerhausen, M. Gärtner, R. Fischer, J. Langer, L. Yu, M. Reiher, *Chem. Eur. J.* **2007**, *13*, 6292-6306.

[70] I. Resa, E. Carmona, E. Gutierrez-Puebla, A. Monge, *Science* **2004**, *305*, 1136-1138.

[71] Y. Wang, B. Quillian, P. Wei, H. Wang, X.-J. Yang, Y. Xie, R. B. King, P.v. R. Schleyer, H. F. Schaefer, III, G. H. Robinson, *J. Am. Chem. Soc.* **2005**, *127*, 11944-11945.

[72] Z. Zhu, R. J. Wright, M. M. Olmstead, E. Rivard, M. Brynda, P. P. Power, *Angew. Chem.* **2006**, *118*, 5939-5942; *Angew. Chem. Int. Ed.* **2006**, *45*, 5807-5810.

[73] J. Chai, H. Zhu, A. C. Stückl, H. W. Roesky, J. Magull, A. Bencini, A. Caneschi, D. Gatteschi, *J. Am. Chem. Soc.* **2005**, *127*, 9201-9206.

[74] J. Prust, K. Most, I. Müller, E. Alexopoulos, A. Stasch, I. Usón, H. W. Roesky, *Z. Anorg. Allg. Chem.* **2001**, *627*, 2032-2037.

[75] A.-M. Neculai, C. C. Cummins, D. Neculai, H. W. Roesky, G. Bunkoczi, B. Walfort, D. Stalke, *Inorg. Chem.* **2003**, *42*, 8803-8810.

[76] Holleman-Wiberg, Lehrbuch der Anorganischen Chemie, Nils Wiberg, *Inorganic Chemistry*, Academic Press, Oxford, **2001**. pp 1063-1065.

[77] H. J. Emeleus, *The Chemistry of Fluorine and its Compounds*, Academic Press. New York, **1969**.

[78] F. Q. Liu, D. Stalke, H. W. Roesky, *Angew. Chem.* **1995**, *107*, 2004-2006; *Angew. Chem. Int. Ed. Engl.* **1995**, *34*, 1872-1874.

[79] A. Pevec, A. Demsar, V. Gramlich, S. Petricek, H. W. Roesky, *Dalton Trans.* **1997**, 2215-2216.

[80] K. Mochida, T. Yamanishi, *J. Organomet. Chem.* **1987**, *332*, 247-252.

[81] K. J. Klabunde, A. Whetten, *J. Am. Chem. Soc*. **1986**, *108*, 6529-6534.

[82] Y. Imizu, K. J. Klabunde, *Inorg. Chem.* **1984**, *23*, 3602-3605.

[83] E. Kemnitz, U. Gross, S. Rüdiger (Humboldt-Universität zu Berlin, DE), EP 1 586542 A1, **2005,** 1-11.

[84] N. Sata, K. Eberman, K. Eberl, J. Maier, *Nature* **2000**, *408*, 946-949.

[85] J. Maier, *Solid State Ionics* **2003**, *157*, 327-334.

[86] B. G. Ueland, G. C. Lau, R. J. Cava, J. R. O'Brien, P. Schiffer, *Phys. Rev. Lett.* **2006**, *96*, 027216-1-4.

[87] J. Chai, V. Jancik, S. Singh, H. Zhu, C. He, H. W. Roesky, H.-G. Schmidt, M. Noltemeyer, N. S. Hosmane, *J. Am. Chem. Soc.* **2005**, *127*, 7521-7528.

[88] S. Singh, H. W. Roesky, *Dalton Trans.* **2007**, 1360-1370.

[89] P. M. Gurubasavaraj, S. K. Mandal, H. W. Roesky, R. B. Oswald, A. Pal, M. Noltemeyer, *Inorg. Chem.* **2007**, *46*, 1056-1061.

[90] L. W. Pineda, V. Jancik, H. W. Roesky, R. Herbst-Irmer, *Inorg. Chem.* **2005**, *44*, 3537-3540.

[91] S. K. Mandal, P. M. Gurubasavaraj, H. W. Roesky, R. B. Oswald, J. Magull, A. Ringe, *Inorg. Chem.* **2007**, *46*, 7594-7600.

[92] P. M. Gurubasavaraj, H. W. Roesky, P. M. V. Sharma, R. B. Oswald, V. Dolle, R. Herbst-Irmer, A. Pal, *Organometallics* **2007**, *26*, 3346-3351.

[93] W. Maudez, M. Meuwly, K. M. Fromm, *Chem. Eur. J.* **2007**, *13*, 8302-8316.

[94] N. N. Greenwood, A. Earnshaw, *Chemistry of the Elements*; 1st ed Pergamon, Press Oxford, **1984.**

[95] A. F. Wells, *Structural Inorganic Chemistry*; 5th ed.; Clarendon Press: Oxford, **1984.**

[96] E. Y.-X. Chen, T. J. Marks, *Chem. Rev.* **2000**, *100*, 1391-1434.

[97] S. Sensarma, S. Sivaram, *Macromol. Chem. Phys***.** **1999**, *200,* 323-329.

[98] S. Sensarma, S. Sivaram, *Macromol. Chem. Phys.* **1997**, *198*, 495-503.

[99] K. Soga, T. Arai, T. Uozumi, *Polymer* **1997**, *38*, 4993-4995.

[100] Y. Nakayama, J. Saito, H. Bando, T. Fujita, *Chem. Eur. J.* **2006**, *12*, 7546-7556.

[101] A. Hu, K. M. Neyman, M. Staufer, T. Belling, B. C. Gates, N. Rösch, *J. Am Chem. Soc.* **1999**, *121*, 4522-4523.

[102] Ł. John, J. Utko, L. B. Jerzykiewicz, P. Sobota, *Inorg. Chem.* **2005**, *44*, 9131-9133.

[103] D. Voet, G. J. Voet, *Biochemistry, 2nd ed.;* John Wiley & Sons New York, **1995;** pp 500-502, 1246-1250, 1265-1267.

[104] F. Bickelhaupt, *Chem. Soc. Rev.* **1999**, *28*, 17-23.

[105] R. W. Hoffmann, *Chem. Soc. Rev.* **2003**, *32*, 225-230.

[106] K. W. Henderson, W. J. Kerr, *Chem. Eur. J.* **2001**, *7*, 3430-3437.

[107] S. C. Sockwell, T. P. Hanusa, J. C. Huffman, *J. Am. Chem. Soc.* **1992**, *114*, 3393-3399.

[108] S. Harder, *Angew. Chem.* **2003**, *115*, 3553-3556; *Angew. Chem. Int. Ed.* **2003**, *42*, 3430-3434.

[109] M. H. Chisholm, J. Gallucci, K. Phomphrai, *Chem. Commun.* **2003**, 48-49.

[110] W. Clegg, S. J. Coles, E. K. Cope, F. S. Mair, *Angew. Chem.* **1998**, *110*, 841-843; *Angew. Chem. Int. Ed.* **1998**, *37*, 796-798.

[111] A. G. Avent, M. R. Crimmin, M. S. Hill, P. B. Hitchcock, *Dalton Trans.* **2005**, 278-284.

[112] H. M. El-Kaderi, M. J. Heeg, C. H. Winter, *Organometallics* **2004**, *23*, 4995-5002.

[113] M. Gärtner, H. Görls, M. Westerhausen, *Inorg. Chem.* **2007**, *46*, 5118-5124.

[114] D. Pfeiffer, M. J. Heeg, C. H. Winter, *Inorg. Chem.* **2000**, *39*, 2377-2384.

[115] S. Blair, K. Izod, W. Clegg, R. W. Harrington, *Inorg. Chem.* **2004**, *43*, 8526-8531.

[116] K. Izod, C. Wills, W. Clegg, R. W. Harrington, *Inorg. Chem.* **2006**, *46*, 4320-4325.

[117] P. L. Franceschini, M. Morstein, H. Berke, H. W. Schmalle, *Inorg. Chem.* **2003**, *42,* 7273-7282.

[118] J. Utko, J. Ejfler, S. Szafert, Ł. John, L. B. Jerzykiewicz, P. Sobota, *Inorg. Chem.* **2006**, *45*, 5302-5306.

[119] P. B. Hitchcock, M. F. Lappert, G. A. Lawless, B. Royo, *J. Chem. Soc. Chem. Commun.* **1990**, 1141-1142.

[120] K. F. Tesh, T. P. Hanusa, J. C Huffman, C. J. Huffman, *Inorg. Chem.* **1992**, *31*, 5572-5579.

[121] K. F. Tesh, D. J. Burkey, T. P. Hanusa, *J. Am. Chem. Soc.* **1994**, *116*, 2409-2417.

[122] S. Govil, R. C. Mehrotra, *Aust. J. Chem.* **1975**, *28*, 2125-2128.

[123] C. Wang, X. Xu, H. Yu, Y. Wen, K. Zhao, *Solid State Ionics* **1988**, *28-30*, 542-545.

[124] S. S. Pandit, A. Weyl, D. Janke, *Solid State Ionics* **1994**, *69*, 93-99.

[125] T. Yajima, H. Kazeoka, T. Yogo, H. Iwahara, *Solid State Ionics* **1991**, *47*, 271-275.

[126] T. Hibino, K. Mizutani, T. Yajima, H. Iwahara, *Solid State Ionics* **1992**, *57*, 303-306.

[127] C. C. Wang, W. H. Chen, S. A. Akbar, M. A. Alim, *J. Mater. Sci.* **1997**, *32*, 2305-2312.

[128] C. C. Wang, S. A. Akbar, W. Chen, J. R. Schorr, *Sensors and Actuators* **1997**, *A58*, 237-243.

[129] F. J. Feher, T. A. Budzichowski, K. J. Weller, *J. Am Chem. Soc.* **1989**, *111*, 7288-7289.

[130] F. J. Feher, K. J. Weller, *Organometallics* **1990**, *9*, 2638-2640.

[131] F. J. Feher, T. A. Budzichowski, K. J. Weller, *Polyhedron* **1993**, *12,* 591-599.

[132] A. W. Apblett, A. C. Warren, A. R. Barron, *Can. J. Chem***.** **1992**, *70*, 771-778.

[133] A. W. Apblett, A. C. Warren, A. R. Barron, *Chem. Mater***.** **1992**, *4,* 167-182.

[134] A. W. Apblett, A. R. Barron, *Organometallics* **1990**, ***9,*** 2137-2141.

[135] K. W. Terry, P. K. Ganzel, T. D. Tilley, *Chem. Mater.* **1992**, *4*, 1290-1295**.**

[136] R. Mulhaupt, J. Calabrese, S. D. Ittel, *Organometallics* **1991**, *10*, 3403-3406.

[137] J. R. Mangham, *Chem. Abstr.* **1963**, *59,* 6440**,** US**.** Patent No**.** 3,095,433

[138] N. B. Sharma, A. Singh, R. C. Mehrotra, *Main Group Metal Chem.* **2004***, 27,* 191-198.

[139] Sonika, S. Kumar, A. K. Narula, *J. Ind. Chem. Soc.* **2004**, *81,* 639-643.

[140] S. U. Ghazi, R. Kumar, M. J. Heeg, J. P. Oliver, *Inorg. Chem.* **1994**, *33*, 411-414.

[141] B. M. Chamberlain, M. Cheng, D. R. Moore, T. M. Ovitt, E. B. Lobkovsky, G. W. Coates, *J. Am. Chem. Soc.* **2001**, *123*, 3229-3238.

[142] D. Neculai, H. W. Roesky, A. M. Neculai, J. Magull, H.-G. Schmidt, M. Noltemeyer, *J. Organomet. Chem.* **2002,** *643-644*, 47-52.

[143] J. M. Smith, R. J. Lachicotte, P. L. Holland, *Chem. Commun.* **2001**, 1542-1543.

[144] H. W. Roesky, K. Keller, *J. Fluor.Chem.* **1998**, *89*, 3-4.

[145] C. Ruspic, S. Nembenna, A. Hofmeister, J. Magull, S. Harder, H. W. Roesky, *J. Am. Chem. Soc.* **2006**, *128*, 15000-15004.

[146] H. Hao, H. W. Roesky, Y. Ding, C. Cui, M. Schormann, H.-G. Schmidt, M. Noltemeyer, B. Žemva, *J. Fluor. Chem*. **2002**, *115*, 143-147.

[147] B. G. Hyde, S. Anderson, *Inorganic Crystal Structures*, Wiley, 1st edn., New York, **1989**, p.187.

[148] D. C. Bradley, M. B. Hursthouse, A. A. Ibrahim, K. M. A. Malik, M. Motevalli, R. Möseler, H. Powell, J. D. Runnacles, A. C. Sullivan, *Polyhedron* **1990**, *9*, 2959-2964.

[149] S. Harder, *Organometallics* **2002**, *21*, 3782-3787.

[150] U. Wannagat, H. Autzen, H. Kuckertz, H.-J. Wismar, *Z. Anorg. Allg. Chem.* **1972**, *394*, 254-262.

[151] L. M. Engelhardt, B. S. Jolly, P. C. Junk, C. L. Raston, B. W. Skelton, A. H. White, *Aust. J. Chem.* **1986**, *39*, 1337-1345.

[152] M. Westerhausen, *Inorg. Chem.* **1991**, *30*, 96-101.

[153] C. E. Holloway, M. Melnik, *J. Organomet. Chem.* **1994**, *465,* 1-63.

[154] R.-C. Yu, C.-H. Hung, J.-H. Huang, H.-Y. Lee, J.-T. Chen, *Inorg. Chem.* **2002**, *41*, 6450-6455.

[155] N. Kuhn, S. Fuchs, E. Niquet, M. Richter, M. Steimann, *Z. Anorg. Allg. Chem.* **2002**, *628*, 717-718.

[156] C. Lee, W. Yang, R. G. Parr, *Phys. Rev. B* **1988**, *37*, 785-789.

[157] B. Miehlich, A. Savin, H. Stoll, H. Preuss, *Chem. Phys. Lett.* **1989**, *157*, 200-206.

[158] Gaussian 03, Revision C.02, M. J. Frisch, G. W. Trucks, H. B. Schlegel, G. E. Scuseria, M. A. Robb, J. R. Cheeseman, Jr. J. A Montgomery, T. Vreven, K. N. Kudin, J. C. Burant, J. M. Millam, S. S. Iyengar, J. Tomasi, V. Barone, B. Mennucci, M. Cossi, G. Scalmani, N. Rega, G. A. Petersson, H. Nakatsuji, M. Hada, M. Ehara, K. Toyota, R. Fukuda, J. Hasegawa, M. Ishida, T. Nakajima, Y. Honda, O. Kitao, H. Nakai, M. Klene, X. Li, J. E. Knox, H. P. Hratchian, J. B. Cross, V. Bakken, C. Adamo, J. Jaramillo, R. Gomperts, R. E. Stratmann, O. Yazyev, A. J. Austin, R. Cammi, C. Pomelli, J. W. Ochterski, P. Y. Ayala, K. Morokuma, G. A. Voth, P. Salvador, J. J. Dannenberg, V. G. Zakrzewski, S. Dapprich, A. D. Daniels, M. C. Strain, O. Farkas, D. K. Malick, A. D. Rabuck, K. Raghavachari, J. B. Foresman, J. V. Ortiz, Q. Cui, A. G. Baboul, S. Clifford, J. Cioslowski, B. B. Stefanov, G. Liu, A. Liashenko, P. Piskorz, I. Komaromi, R. L. Martin, D. J. Fox, T. Keith, M. A. Al-Laham, C. Y. Peng, A. Nanayakkara, M. Challacombe, P. M. W. Gill, B. Johnson, W. Chen, M. W. Wong, C. Gonzalez, and J. A Pople, Gaussian, Inc., Wallingford CT, **2004**.

[159] R. Ditchfield, W. J. Hehre, J. A. Pople, *J. Chem. Phys.* **1971**, *54*, 724-728.

[160] W. J. Hehre, R. Ditchfield, J. A. Pople, *J. Chem. Phys.* **1972**, *56*, 2257-2261.

[161] P. C. Hariharan, J. A. Pople, *Mol. Phys.* **1974**, *27*, 209-214.

[162] V. A. Rassolov, M. A. Ratner, J. A. Pople, P. C. Redfern, L. A. Curtiss, *J. Comp. Chem.* **2001,** *22*, 976-984.

[163] A. P. Dove, V. C. Gibson, P. Hormnirun, E. L. Marshall, J. A. Segal, A. J. P. White, D. J. Williams, *Dalton Trans.* **2003,** 3088-3097.

[164] P. J. Bailey, C. M. E. Dick, S. Fabre, S. Parsons, *J. Chem. Soc. Dalton Trans.* **2000**, 1655-1661.

[165] P. J. Bailey, R. A. Coxall, C. M. E. Dick, S. Fabre, S. Parsons, *Organometallics* **2001***, 20*, 798-801.

[166] S. Nembenna, H. W. Roesky, S. K. Mandal, R. B. Oswald, A. Pal, R. Herbst- Irmer, M. Noltemeyer, H.-G. Schmidt, *J. Am. Chem. Soc.* **2006**, *128*, 13056-13057.

[167] M. Veith, O. Recktenwald, *Z. Naturforsch.* **1981**, *36b*, 144-149.

[168] B. Cetinkaya, I. Gümrükcü, M. F. Lappert, J. L. Atwood, R. D. Rogers, M. J. Zaworotko, *J. Am. Chem. Soc.* **1980**, *102*, 2088-2089.

[169] M. R. Crimmin, I. J. Casely, M. S. Hill, *J. Am. Chem. Soc.* **2005**, *127*, 2042-2043.

[170] S. Datta, P. W. Roesky, S. Blechert, *Organometallics* **2007**, *26*, 4392-4394.

[171] C. Eaborn, P. B. Hitchcock, K. Izod, Z.-R. Lu, J. D. Smith, *Organometallics* **1996**, *15*, 4783-4790.

[172] F. Weber, H. Sitzmann, M. Schultz, C. D. Sofield, R. A. Andersen, *Organometallics* **2002**, *21*, 3139-3146.

[173] S. Harder, *Angew. Chem.* **2004**, *116*, 2768-2773; *Angew. Chem. Int. Ed.* **2004**, *43*, 2714-2718.

[174] M. R. Crimmin, A. G. M. Barrett, M. S. Hill, P. B. Hitchcock, P. A. Procopiou, *Organometallics* **2007**, *26*, 2953-2956.

[175] M. R. Crimmin, A. G. M. Barrett, M. S. Hill, P. A. Procopiou, *Org. Lett*. **2007**, *9*, 331-333.

[176] A. G. M. Barrett, M. R. Crimmin, M. S. Hill, P. B. Hitchcock, P. A. Procopiou, *Organometallics* **2007**, *26*, 4076-4079.

[177] Z. Zhong, P. J. Dijkstra, C. Birg, M. Westerhausen, J. Feijen, *Macromolecules* **2001**, *34*, 3863-3868.

[178] R. A. Williams, T. P. Hanusa, J. C. Huffman, *Organometallics* **1990**, *9*, 1128-1134.

[179] M. Rieckhoff, U. Pieper, D. Stalke, F. T. Edelmann, *Angew. Chem.* **1993**, *105*, 1102-1104; *Angew. Chem. Int. Ed. Engl.* **1993**, *32*, 1079-1081.

[180] D. Stalke, *Angew. Chem.* **1994**, *106*, 2256-2259; *Angew. Chem. Int. Ed. Engl.* **1994,** *33*, 2168-2171.

[181] R. A. Williams, T. P. Hanusa, J. C. Huffman, *J. Am. Chem. Soc.* **1990**, *112*, 2454-2455.

[182] K. Izod, W. Clegg, S. T. Liddle, *Organometallics* **2000**, *19*, 3640-3643.

[183] C. Ruspic, J. Spielmann, S. Harder, *Inorg. Chem.* **2007**, *46*, 5320-5326.

[184] F. Buch, J. Brettar, S. Harder, *Angew. Chem.* **2006**, *118*, 2807-2811; *Angew. Chem. Int. Ed.* **2006**, *45*, 2741-2745.

[185] G. M. Sheldrick, *Acta Cryst. A* **1990**, *46*, 467-473.

[186] G. M. Sheldrick, SHELXL-97. *Program for crystal structure refinement*, University of Göttingen, Göttingen (Germany), **1997**.

[187] M. J. S. Gynane, D. H. Harris, M. F. Lappert, P. P. Power, P. Rivière, M. Rivière-Baudet, *J. Chem. Soc. Dalton Trans.* **1977**, 2004-2009.

8. Curriculum Vitae

Name	Sharanappa Nembenna
Date of Birth	01–06–1975
Marital status	Unmarried
Place of Birth	Kallur (India)
Nationality	Indian
Parents	Channabasamma – Mother Nembennagouda – Father

School Education

1981 – 1983	Govt. Primary School, Kallur
1983 – 1986	Govt. Primary School, Hallihosur
1986 – 1988	Govt. Primary School, Kallur
1988 – 1991	Govt. High School, Kallur

University Education

1993 – 1996	Bachelor of Science (Chemistry, Botany, Zoology) Karnatak University, Dharwad, India
1997 – 1999	Master of Science (Organic Chemistry) Karnatak University, Dharwad, India

Doctoral Degree

2004 – present	Begin the PhD studies at the Institute of Inorganic Chemistry, Universität Göttingen, Germany, under the supervision of Prof. Dr. Herbert W. Roesky. Topic: β−Diketiminate Ligand Supported Group 2 Metal Hydroxide, Halide, Oxygen Bridged Heterobimetallic and Heterotrimetallic Complexes: Synthesis and X-ray Structural Studies

Work Experience

2001 – 2004	Worked as a Project Assistant in the department of Inorganic Chemistry, National Chemical Laboratory, India
2000 – 2001	Worked as a part-time lecturer at B.V.B. College of Engg and Tech Hubli

Lebenslauf

Name	Sharanappa Nembenna
Geburtsdatum	01–06–1975
Familienstand	Ledig
Geburtsort	Kallur (India)
Staatsangehörigkeit	Indisch
Eltern	Channabasamma – Mutter Nembennagouda – Vater

Schulausbildung

1981 – 1983	Govt. Primary School, Kallur
1983 – 1986	Govt. Primary School, Hallihosur
1986 – 1988	Govt. Primary School, Kallur
1988 – 1991	Govt. High School, Kallur

Studium

1993 – 1996	Bachelor of Science (Chemie, Botanik, Zoology) Karnatak University, Dharwad, India
1997– 1999	Master of Science (Organische Chemie) Karnatak University, Dharwad, India

Promotionsstudium

2004 – present	Beginn der Dissertation in Anorganishe Chemie bei Prof. Dr. Herbert W. Roesky am Anorganische –Chemie Universität Göttingen Thema: β−Diketiminate Ligand Supported Group 2 Metal Hydroxide, Halide, Oxygen Bridged Heterobimetallic and Heterotrimetallic Complexes: Synthesis and X-ray Structural Studies

Berufstätigkeit

2001 – 2004	Worked as a Project Assistant in the department of Inorganic Chemistry, National Chemical Laboratory, India
2000 –2001	Worked as a part-time lecturer at B.V.B. College of Engg and Tech Hubli

9. List of publications

[1] *A Well-Defined Hydrocarbon-Soluble Calcium monofluoride of Composition [{LCaF·(thf)}$_2$]: The Application of Soluble Calcium Derivatives for Surface Coating*. **Sharanappa Nembenna**, Herbert W. Roesky, Selvarajan Nagendran, Anja Hofmeister, Jörg Magull, Peter-J. Wilbrandt, Matthias Hahn, *Angew. Chem.* **2007**, *119,* 2564-2566; *Angew. Chem. Int. Ed.* **2007**, *46*, 2512-2514.

[2] *Soluble Molecular Compounds with the Mg–O–Al Structural Motif***:** *A Model Approach for the Fixation of Organometallics on a MgO Surface*. **Sharanappa Nembenna**, Herbert W. Roesky, Swadhin K. Mandal, Rainer B. Oswald, Aritra Pal, Regine Herbst-Irmer, Mathias Noltemeyer, and Hans-Georg Schmidt, *J. Am. Chem. Soc.* **2006**, *128*, 13056-13057.

[3] *A Well-Defined Hydrocarbon-Soluble Calcium Hydroxide: Synthesis, Structure, and Reactivity*. Christian Ruspic, **Sharanappa Nembenna**, Anja Hofmeister, Jörg Magull, Sjoerd Harder, and Herbert W. Roesky, *J. Am. Chem. Soc.* **2006**, *128,* 15000-15004.

[4] *Polyhedral Cobalt(II) and Iron(II) Siloxanes: Synthesis and X-ray Crystal Structure of* $[(RSi(OH)O_2)Co(OPMe_3)]_4$ *and* $[(RSiO_3)_2(RSi(OH)O_2)_4(\mu_3\text{-}OH)_2Fe_8(THF)_4]$ *(R = (2,6-*$iPr_2C_6H_3)N(SiMe_3)$*)*. Umesh N. Nehete, Herbert W. Roesky, Hongping Zhu, **Sharanappa Nembenna**, Hans-Georg Schmidt, Mathias Noltemeyer, Dmitrij Bogdanov, and Konrad Samwer, *Inorg. Chem.* **2005**, *44*, 7243-7248.

[5] *Low-Valent Lead and Bismuth Organohalides bearing a β–diketiminato Ligand.* Leslie W. Pineda, Vojtech Jancik, **Sharanappa Nembenna**, and Herbert W. Roesky, *Z. Anorg. Allg. Chem.* **2007**, *633*, 2205-2209.

Articles accepted and /or in preparation

[6] *A Tailor-Made Trimetallic Oxide containing a Sub-Valent O–Sn(II)–O Core*. **Sharanappa Nembenna**, Sanjay Singh, Herbert W. Roesky, Holger Ott, and Dietmar Stalke. *Organometallics*

[7] *A Hydrocarbon-Soluble Strontium Hydroxide Complex* $[LSr(thf)(\mu\text{-}OH)_2Sr(thf)_2L]$ *Derived from Strontium Amide*. Sankaranarayanapillai Sarish, **Sharanappa Nembenna**, Selvarajan Nagendran, Herebert W. Roesky, Aritra Pal, Regine Herbst-Irmer, and Jörg Magull. *Organometallics*

[8] *Antimony Oxide-Amide and Antimony Oxide-Chloride Wrapped in an Organoaluminum Framework*. Sanjay Singh, **Sharanappa Nembenna,** Vojtech Jancik, and Herbert W. Roeky. *E. J. Inorg. Chem*. **Accepted**

[9] *β-Diketminate Supported Magnesium Halide, Hydroxide, and Heterobimetallic Complexes: Synthesis and X-ray Structural Studies*. **Sharanappa Nembenna**, Herbert W. Roesky, Holger Ott, Dietmar Stalke, Hans-Georg Schmidt, and Mathias Noltemeyer. *E. J. Inorg. Chem*.